Winter 2012

Enhancing Spectrum Utilization in Dynamic Cognitive Radio Systems

Dusadee Treeumnuk
Old Dominion University

ENHANCING SPECTRUM UTILIZATION IN DYNAMIC COGNITIVE RADIO SYSTEMS

by

Dusadee Treeumnuk
B.E. May 1995, Kasetsart University, Thailand
M.S. May 2009, Old Dominion University

A Dissertation Submitted to the Faculty of
Old Dominion University in Partial Fulfillment of the
Requirements for the Degree of

DOCTOR OF PHILOSOPHY

ELECTRICAL AND COMPUTER ENGINEERING

OLD DOMINION UNIVERSITY
December 2012

Approved by:

Dimitrie C. Popescu (Director)

Jiang Li (Member)

Linda L. Vahala (Member)

Hideaki Kaneko (Member)

ABSTRACT

ENHANCING SPECTRUM UTILIZATION IN DYNAMIC COGNITIVE RADIO SYSTEMS

Dusadee Treeumnuk
Old Dominion University, 2012
Director: Dr. Dimitrie C. Popescu

Cognitive radio (CR) is regarded as a viable solution to enabling flexible use of the frequency spectrum in future generations of wireless systems by allowing unlicensed secondary users (SU) to access licensed spectrum under the specific condition that no harmful interference be caused to the licensed primary users (PU) of the spectrum. In practical scenarios, the knowledge of PU activity is unknown to CRs and radio environments are mostly imperfect due to various issues such as noise uncertainty and multipath fadings. Therefore, important functionalities of CR systems are to efficiently detect availability of radio spectrum as well as to avoid generating interference to PUs, by missing detection of active PU signals.

Typically, CR systems are expected to be equipped with smart capabilities which include sensing, adapting, learning, and awareness concerned with spectrum opportunity access, radio environments, and wireless communications operations, such that SUs equipped with CRs can efficiently utilize spectrum opportunities with high quality of services. Most existing researches working on CR focus on improving spectrum sensing through performance measures such as the probabilities of PU detection and false alarm but none of them explicitly studies the improvement in the actual spectrum utilization. Motivated by this perspective, the main objective of the dissertation

is to explore new techniques on the physical layer of dynamic CR systems, that can enhance actual utilization of spectrum opportunities and awareness on the performance of CR systems.

Specifically, this dissertation investigates utilization of spectrum opportunities in dynamic scenarios, where a licensed radio spectrum is available for limited time and also analyzes how it is affected by various parameters. The dissertation proposes three new methods for adaptive spectrum sensing which improve dynamic utilization of idle radio spectrum as well as the detection of active PUs in comparion to the conventional method with fixed spectrum sensing size. Moreover, this dissertation presents a new approach for optimizing cooperative spectrum sensing performance and also proposes the use of hidden Markov models (HMMs) to enabling performance awareness for local and cooperative spectrum sensing schemes, leading to improved spectrum utilization. All the contributions are illustrated with numerical results obtained from extensive simulations which confirm their effectiveness for practical applications.

This work is dedicated to the Treeumnuk family.

ACKNOWLEDGMENTS

First of all, I would like to express my sincere gratitude and deepest appreciation to my advisor, Prof. Dimitrie C. Popescu, for his excellent guidance, continuous motivation, and warm mentorship throughout many years of my study at Old Dominion University. With his professional knowledge and vision in the research area, he has advised, inspired, and conducted me to gain a lot of knowledge along with experiencing high quality research applicable to both academia and industry.

I would like to thank my dissertation committee members, Prof. Jiang Li, Prof. Linda L. Vahala, and Prof. Hideaki Kaneko, for their valuable suggestions on completing my doctoral dissertation. I am grateful to Prof. Shirshak K. Dhali and Prof. Oscar R. González, who are the Chair and Graduate Program Director of the Department of Electrical and Computer Engineering, respectively, for their best advice and support over the years. I express my thanks to Linda Marshall who was always willing to help me whenever I had questions and problems. I am also thankful to all professors and people in the department for providing all the excellent classes, facilities, support, and atmosphere that help grow my knowledge and research. I appreciate and thank Danda B. Rawat, Deepak R. Joshi, and also other friends in the department for their direct and indirect support along with friendship.

Particularly, I would like to express my thanks to my wife Panida for all the support and patience associated with true love and I also thank my daughters, Rutfah and Proadfah, who always make me happy with their lovely smiles. With similar feeling, I am thankful to my elder sister, Suntaree, my younger brother, Krawee, my brother-in-law, Khunlor, and my sister-in-law, Tawarat, for their overseas help and

support. I am forever thankful to my parents, Santi and Chuanpit, for their endless love, advice, guidance, and inspiration. Without their support, I would never have made this part of my life successful. I also express my thanks to everyone in the Treeumnuk family who are also behind my success.

I would like to send a lot of thanks to all Thai, American, and international friends who have filled my life with their sincere friendship during my stay in the US. Without them, I doubt if I could keep living far away from my home country. Finally I owe a debt of gratitude to the Royal Thai government who has financed and supported me for my entire education. The work presented in this dissertation is a result of dedicated study which could not be made possible without the support from the Royal Thai government.

TABLE OF CONTENTS

LIST OF TABLES

LIST OF FIGURES

CHAPTER I

INTRODUCTION

Wireless communication systems along with the services they provide have become an essential component of our daily lives. In recent years, wireless networks have become more ubiquitous and less expensive, and there is increasing demand for new wireless services and applications beyond cellular telephones and wireless local area networks (WLANs). These are equipped with emerging wireless technologies geared toward diverse applications that include travel assistance, rescue, weather forecasting, mobile entertainment, and a lot more. However, progress toward new wireless systems and technologies is hindered by the lack of available radio frequency (RF) spectrum: as most of the spectrum has already been allocated it is becoming increasingly difficult to find vacant/open frequency bands for new wireless applications and services.

Cognitive radio (CR) [1, 2] is an emerging concept that aims to enable dynamic access to the RF spectrum for secondary users (SU) through the reuse of licensed frequencies under specific conditions that no harmful interference be caused to the licensed primary users (PU) of the spectrum. Specifically, CR systems are expected to detect spectrum holes [3] or idle frequency bands that are not actively used by PU, to take advantage of them for providing service to SU, and to release them to the PU upon request.

In this chapter, a brief review of CR systems is given in Section I.1. Section I.2 and I.3 present background material on energy detection and hidden Markov models, respectively, which are key concepts used in this dissertation. The problems studied

along with the main contributions of the dissertation are formally stated in Section I.4, with the dissertation outline in Section I.5.

I.1 COGNITIVE RADIO SYSTEMS

The CR concept was introduced by Joseph Mitola in his doctoral research in the early 2000s [4]. The idea of CR was originated from the existence of software defined radio (SDR) in which modulation and demodulation parts are programmable and adaptable [5, 6].

CR has attracted a lot of attention and the term *cognitive radio* has been interpreted in diverse meanings. In the US, the Federal Communications Commission (FCC) defines CR as "*A radio or system that senses its operational electromagnetic environment and can dynamically and autonomously adjust its radio operating parameters to modify system operation, such as maximize throughput, mitigate interference, facilitate interoperability, access secondary markets*" [7, 8]. Thus, CR is an intelligent technology that is expected to not only solve the spectrum scarcity problem but also to increase quality of service of wireless systems with smart capabilities.

Typical capabilities of CR include spectrum sensing, spectrum management, and spectrum sharing [9]. Spectrum sensing is used to identify licensed spectrum bands that are underutilized or not actively used by PUs. Spectrum management allows CRs to appropriately select the best frequency band among multiple idle frequency bands identified by the spectrum sensing process. Spectrum sharing enables CRs to share spectrum opportunities with multiple CRs as well as PUs in order to achieve high spectrum utilization efficiency. Among these functions, spectrum sensing plays

a critical role in CR systems because it is the first process of CR spectrum utilization. A brief review of spectrum sensing techniques used in CR systems is given as follows.

I.1.1 SPECTRUM SENSING

1. Energy Detection: Energy detection [10] is a non-coherent sensing technique which does not require *a priori* knowledge of PU signals. The concept is that energy of the received signal is first estimated and then compared to a specified threshold resulting in a binary output decision. More details of energy detection in CR spectrum sensing are given in Section I.2.

2. Waveform-based Detection: Unlike energy detection, this type of sensing technique [7, 11] requires knowledge of the PU's waveform patterns transmitted such as preambles, midambles, spread sequences, and so on. These patterns are generally used for synchronization, medium access control (MAC) or other purposes in wireless communication systems. The concept is that the detector correlates the received signal with a known waveform pattern of the PU signal. The output decision is performed by comparing the result of correlation with a predetermined threshold. High correlation result above the threshold will infer the presence of the PU. The sensing performance can be improved when the length of the known waveform pattern increases [7]. In CR systems, the knowledge of PU signals is very limited such that the use of this sensing technique may not be applicable in many instances.

3. Cyclostationary Detection: This sensing technique [7, 12–16] exploits periodicity features of the received signal autocorrelation to distinguish between the

PU signal and noise. The key concept is that PU signals are generally cyclostationary, which embeds periodical features into their statistics due to sinusoidal carriers, modulation schemes, or spreading codes while noise is in general wide-sense stationary, with no specific correlation features. Employing the cyclic spectral density (CSD) function, cyclostationary detection can distinguish different types of PU signals as well as noise. This sensing technique is robust to noise uncertainty. However, it requires prior knowledge of PU signals and has high computational complexity.

I.1.2 COOPERATIVE SPECTRUM SENSING

The spectrum sensing techniques discussed in Section I.1.1 are applied locally at individual receivers where their sensing performance can be severely degraded by noise uncertainty, multipath fading, and shadowing in practical scenarios. In particular, local spectrum sensing is affected by the hidden node problem where a SU falsely infers the absence of a PU because the PU signal is received at the SU through a degraded channel. As a consequence, the SU unintentionally causes interference to the PU. Cooperative spectrum sensing where multiple SUs cooperate to decide if a PU signal is present or not [9, 17, 18] is a promising approach to solving the hidden node problem as well as to improving the performance of spectrum sensing.

Generally, cooperative spectrum sensing can be classified into 3 categories as shown in Fig. 1 [17].

1. Centralized Cooperative Sensing: In this category [17, 19–23], a central SU called fusion center (FC) is responsible for collecting local sensing reports from

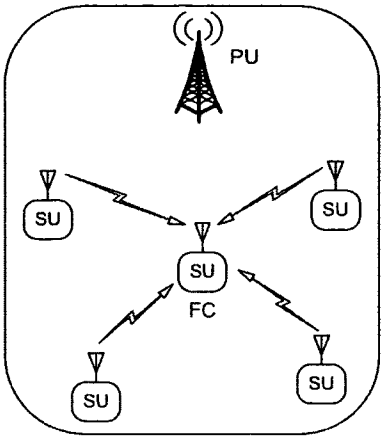

(a) Centralized cooperative sensing

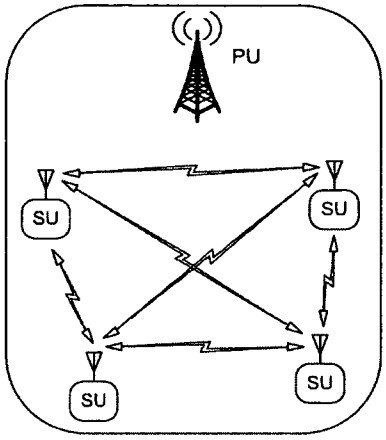

(b) Distributed cooperative sensing

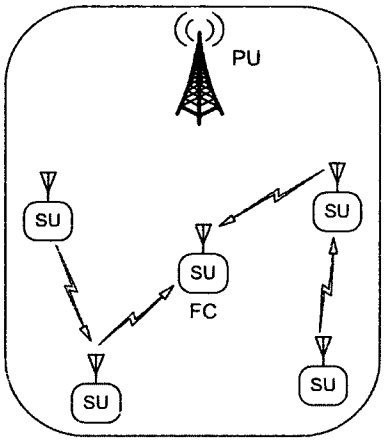

(c) Relay-assisted cooperative sensing

Fig. 1: Classification of cooperative spectrum sensing.

cooperating SUs via report/control channels and decide on the presence of the PU based on a data fusion rule. The FC then reports a fused decision to all cooperating SUs.

2. Distributed Cooperative Sensing: Without employing a FC, cooperative SUs in this cooperative sensing category [7, 17, 24–26] exchange their local sensing information with each other. Each SU makes a decision based on combining its

local decision with decision data received from other SUs.

3. Relay-Assisted Cooperative Sensing: Some cooperative SUs in the system may experience poor communications channels to report their data to the FC. Using relay-assisted cooperative sensing [17, 27–29] , these cooperating SUs can relay their local sensing data to the FC via their neighbors instead of direct report.

I.2 ENERGY DETECTION

Energy detection [10] is a widely used signal processing technique for spectrum sensing. Its popularity is due to the fact that it does not require prior knowledge of PU signals and it has low complexity [7]. The idea behind energy detection is to evaluate the energy in a given frequency band and to compare it against a specified threshold. The band is said to be idle if the estimated energy is below the specified threshold and occupied if the corresponding energy value is above the threshold. Energy detection for spectrum sensing in CR systems has been used in many approaches [30–33].

To introduce the energy detection technique for spectrum sensing, let us start by considering the two possible hypotheses in a CR system: H_0 and H_1, corresponding to the absence, respectively presence, of a PU. The discrete received signal $y(n)$ at the CR under the two hypotheses is written as:

$$y(n) = \begin{cases} w(n), & \text{for } H_0 \\ h \cdot s(n) + w(n), & \text{for } H_1 \end{cases} \tag{I.2.1}$$

where $s(n)$ denotes the transmitted PU signal, h denotes the channel gain between the PU and SU, $w(n)$ denotes the additive white Gaussian noise (AWGN) with zero mean and variance σ_w^2, and n denotes the sample index. It is assumed that the sensing time

is much smaller than the coherence time of the channel. Therefore h can be assumed to be constant during the sensing process.

In energy detection, the test statistic for distinguishing between the two hypotheses H_0 and H_1 is:

$$T_y = \frac{1}{W}\sum_{n=0}^{W-1}|y(n)|^2 \underset{H_0}{\overset{H_1}{\gtrless}} \lambda \tag{I.2.2}$$

where W denotes the number of samples for energy estimation and λ denotes the decision threshold. It should be noted that W is regarded as the sensing window of the energy detection.

According to Parseval's Theorem [34, Sec. 7.2.3], an energy detector can be implemented by using samples of the received signal in either time or frequency domain. Let $Y(k)$ be the discrete Fourier transform (DFT) of the discrete time received signal $y(n)$ with length W. The theorem states that:

$$\sum_{n=0}^{W-1}|y(n)|^2 = \frac{1}{W}\sum_{k=0}^{W-1}|Y(k)|^2$$

Therefore, two basic structures of energy detection are shown in Fig. 2 [35].

Let γ be the signal-to-noise ratio (SNR) at the CR, which is defined as:

$$\gamma = \frac{\sigma_s^2}{\sigma_w^2} \tag{I.2.3}$$

where $\sigma_s^2 = E\{[h \cdot s(n)]^2\}$ denotes the PU signal variance. It is noted that when W is sufficiently long the tail of the test statistic T_y's pdf can be approximated by that of a normal distribution corresponding to the hypothesis that is true [30], that is:

$$T_y \sim \begin{cases} \mathcal{N}\left(\sigma_w^2, \frac{2}{W}\sigma_w^4\right), & \text{for } H_0 \\ \mathcal{N}\left((1+\gamma)\sigma_w^2, \frac{2}{W}(1+2\gamma)\sigma_w^4\right), & \text{for } H_1 \end{cases} \tag{I.2.4}$$

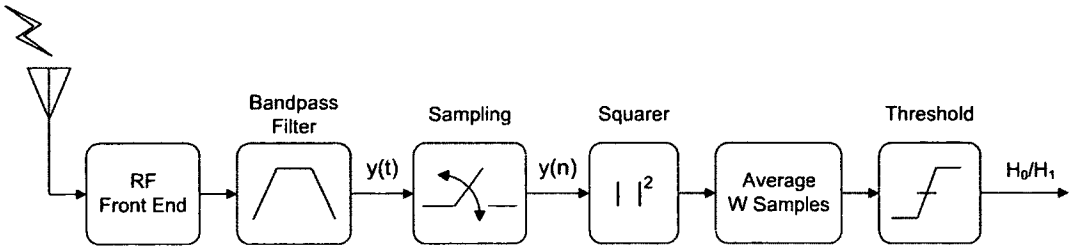

(a) Squarer in time domain.

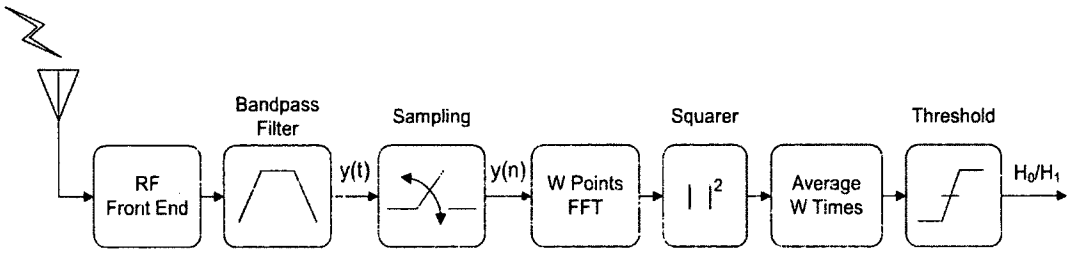

(b) Squarer in frequency domain.

Fig. 2: Basic block diagrams of CR energy detector.

where $\mathcal{N}(\mu, \sigma^2)$ denotes a Gaussian distribution with mean μ and variance σ^2. Generally the performance of spectrum sensing is evaluated through the probability of detection – P_d – which is the probability of correctly detecting an active PU and the probability of false alarm – P_f – which is the probability of incorrectly classifying a given band as occupied when no PU is active. The probabilities of detection P_d and false alarm P_f are then computed as [30]:

$$P_d = P\{T_y > \lambda \mid H_1\} = Q\left(\frac{\lambda - (1+\gamma)\,\sigma_w^2}{\sigma_w^2\sqrt{(1+2\gamma)\,2/W}}\right) \tag{I.2.5}$$

$$P_f = P\{T_y > \lambda \mid H_0\} = Q\left(\frac{\lambda - \sigma_w^2}{\sigma_w^2\,\sqrt{2/W}}\right) \tag{I.2.6}$$

where $Q(\cdot)$ denotes the complementary cumulative distribution function which is defined as [36, Sec. 2.2.1]:

$$Q(x) = \frac{1}{\sqrt{2\pi}} \int_x^{\infty} \exp\left(-\frac{t^2}{2} \right) dt \tag{I.2.7}$$

It is noted that a high value for P_d implies a high capability of the CR to avoid interference with the active PU, while a low P_f value implies a high capability of the CR to utilize spectrum opportunities.

I.3 HIDDEN MARKOV MODELS

The theory of Hidden Markov Models (HMMs) was published by Baum and colleagues in the late 1960s [37–40]. Since the late 1980s, the concept of HMMs has been extensively adopted to speech and image recognition research areas [41]. Recently, HMMs have attracted the attention of researches working on CRs. In [42–44], HMMs are applied to blind spectrum sensing. In [45], the existence of Markov chain for sub-band utilization is experimentally validated and HMMs are used to predict the true states of a sub-band. The use of HMMs for channel state prediction is studied in [46–50]. In [51, 52], sequence detection algorithms are proposed for spectrum sensing based on modeling PU access pattern with HMMs and in [53–55], HMMs are applied to dynamic spectrum access. In this dissertation, the theory of HMMs is applied to studying the performance awareness and evaluation of CR spectrum sensing which is a novel application different from previous works.

A HMM is a Markov model that describes a system's output sequence whose actual states are unknown or hidden but observable through the sequence [41]. Let $S=\{S_1, ..., S_N\}$ be the state space having N possible states and q_t be the actual state

at time instant t. An important property of the first order Markov chain is that the state at any time t depends only on the last state:

$$P[q_t = S_j \mid q_{t-1} = S_i, q_{t-2} = S_k, ...] = P[q_t = S_j \mid q_{t-1} = S_i]$$

The idea behind HMMs is that they can represent the statistical behavior of an observable stochastic sequence in terms of probabilistic state transitions. An observable symbol of each sequence can either stay in the same state or transit to another state depending on the state transition probabilities which are not given but computable with a given set of observable symbol sequences.

Elements of an HMM

The complete parameter set that describes an HMM is $\varphi = (A, B, \pi)$ whose elements are described below:

- N: The number of states in the system. It is noted that the number of HMM states is not known exactly, but with some physical clues about the stochastic process, a suitable number of states can be assumed.

- M: The number of distinct observation symbols per state.

- $A_{N\times N} = \{a_{ij}\}$: The state transition probability matrix. Element a_{ij} of the matrix is expressed as $a_{ij} = P\{q_{t+1} = j \mid q_t = i\}$ for $0 \leq i, j \leq N-1$, where q_t denotes the state at sequence index t, with the constraints: $0 \leq a_{ij} \leq 1$ and $\sum_{j=0}^{N-1} a_{ij} = 1$ for $0 \leq i \leq N-1$.

- $B_{M\times N} = \{b_j(k)\}$: The observation symbol probability matrix. Element $b_j(k)$ of the matrix is the probability that the HMM system will generate the observable

symbol v_k at state j and sequence index t and is formally defined as $b_j(k) = P\{\mathcal{O}_t = v_k \mid q_t = j\}$ for $0 \leq j \leq N-1$, $0 \leq k \leq M-1$, where $v_k = k$. The elements $b_j(k)$ are also known as the emission probabilities [56].

- $\pi_{1\times N} = \{\pi_i\}$: The initial state probability vector, where $\pi_i = P\{q_1 = i\}$, for $0 \leq i \leq N-1$ is the probability that the first state will be state i.

Types of HMMs

Various types of HMMs can be specified by the number of states N and their corresponding state transition probability matrix $A_{N\times N}$. Two examples of HMM types are shown in Fig. 3. Fig. 3(a) shows a 2-state ergodic HMM the two states of

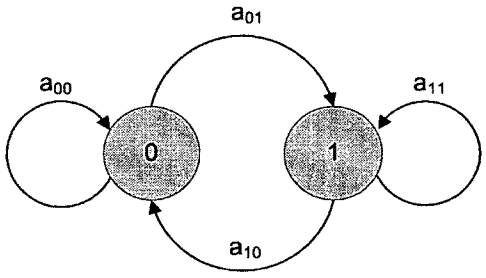

(a) A 2-state ergodic HMM

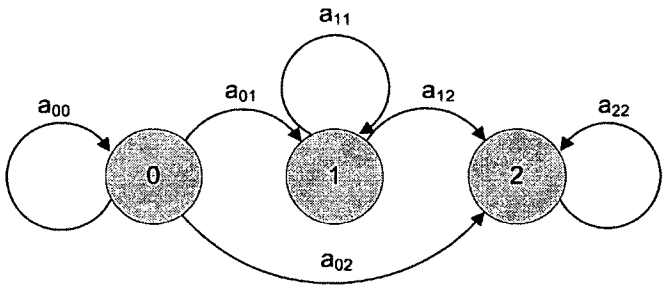

(b) A 3-state left-right HMM

Fig. 3: Examples of HMM types.

which are fully connected while Fig. 3(b) shows a 3-state left-right HMM. Their state transition probability matrices are given by:

$$A_{2\times 2} = \begin{bmatrix} a_{00} & a_{01} \\ a_{10} & a_{11} \end{bmatrix}, \qquad A_{3\times 3} = \begin{bmatrix} a_{00} & a_{01} & a_{02} \\ 0 & a_{11} & a_{12} \\ 0 & 0 & a_{22} \end{bmatrix}$$

Three Basic Problems for HMMs

Given the observation sequence $O = \{\mathcal{O}_t\}_{,1\leq t\leq T}$, where T is the observation length, there are three problems needed to be solved for HMMs:

(1) Given the parameter set φ, how can we compute the likelihood or the probability of the observed sequence given parameter set, $P(O \mid \varphi)$, efficiently.

(2) Given the parameter set φ, how can we determine the optimal state sequence $Q = \{q_t\}_{,1\leq t\leq T}$ corresponding to the observation sequence O.

(3) How can we estimate the parameter set φ to maximize the likelihood $P(O \mid \varphi)$.

It should be noted that these three problems are important in applying HMMs to practical applications including the ones presented in this dissertation.

I.4 DISSERTATION MOTIVATION AND CONTRIBUTIONS

CR is an intelligent technology that enables efficient usage of temporarily unoccupied radio frequencies along with enhancing service quality with cognitive and adaptive capabilities. With this perspective, the physical layer of CR systems is accounted as the most important part that provides sensing, adapting, and awareness

capabilities concerned with spectrum opportunities, radio environments, communication operations, and so on. Research in the CR physical layer is still open for new techniques that can enhance spectrum utilization. However, most existing works focus on improving spectrum sensing performance of CR systems without explicitly considering actual utilization of spectrum holes. It is noted that the work in [57] which presents a method for adapting the sensing window size of the energy detector based on a sequential shift chi-square test (SSCT) but does not consider actual utilization of spectrum holes. Other works discussing CR in dynamic spectrum sensing are [58], which proposes the use of a side detector to monitor when a PU becomes active and adjusting the sensing window accordingly, and [59] which presents an experimental study of adaptive energy detection, neither of which consider the impact of the sensing overhead in the utilization of spectrum holes.

It is also noted that the work in [60] which analyzes the impact of the sensing overhead on the spectrum hole utilization, as well as the work in [30] which studies the tradeoff between the sensing duration and achievable CR throughput. To the best of our knowledge, research that explicitly studies and improves the actual utilization of spectrum holes by CR is not available in the literature, which motivates the work in this dissertation. The main objective of the dissertation is to explore new methods on the physical layer of CR systems, that can efficiently enhance spectrum utilization along with improving sensing performance and awareness of dynamic CR systems. The contributions of the dissertation are presented as follows:

- **Analyzing Spectrum Utilization in Dynamic Scenarios:**

  This dissertation defines a formal measure for CR spectrum hole utilization

which depends on the size of the spectrum sensing window and on the actual duration of the spectrum hole and analyzes the effects of sensing window duration on the spectrum hole utilization. This dissertation also proposes an energy detector with adaptive sensing window that can improve the spectrum hole utilization and probability of detection in dynamic CR systems.

- **Optimizing Sensing Window for Improved Spectrum Utilization:**

  This dissertation proposes methods for adapting the size of energy-based spectrum sensing window that improves the detection of PU signals as well as the utilization of spectrum opportunities, based on jointly optimizing the spectrum hole utilization and probability of detection in dynamic CR systems.

- **Optimizing Performance of Cooperative Sensing for Increased Spectrum Utilization:**

  This dissertation introduces a new metric for evaluating the performance of cooperative sensing that includes both the detection capability of PU signals and the utilization of spectrum holes and also presents numerical results showing that the proposed metric can be used for optimizing performance of cooperative spectrum sensing leading to enhanced spectrum hole utilization in dynamic CR systems.

- **Using Hidden Markov Models to Evaluate Sensing Performance of CR systems:**

  This dissertation presents the use of HMM to describe the output of energy-based local spectrum sensing and cooperative spectrum sensing, and specifically proposes a new method based on HMM, that enables performance evaluation

and awareness for both local and cooperative spectrum sensings in dynamic CR systems.

I.5 DISSERTATION ORGANIZATION

The organization of this dissertation is shown in Table 1. Chapter II evaluates utilization of spectrum holes with energy-based spectrum sensing in dynamic CR systems and defines a formal measure for spectrum hole utilization. Specifically, this chapter presents a heuristic method for adapting the size of the spectrum sensing window that improves the probability of detection of an active PU as well as the actual utilization of spectrum holes when compared to a scheme with fixed sensing window size.

Chapter III presents optimizing the sensing performance of energy-based spectrum sensing with its sensing window size in dynamic scenarios and proposes methods for adapting the size of energy-based spectrum sensing window that improves the

Table 1: Organization of the dissertation.

<table>
<tr><td colspan="4">Chapter I
Introduction</td></tr>
<tr><td>Chapter II
Spectrum Hole Utilization in Dynamic Scenarios</td><td>Chapter III
Sensing Window Adaptation Techniques</td><td>Chapter IV
Optimizing Performance of Cooperative Sensing</td><td>Chapter V
Using HMM for Performance Evaluation of CR</td></tr>
<tr><td colspan="4">Chapter VI
Conclusions and Future Research</td></tr>
</table>

detection of PU signals as well as the utilization of spectrum opportunities, based on optimization between the probability of detection and spectrum hole utilization.

Chapter IV investigates the performance of cooperative sensing in dynamic CRs, by considering the time delay introduced by a CR fusion center (FC) for processing of the local sensing information. Specifically, this chapter introduces a new metric for evaluating the performance of cooperative sensing that includes both the probability of detection and the spectrum hole utilization, and presents numerical performance studies in dynamic scenarios where the activity of the PU changes in time and/or is affected by fading, such that optimal cooperative sensing performance can be achieved through the use of the metric.

Chapter V presents the use of HMM to describe the decision output of locally energy-based spectrum sensing which relies on accurate estimation of the noise energy as well as to describe the decision output of cooperative spectrum sensing which relies on local sensing information of cooperative CRs, and also proposes a HMM-based method that uses the history of sensing decisions to estimate the sensing performance in terms of the probabilities of detection and false alarm for both local and cooperative spectrum sensing in practical scenarios where radio environments are not perfect.

Chapter VI concludes all the work in this dissertation with final remarks and proposes some interesting directions for future research.

The results in this dissertation have been presented at various IEEE conferences and submitted for journal publication. The study presented in Chapter II was presented in part at the 2012 IEEE Radio and Wireless Symposium (RWS'12) [61] and also the 2012 IEEE International Conference on Communications (ICC'12) [62]. The

work presented in Chapter III was presented in part at the 2012 IEEE Global Telecommunications Conference (GLOBECOM'12) [63] and also submitted for publication in the IEEE Transactions on Wireless Communications [64]. The work presented in Chapter IV was submitted to the 2013 IEEE International Conference on Communications (ICC'13) [65]. The results presented in Chapter V was presented in part at the 44th Conference on Information Sciences and Systems (CISS'12) [66] and also submitted to the IEEE Communications Letters [67].

CHAPTER II

SPECTRUM HOLE UTILIZATION IN DYNAMIC SCENARIOS

Cognitive radio systems are expected to detect spectrum holes [3] or idle frequency bands that are not actively used by PU, to take advantage of them for providing service to SU, and to release them to the PU upon request. It should be noted that, taking advantage of a spectrum hole that is available only for a limited time (between two PU transmissions) involves two distinct steps: first, a spectrum sensing procedure is employed to determine the availability of the spectrum hole, followed by the actual utilization of the spectrum hole. Thus, the duration of the spectrum sensing procedure directly affects the actual utilization of the spectrum hole: the longer the duration of the spectrum sensing is, the shorter the actual utilization of the spectrum hole will be as illustrated in Fig. 4.

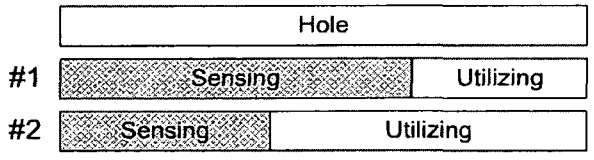

Fig. 4: Sensing versus hole utilization time for a spectral hole with finite duration.

In this chapter, energy detectors are considered for spectrum sensing and how the size of spectrum sensing window affects the utilization of spectrum holes is analyzed. A new method is proposed for adapting the size of the spectrum sensing window that improves both the detection of the spectrum holes as well as their actual utilization.

In this direction, it is noted that the related work in [68] which defines the spectrum hole utilization efficiency and the work in [57] which presents a method for adapting the sensing window size of the energy detector based on a sequential shift chi-square test (SSCT) but which does not consider actual utilization of spectrum holes. Other related references discussing adaptive spectrum sensing based on energy detection in dynamic scenarios are [58], which proposes the use of a side detector to monitor when PU become active and adjust the sensing window accordingly. Also, [59] which presents an experimental study of adaptive energy detection, and [69] studies maximizing spectrum utilization in relation with the data transmission duration, neither of which consider the impact of the sensing overhead in the utilization of spectrum holes. It is also noted that the work in [60] which analyzes the impact of the sensing overhead on the spectrum hole utilization, as well as the work in [30] which studies the tradeoff between the sensing duration and achievable CR throughput.

The rest of the chapter is organized as follows: the system model is introduced and the problem is formally stated in Section II.1, followed by the definition and analysis of spectrum hole utilization in Section II.2. The description of the proposed spectrum sensing technique with adaptive sensing window size is presented in Section II.3. In Section II.4, numerical results obtained from simulations are presented and concluding remarks are in Section II.5.

II.1 SYSTEM MODEL

The sequence $\{\mathcal{A}_i\}$ of spectrum holes is considered, as shown schematically in Fig. 5. The duration of spectrum hole $\mathcal{A}_i$ denoted by D_i is determined by the time

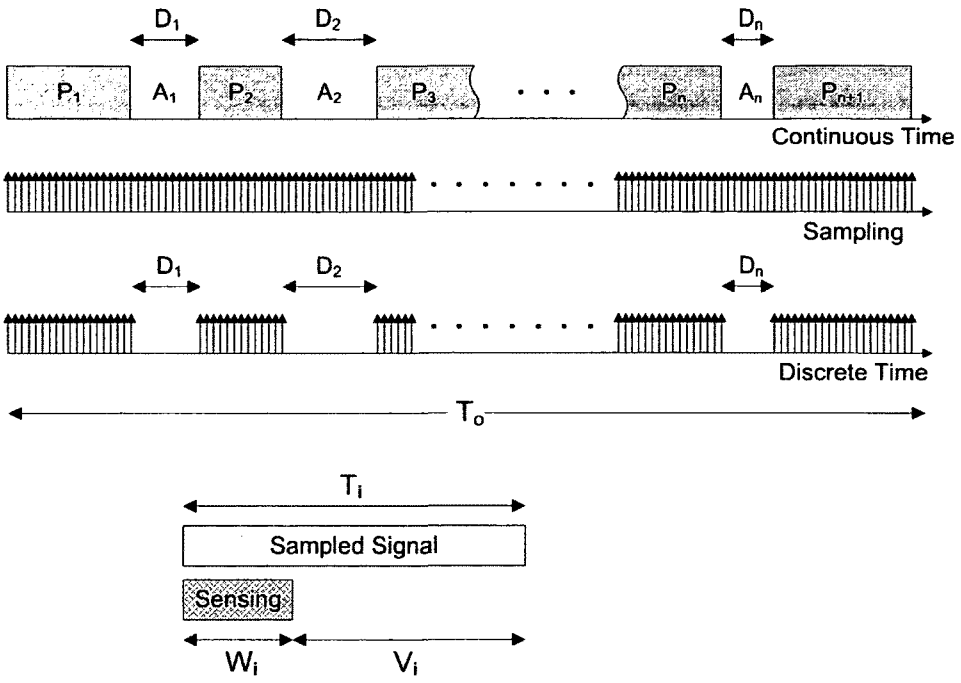

Fig. 5: Sensing spectrum holes with finite duration in discrete time domain.

interval between two consecutive PU transmissions. $\{\mathcal{P}_i\}$ denotes a sequence of PU transmissions and it is noted that appearance of $\mathcal{A}_i$ implies the absence of $\mathcal{P}_i$ during that period of time. It is assumed that the duration of a spectrum opportunity $\{\mathcal{A}_i\}$ is exponentially distributed with mean μ, and that the time between two consecutive spectrum opportunities has a Poisson distribution with mean τ.

Energy-based spectrum sensing is considered with a variable sensing window and is used to determine the availability of spectrum holes, as shown in Fig. 6, and the discrete received signal $y(n)$ is considered at the CR under the two hypotheses: H_0 and H_1 according to Eq. (I.2.1). Energy estimation and decision are made by using Eq. (I.2.2).

It is noted that the value of the sensing threshold λ used for making the decision is obtained from the desired performance of the energy detector by imposing specific

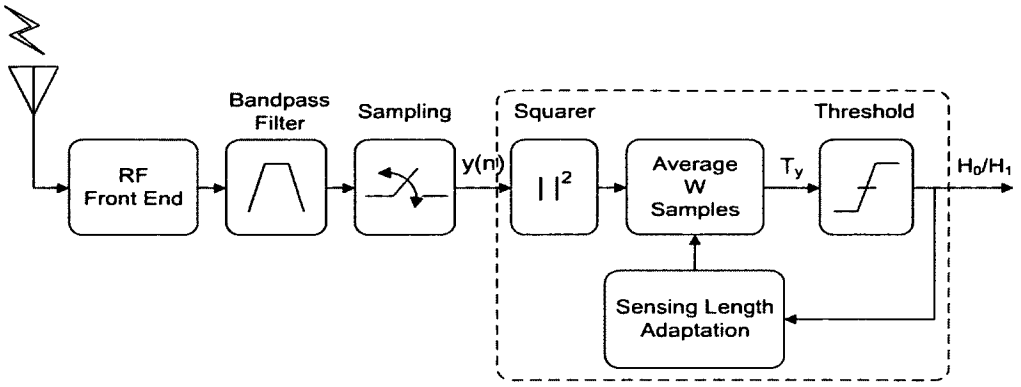

Fig. 6: Energy detector with adaptive sensing window.

values for P_d and/or P_f: a large value of the probability of detection P_d (or equivalently a small value of the probability of missed detection $P_m = 1 - P_d$) implies accurate detection of active PU transmissions, while a low value of the probability of false alarm P_f implies accurate detection of spectrum holes [30]. Thus, one can achieve both good detection performance and high utilization of the spectrum holes by setting the probability of missed detection $P_m = 1 - P_d$ equal to the probability of false alarm P_f. Using Eq. (I.2.5) and Eq. (I.2.6), the optimal threshold λ is then computed as follows:

$$P_m(\lambda) = P_f(\lambda) \tag{II.1.1}$$

$$1 - Q\Big(\frac{\lambda - m_1}{\sigma_1}\Big) = Q\Big(\frac{\lambda - m_0}{\sigma_0}\Big) \tag{II.1.2}$$

where m_0 and σ_0 denote the mean and standard deviation of the normal distribution corresponding to H_0, repectively, while m_1 and σ_1 denote the mean and standard deviation of the normal distribution corresponding to H_1, repectively, i.e.,

$$m_0 = \sigma_w^2, \quad \sigma_0 = \sigma_w^2\sqrt{2/W} \tag{II.1.3}$$

$$m_1 = (1+\gamma)\,\sigma_w^2, \quad \sigma_1 = \sigma_w^2\sqrt{(1+2\gamma)\,2/W} \tag{II.1.4}$$

Since $Q(-x) = 1 - Q(x)$ and $Q(x)$ is a monotonically decreasing function, it is then written:

$$Q\Big(\frac{-(\lambda - m_1)}{\sigma_1}\Big) = Q\Big(\frac{\lambda - m_0}{\sigma_0}\Big) \tag{II.1.5}$$

$$\frac{-\lambda + m_1}{\sigma_1} = \frac{\lambda - m_0}{\sigma_0} \tag{II.1.6}$$

$$\begin{aligned}
\lambda &= \frac{m_0\sigma_1 + m_1\sigma_0}{\sigma_0 + \sigma_1} \\
&= \frac{\sigma_w^4\sqrt{(1+2\gamma)\,2/W} + \sigma_w^4(1+\gamma)\sqrt{2/W}}{\sigma_w^2\sqrt{2/W} + \sigma_w^2\sqrt{(1+2\gamma)\,2/W}} \\
&= \frac{\sigma_w^2\big(\sqrt{1+2\gamma} + (1+\gamma)\big)}{1+\sqrt{1+2\gamma}} \\
&= \sigma_w^2\Big(1 + \frac{\gamma}{1+\sqrt{1+2\gamma}}\Big)
\end{aligned} \tag{II.1.7}$$

and after some algebra, we obtain:

$$\lambda = \sigma_w^2\Big(1 + \frac{\gamma}{1+\sqrt{1+2\gamma}}\Big) \simeq \begin{cases} \sigma_w^2\big(1+\gamma/2\big), & \gamma < 1 \\ \\ \sigma_w^2\big(1+\sqrt{\gamma/2}\big), & \gamma > 1 \end{cases} \tag{II.1.8}$$

It is noted that the threshold derived is not a function of the sensing window size W.

To study the utilization of spectrum holes in dynamic scenarios, it should be noted that the size of the spectrum sensing window, W, is a significant factor:

- If W is too short, the performance of energy estimation will be less accurate and may result in low P_d, especially in the low SNR regime.

- Extending W will result in more accurate estimation of the signal energy and improved sensing performance [70, 71]. However, if W becomes too long, it can result in missed detection of utilizable spectrum holes as shown in Fig. 7 for window #1.

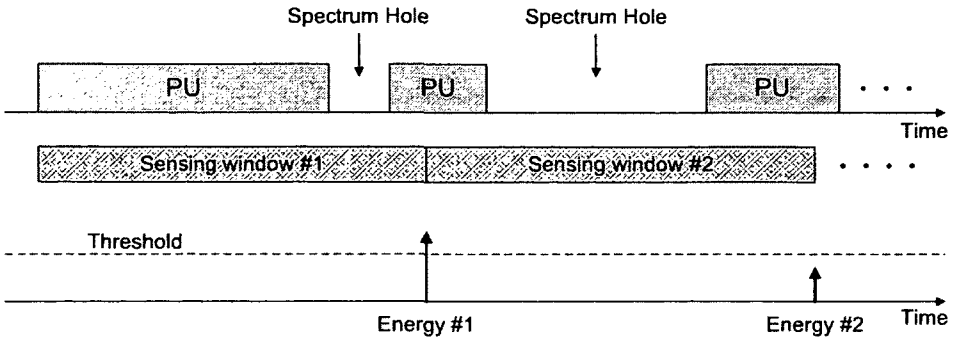

Fig. 7: Illustration of how a long spectrum sensing window may miss spectrum holes with short duration (sensing window #1), or not identify them in time for utilization (sensing window #2).

- Even when W correctly identifies a spectrum hole, the duration of the spectrum hole may be too short for the SU to utilize it before a new PU transmission requests again the spectrum, as shown in Fig. 7 for window #2.

Given the importance of the sensing window size W in reliably detecting active PU signals as well as in the actual utilization of available spectrum holes in dynamic scenarios, a formal measure is defined for spectrum hole utilization which depends on the size of the spectrum sensing window and on the actual duration of the spectrum hole. This chapter analyzes spectrum hole utilization that is influenced by the sensing window size and presents a novel technique for spectrum sensing which uses an adaptive sensing window with variable size as shown in Fig. 6. The proposed technique improves P_d and enables increased utilization of the spectrum holes.

II.2 SPECTRUM HOLE UTILIZATION

In this section, the effect of the sensing window size on the utilization of spectrum holes in dynamic scenarios is studied by assuming that the energy detector identifies

spectrum holes using a sensing window with variable size. In addition, it is assumed that the sequence of occurrences of active PU transmissions and spectrum holes is unknown to the CR system, and that the spectrum sensing is not perfect. Thus, spectrum holes identified by the CR system, along with their durations, may not be entirely accurate when compared to the actual spectrum holes, and the following parameters are introduced and shown in Fig. 5:

- T_i is the duration of spectrum hole i as identified by the CR system. It is noted that this may not coincide with the actual spectrum hole $\mathcal{A}_i$.
- W_i is the size of the sensing window used while detecting hole i.
- $V_i = T_i - W_i$ is the duration of spectrum hole i after the spectrum sensing is complete. It should be noted that V_i may not be 100% usable as it may contain portions of PU signal due to imperfections in the spectrum sensing.
- E_i is the overlap duration between V_i and the actual duration of spectrum hole during the same period of time. $E_i > 0$ represents the actual usable duration of the spectrum hole. $E_i = 0$ implies that no duration of the spectrum hole is available for utilization due to false detection or excessive sensing overhead.
- D_i is the actual duration of the i-th spectrum hole determined by the time interval between the i and $(i+1)$ PU transmissions.
- N_h denotes the cardinality of $\{\mathcal{A}_i\}$ determined within the given observation time T_o.
- N_{hd} denotes the total number of spectrum holes detected by the SU within the given observation time T_o. It is noted that N_{hd} is not necessarily equal to N_h.

In the above definitions, time and duration are taken in a discrete context (samples). The spectrum hole utilization measure is then formally defined as:

$$U_h = \frac{\sum_{i}^{N_{hd}} E_i}{\sum_{i}^{N_h} D_i} \tag{II.2.1}$$

and represents essentially the fraction of usable duration of spectrum holes correctly detected within the given observation period T_o. While $U_h < 1$ in practical systems, it may become very close to 1 in cases where all spectrum holes are much larger than the size of the sensing window.

Following the definition in Eq. (II.2.1), an analysis of how a sensing window size can influence the hole utilization is performed. Let $\boldsymbol{D}$ be the random variable representing the actual duration of spectrum hole which follows an exponential distribution with mean μ according to the system model. Thus the cumulative distribution function (cdf) and probability density function (pdf) for $\boldsymbol{D}$ are:

$$\left.\begin{aligned} F_D(D) &= 1 - \exp\left(-D/\mu\right) \\ f_D(D) &= (1/\mu)\, \exp\left(-D/\mu\right) \end{aligned}\right\}, \; D \geq 0 \tag{II.2.2}$$

Using the sensing window size W, the utilizable duration $\boldsymbol{U}$ is equal to:

$$\boldsymbol{U} = \boldsymbol{D} - W \tag{II.2.3}$$

$\boldsymbol{U}$ is also a random variable and $\boldsymbol{U}$ must be positive to be utilizable.

$$\begin{aligned} \mathrm{P}\{\boldsymbol{U} \leq U\} &= \mathrm{P}\{\boldsymbol{D} - W \leq U\} \\ &= \mathrm{P}\{\boldsymbol{D} \leq U + W\} \\ &= F_D(U + W) \end{aligned} \tag{II.2.4}$$

Therefore the cdf and pdf for $\boldsymbol{U}$ are then writen as:

$$\left.\begin{aligned} F_U(U) &= 1 - \exp\big(-(U+W)/\mu\big) \\ f_U(U) &= (1/\mu)\exp\big(-(U+W)/\mu\big) \end{aligned}\right\}, U \geq 0 \qquad \text{(II.2.5)}$$

$\bar{U}$ is denoted by the expected value of $\boldsymbol{U}$ which is derived as:

$$\begin{aligned} \bar{U} = \mathrm{E}\{\boldsymbol{U}\} &= \int_0^\infty U \frac{1}{\mu} \exp\big(-(U+W)/\mu\big)\,\mathrm{d}U \\ &= \Big[(U+\mu)\exp\big(-(U+W)/\mu\big)\Big]\Big|_0^\infty \\ &= \mu \exp\Big(-\frac{W}{\mu}\Big) \end{aligned} \qquad \text{(II.2.6)}$$

$\bar{U}$ represents the average utilizable duration of spectrum holes in ideal conditions which assume perfect detection. However, with some of the spectrum holes reported as used due to false alarm detections, the *actual* value of the average utilizable duration of the spectrum holes depends on the probability of false alarm P_f and is written as:

$$\begin{aligned} \tilde{U} &= \mu \exp\Big(-\frac{W}{\mu}\Big)\Big[1 - P_f\Big] \\ &= \mu \exp\Big(-\frac{W}{\mu}\Big)\left[1 - Q\left(\frac{\lambda - \sigma_w^2}{\sigma_w^2\sqrt{2/W}}\right)\right] \end{aligned} \qquad \text{(II.2.7)}$$

Using the definition of the spectrum hole utilization (II.2.1) and assuming that the observation time is large ($T_o \to \infty$) the analytical expression of the spectrum hole utilization is obtained in terms of the ratio of the average values of the corresponding random variables:

$$\begin{aligned} \hat{U}_h &= \frac{\tilde{U}}{E\{\boldsymbol{D}\}} = \frac{\tilde{U}}{\mu} \\ &= \exp\Big(-\frac{W}{\mu}\Big)\left[1 - Q\left(\frac{\lambda - \sigma_w^2}{\sigma_w^2\sqrt{2/W}}\right)\right] \end{aligned} \qquad \text{(II.2.8)}$$

The equation (II.2.8) shows that the expected value of the spectrum hole utilization measure depends on the size of the sensing window, the average duration of spectrum holes, and the variance of the noise.

II.3 ADAPTIVE SENSING WINDOW ALGORITHM

Motivated by the observation that spectrum hole utilization depends on the size of the sensing window, in this section an energy-based sensing method is proposed with adaptive sensing window whose parameters are defined as follows:

- W_{sen} is the actual size of the sensing window.
- W_{min} denotes the minimum allowed size of sensing window, and assures that if $W_{sen} \geq W_{min}$, the SU is able to detect PU signal.
- W_{max} denotes the maximum allowed size of the sensing window. If the $W_{sen} > W_{max}$ the performance of energy sensing has no more improvement.

In the proposed method, the sensing window size varies between a lower bound W_{min} and an upper bound W_{max}, and is adapted to reduce the possibility of missing spectrum holes with short duration as follows:

- W_{sen} is initialized with W_{max} to ensure that maximum accuracy is used to detect active PU signals.
- If $W_{sen} > W_{min}$ during an interval when a PU is active the sensing window size is decreased by W_{min} to reduce possibility of missing an incoming spectrum hole with a small duration. However, W_{sen} will not decrease below W_{min}.

- During an interval when no PU is active $W_{sen} = W_{max}$ to have high performance in detecting an incoming PU signal.

Using this approach an algorithm was implemented by using variable *window_count* to keep track of the number of consecutive windows with active PU signals, and variable α as the number of consecutive windows after which the size of the sensing window is decreased by W_{min}. The flowchart of the proposed algorithm with adaptive sensing window is shown in Fig. 8.

The proposed algorithm can also be modeled by the state transition diagram shown in Fig. 9 with two states denoting the *absence*, respectively *presence* of a PU signal. More precisely, the *absence* state corresponds to the case in which a spectrum hole is available and in this case the size of the sensing window is kept maximum, while the *presence* state is the state in which a PU signal is detected, and the size of the sensing window is uniformly decreased until W_{min} is reached or kept at this value.

II.4 SIMULATION AND NUMERICAL RESULTS

In this section, numerical results obtained from simulations are presented to illustrate the performance of the proposed algorithm for spectrum sensing with adaptive sensing window size and compare it with that of a conventional energy detector with fixed size of the spectrum sensing window. The following simulation setup is considered: the minimum and maximum size of the sensing window are set to $W_{min} = 100$ and $W_{max} = 1000$ samples, respectively. The number of consecutive sensing windows after which the size of the spectrum sensing window is decreased is taken to be $\alpha = 1$, 2, and 5, respectively.

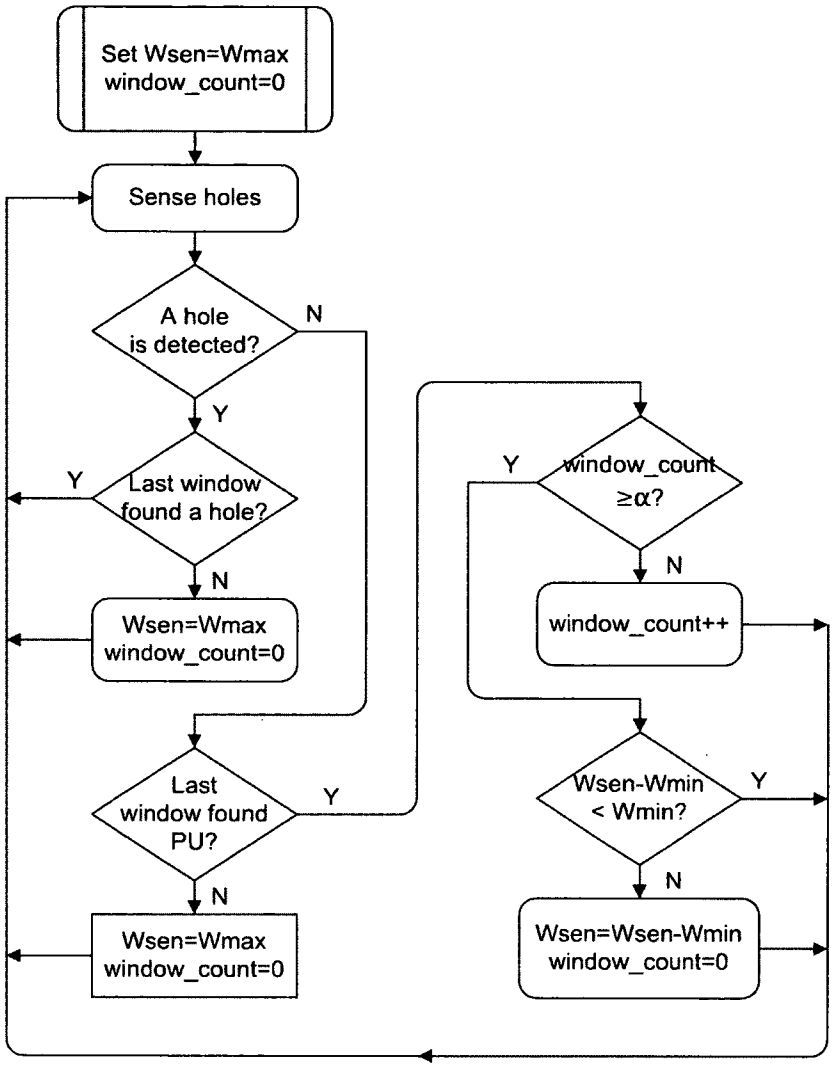

Fig. 8: Flowchart of the proposed algorithm for spectrum sensing with adaptive window size.

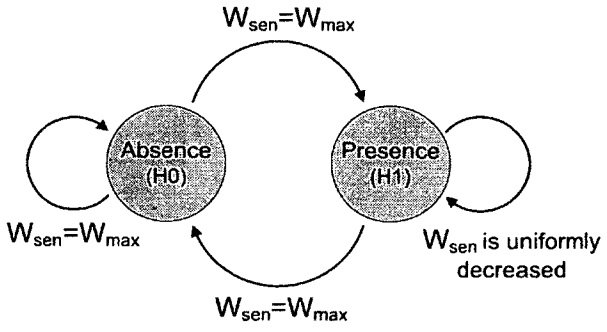

Fig. 9: State transition diagram modeling the algorithm.

During the simulations the SNR is varied and the performance of the proposed adaptive spectrum sensing technique is evaluated in terms of the spectrum hole utilization measure U_h, as well as in terms of the probability of detection P_d. Empirically, the spectrum hole utilization U_h is determined by Eq. (II.2.1) while P_d is calculated from:

$$P_d = \frac{N'_{pu}}{N_{pu}} \tag{II.4.1}$$

where N'_{pu} and N_{pu} represent the total duration of PU transmissions correctly identified by the spectrum sensing procedure and the actual duration of total PU transmissions, respectively, assuming sufficiently large observation time T_o. The analytical expressions (II.2.8) and (I.2.5) are also used to evaluate the hole utilization and probability of detection, respectively, when a fixed sensing window size is used.

In the first simulation, the arrival rate and duration time describing the appearance of a spectrum hole becomes available are taken as $\tau = 140$ and $\mu = 30$ symbol intervals, respectively. The results are shown in Fig. 10. From Fig. 10(a), it is noted that when energy detection with fixed window size $W_{sen} = W_{min}$ is used the spectrum holes are utilized more efficiently than when energy detection with $W_{sen} = W_{max}$ is used, especially at high SNR values, and the simulated results agree with the analytical results. However, when $W_{sen} = W_{min}$ the probability of detection of the PU is lower than when $W_{sen} = W_{max}$ at low SNR values as seen from the corresponding curves in Fig. 10(b). By comparison, the proposed method for spectrum sensing with adaptive sensing window size improves the utilization of spectrum holes compared to the fixed sensing window size scenario with $W_{sen} = W_{max}$ while having comparable probability of detection (higher than when the fixed sensing window size with

$W_{sen} = W_{min}$). As α decreases, the spectrum hole utilization improves while the probability of detection does not change significantly.

In the second simulation, the spectrum hole opportunity is considered to be less dynamic than the first simulation by setting $\tau = 800$ and $\mu = 240$ symbol intervals. The results are shown in Fig. 11. With the considered SNR range, Fig. 11(a) shows that energy detection with fixed sensing size $W_{sen} = W_{min}$ does not always give higher hole utilization than that with fixed sensing size $W_{sen} = W_{max}$ like in the the first simulation and the simulated results agree with the analytical results. According to Eq. (II.2.8), this is due to the fact that when the spectrum sensing overhead is increased, probability of false alarm can be improved for low SNR values. According to the average duration of holes μ, when most spectrum holes are likely to be much larger than the sensing window size, thus more utilization of holes can be obtained. However, if spectrum holes are not likely to be larger than the sensing window size, like in the first simulation, the hole utilization would be reduced since the increased sensing size causes missed detection of small holes.

The results in this scenario also show that the proposed adaptive sensing method can improve the hole utilization when compared to the fixed sensing window size with $W_{sen} = W_{min}$ and $W_{sen} = W_{max}$ at SNR ≤ -2.5 dB and SNR ≥ -7.5 dB, respectively, while keeping probability of detection comparable to that for fixed sensing window size with $W_{sen} = W_{max}$ as seen in Fig. 11(b). The proposed method can also result in high hole utilization close to 100% which is comparable to that of the fixed sensing size with $W_{sen} = W_{min}$ for high SNR values. Moreover the three α values considered do not significantly give different results in this scenario.

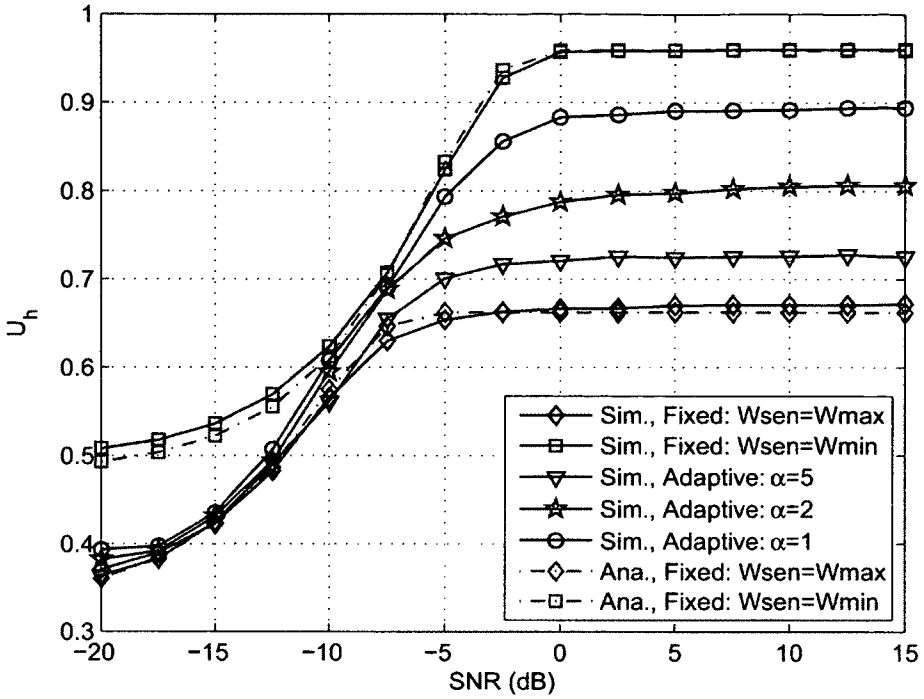

(a) Spectrum hole utilization.

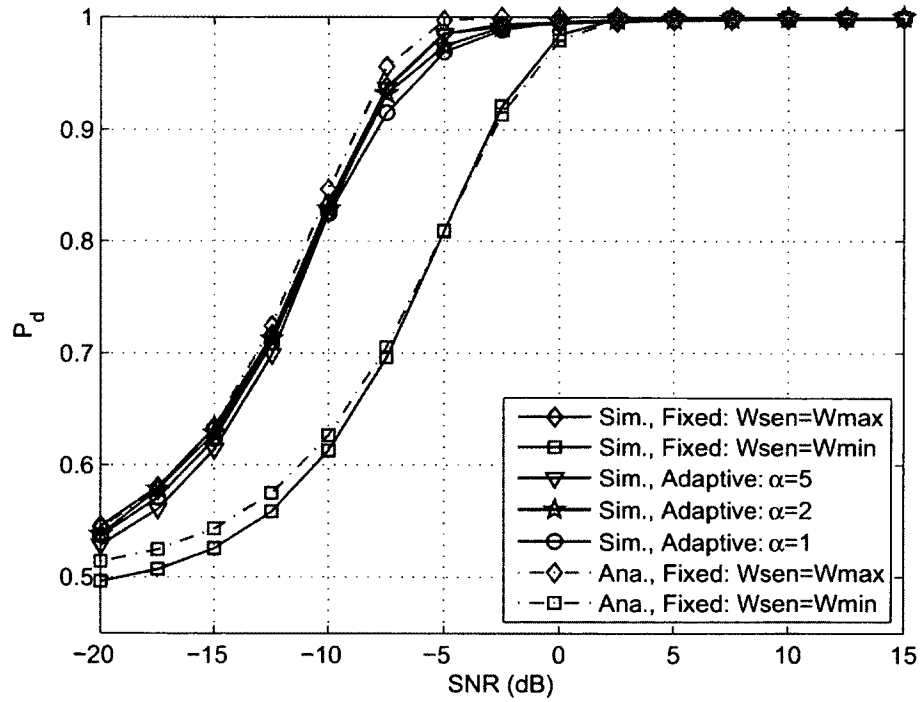

(b) Probability of detection.

Fig. 10: Spectrum hole utilization and probability of detection vs. SNR with fixed and variable size of the sensing window for $\tau = 140$ and $\mu = 30$.

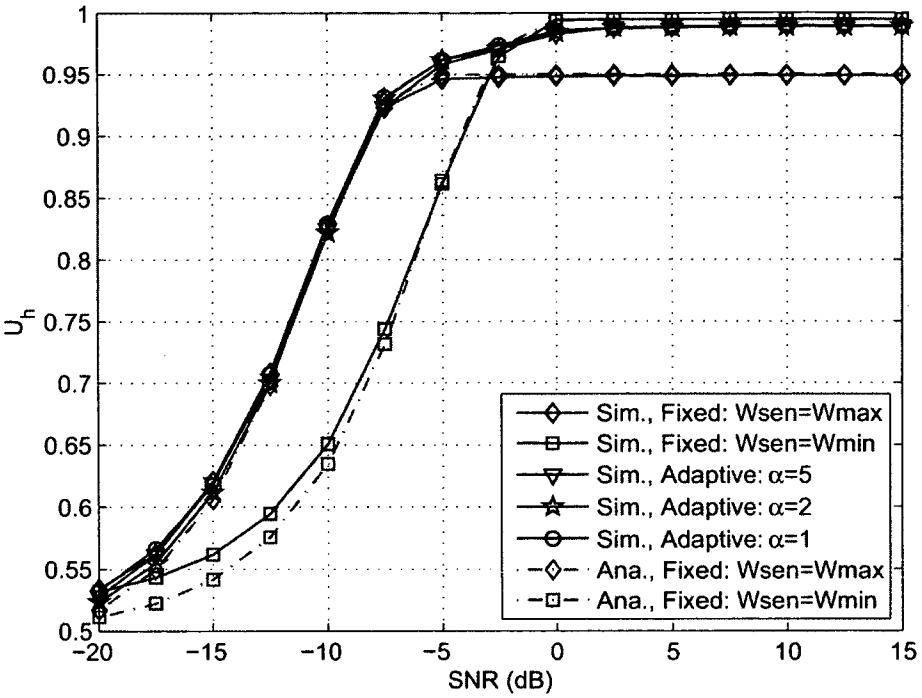

(a) Spectrum hole utilization.

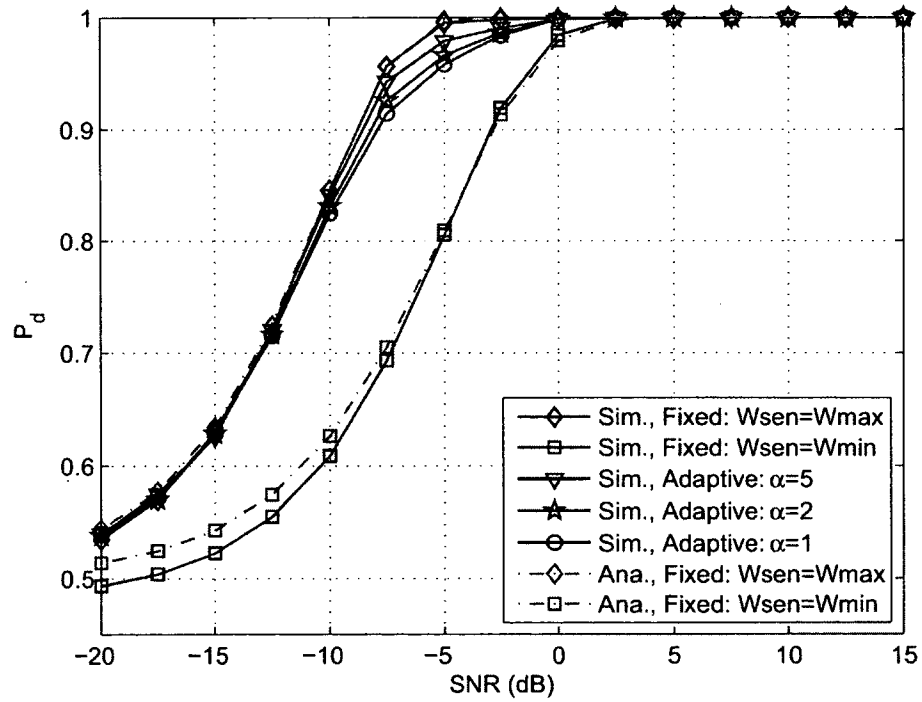

(b) Probability of detection.

Fig. 11: Spectrum hole utilization and probability of detection vs. SNR with fixed and variable size of the sensing window for $\tau = 800$ and $\mu = 240$.

From these results, it can be noted that using the proposed method with adaptive sensing window is particularly useful for SNR values above -10 dB comparing to the fixed sensing size methods with $W_{sen} = W_{min}$ and $W_{sen} = W_{max}$ in terms of both hole utilization and probability of detection.

II.5 CHAPTER SUMMARY

This chapter studies utilization of spectrum holes and proposes a new method for spectrum sensing that improves it in dynamic scenarios. This method uses energy detection with an adaptive sensing window and improves the spectrum hole utilization over the conventional energy detection with fixed spectrum sensing window. The performance of the proposed method was illustrated with numerical results obtained from simulations which show how the size of the sensing window, SNR, and average duration of spectrum holes affect the performance of detection and spectrum hole utilization. The tradeoffs related to adaptation of the sensing window size are also discussed.

The proposed method with adaptive sensing window appears to be useful for SNR values above -10 dB where detection of an active PU signal can be accomplished reliably with a short sensing window.

CHAPTER III

SENSING WINDOW ADAPTATION FOR IMPROVED SPECTRUM UTILIZATION

Chapter II has discussed that the duration of the spectrum sensing procedure is an overhead factor that affects the actual utilization of the spectrum in dynamic CR systems and also proposed an energy-based spectrum sensing algorithm with adaptive sensing window size, that can improve the spectrum hole utilization and probability of detection, when compared to the conventional energy-based sensing with fixed sensing window.

This chapter extends the work in Chapter II by presenting two new methods that improve detection of PU signals as well as utilization of spectrum opportunities over the conventional fixed sensing scheme and the adaptive sensing method presented in Chapter II as well. The two proposed methods use knowledge of the average duration of spectrum opportunities and adapt the size of the sensing window to jointly maximize the probability of detection and the spectrum hole utilization.

This chapter is organized as follows: Section III.1 presents the system model of this study. Section III.2 proposes the adaptive sensing method that optimizes its sensing window size with adaptive weighting followed by Section III.3 which presents the adaptive sensing method based on optimizing the sensing window size with a heuristic algorithm. Numerical results obtained from simulation are presented in Section III.4 and finally, the results of the study are concluded in Section III.5.

III.1 SYSTEM MODEL

Similar to Chapter II, the PU activity is considered to have a sequence of PU transmissions and spectrum holes, as shown schematically in Fig. 5. However, in this study, a more practical PU activity in dynamic scenarios is considered by assuming that the duration D_i of a spectrum opportunity $\{\mathcal{A}_i\}$ and that the time between two consecutive spectrum opportunities are exponentially distributed with mean μ and τ, respectively, which corresponds to a dynamic occupancy of the spectrum by a PU as discussed in [72].

It is assumed that the received signal $y(n)$ at the CR in a discrete time domain is corrupted by AWGN and is tested under two hypotheses: H_0 and H_1 according to Eq. (I.2.1). It is considered that the SU uses energy-based spectrum sensing with a variable sensing window size W that is used to determine the availability of spectrum holes and the energy detector uses an adaptive sensing threshold λ that is computed by Eq. (II.1.8) corresponding to the SNR γ received at the SU. The probability of detection P_d and spectrum hole utilization U_h, introduced in Chapter I and respectively Chapter II, are also taken into account as performance measures for evaluating the proposed methods.

III.2 OPTIMIZING SENSING WINDOW WITH ADAPTIVE WEIGHTING

Motivated by the fact that adapting the duration of the sensing procedure to provide reliable detection of spectrum opportunities with optimized sensing time will enhance the utilization of spectrum holes in dynamic CR systems, a new method

for adapting the size of energy-based spectrum sensing window to the actual SNR is proposed that improves both the detection of the spectrum holes as well as their actual utilization. Fig. 12 illustrates block diagram of the proposed sensing method, in which the sensing window adaptation process uses the channel state information, e.g., the received SNR and average duration of spectrum opportunities, at the energy detector to compute an optimal value on the sensing window size, that can optimally improve both the probability of detection and spectrum hole utilization.

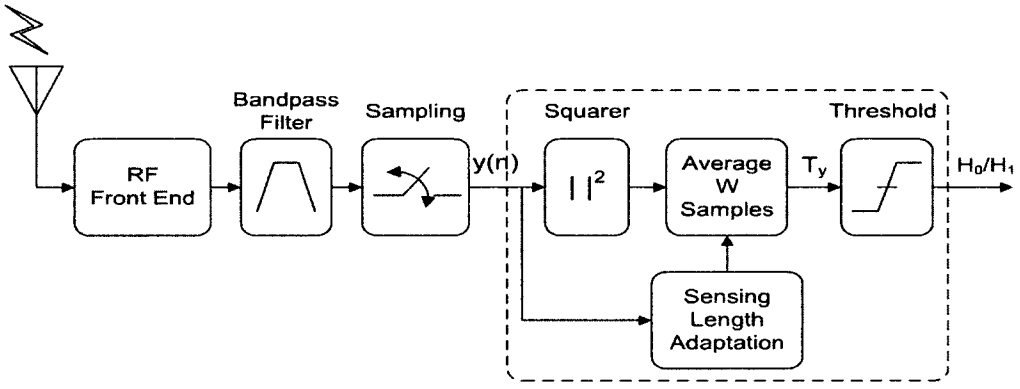

Fig. 12: Energy detector with adaptive sensing window based on weighted adaptation.

In order to introduce the proposed technique for adapting the sensing window size W, the effect of W on the spectrum hole utilization $\hat{U}_h$ and on the probability of detection P_d is evaluated for spectrum holes with finite duration. Using Eq. (I.2.5) and Eq. (II.2.8), P_d and $\hat{U}_h$ are plotted versus W for different SNR values in Fig. 13, by considering that the received SNRs are above the SNR wall [73] where increasing the sensing length can improve sensing performance.

The plots clearly show that increasing W improves the probability of detection, and up to a certain value, spectrum hole utilization as well. However, when W

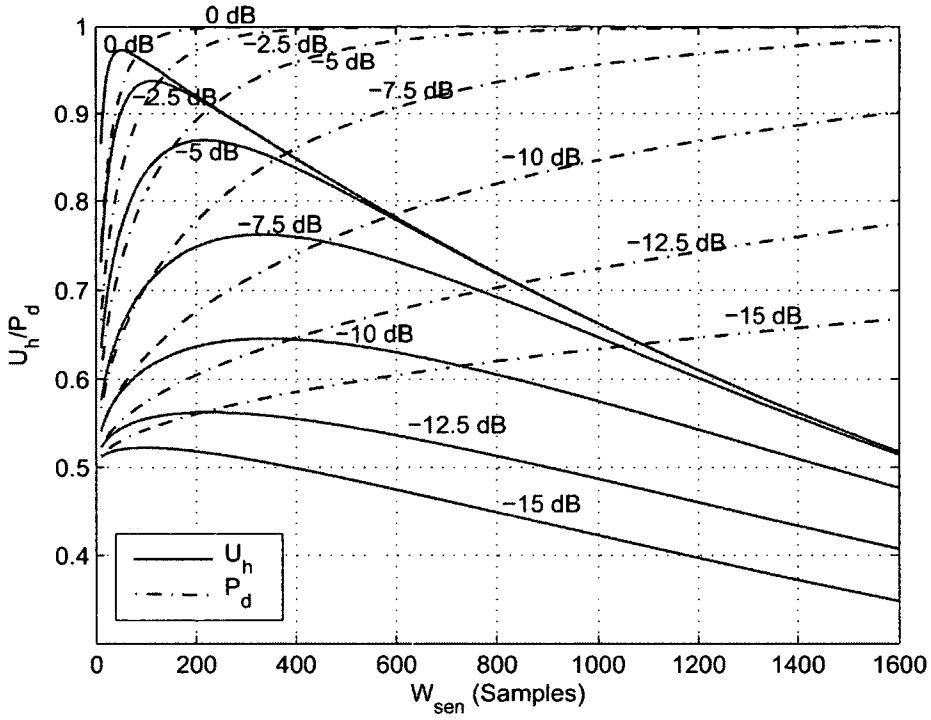

Fig. 13: Illustration of how the size of sensing window can effect the spectrum hole utilization and probability of detection at different SNR values based on an average duration of spectrum holes.

becomes too long, the spectrum hole utilization starts decreasing, and it is noted that there is an optimal sensing size W that maximizes the spectrum hole utilization. This indicates that using a fixed size for the sensing window would limit the probability of detection and utilization of spectrum holes, and that adapting W to maximize $\hat{U}_h$ for the given SNR can improve over performance. With these perspectives, the following parameters are defined:

- W_{sen} is the actual size of the sensing window.
- W_{min} denotes the minimum allowed size of sensing window, and assures that if $W_{sen} \geq W_{min}$, the SU is able to detect PU signal.

- W_{max} denotes the maximum allowed size of the sensing window. W_{max} is used to limit degradation of spectrum hole utilization when the sensing length becomes too long.

- W_u and W_d denote the sensing window sizes that maximize the hole utilization and the probability of detection, respectively with the contraint $W_{min} \leq W_u$, $W_d \leq W_{max}$.

It is noted that all the above parameters are positive integers, i.e, $\in \mathbb{Z}^+$. In this approach, the sensing window size W_{sen} varies between a lower bound W_u and an upper bound W_d in order to optimize for the spectrum hole utilization and the probability of detection for different received SNR values. It can be written:

$$W_{sen} = \left\lfloor \beta W_u + (1-\beta) W_d \right\rfloor \tag{III.2.1}$$

where $\beta \in [0,1]$ denotes the weight that compromises between W_u and W_d and $\lfloor x \rfloor$ denotes the floor function, i.e., the largest integer that is less than or equal to x. The value W_u is obtained by solving $\frac{\partial \hat{U}_h}{\partial W} = 0$ to identify the critical points of $\hat{U}_h$. According to Eq. (II.1.8), it is noted that the threshold λ is not a function of W. From Eq. (II.2.8), it can be written:

$$\begin{aligned} \hat{U}_h &= \exp\Big(-\frac{W}{\mu}\Big)\left[1 - Q\left(\frac{\lambda - \sigma_w^2}{\sigma_w^2\sqrt{2/W}}\right)\right] \\ &= \exp\Big(-\frac{W}{\mu}\Big)\left[1 - Q\Big(\Omega\sqrt{W}\Big)\right] \end{aligned} \tag{III.2.2}$$

where $\Omega = (\lambda - \sigma_w^2)/\sigma_w^2\sqrt{2}$. In order to determine the partial derivative $\frac{\partial \hat{U}_h}{\partial W}$, the formula of the derivative for the erfc function [74] is used to obtain the derivative for

the Q function as follows:

$$\frac{d}{d\,z}\,\mathrm{exfc}(z) = -\frac{2}{\sqrt{\pi}}\,\exp\left(-z^2\right) \tag{III.2.3}$$

$$Q(z) = \frac{1}{2}\,\mathrm{erfc}(\frac{z}{\sqrt{2}}) \;\rightarrow\; \mathrm{erfc}(z) = 2\,Q(\sqrt{2}z)$$

$$\frac{d}{d\,z}\,\mathrm{exfc}(z) = \frac{d}{d\,z}\,2\,Q(\sqrt{2}z) \;\rightarrow\; \frac{d}{d\,z}\,Q(\sqrt{2}z) = -\frac{1}{\sqrt{\pi}}\,\exp\left(-z^2\right)$$

$$\frac{d}{d\,z}\,Q(z) = -\frac{1}{\sqrt{2\pi}}\,\exp\left(-\frac{z^2}{2}\right) \tag{III.2.4}$$

Now,

$$\begin{aligned}\frac{\partial \hat{U}_h}{\partial W} &= \exp\Big(-\frac{W}{\mu}\Big)\frac{\partial}{\partial W}\Big[1-Q\big(\Omega\sqrt{W}\big)\Big] \\ &\quad + \Big[1-Q\big(\Omega\sqrt{W}\big)\Big]\frac{\partial}{\partial W}\exp\Big(-\frac{W}{\mu}\Big) \\ &= \exp(-\frac{W}{\mu})\Bigg[\frac{\Omega}{\sqrt{8\pi W}}\exp(-\frac{\Omega^2 W}{2}) \\ &\quad - \frac{1}{\mu}\Big[1-Q\big(\Omega\sqrt{W}\big)\Big]\Bigg] \;=\; 0\end{aligned} \tag{III.2.5}$$

It is noted that Eq. (III.2.5) is satisfied when $W \rightarrow \infty$ or W is equal to a finite value that achieves:

$$\Delta(W) \triangleq \frac{\Omega}{\sqrt{8\pi W}}\exp(-\frac{\Omega^2 W}{2}) - \frac{1}{\mu}\Big[1-Q\big(\Omega\sqrt{W}\big)\Big] = 0 \tag{III.2.6}$$

However, since $W \in \mathbb{Z}^+$, an integer W_u can be found such that $\Delta(W_u) \approx 0$. With the constraint $W_{min} \leq W_u \leq W_{max}$, we round $W_u = W_{min}$ if $W_u < W_{min}$ and $W_u = W_{max}$ if $W_u > W_{max}$.

To compute W_d, it is noted that the probability of detection is expressed in terms of the standard Q-function, for which we have that $Q(-\infty) = 1$. Hence,

$$\lim_{W\rightarrow\infty} P_d(W) = 1 \tag{III.2.7}$$

According to this expression, W may need to be very large to obtain P_d very close to 1. Setting a tolerance δ for which we can approximate $1-\delta \approx 1$, e.g., $1-\delta = 0.999$, the size of the sensing window can significantly be reduced. Using this perspective, W_d can be computed from Eq. (I.2.5) as follows:

$$Q^{-1}(P_d) = \frac{\lambda - (1+\gamma)\,\sigma_w^2}{\sigma_w^2\sqrt{(1+2\gamma)\,2/W_d}}$$

$$\sqrt{W_d} = \left(\frac{\sigma_w^2\sqrt{(1+2\gamma)\,2}}{\lambda-(1+\gamma)\,\sigma_w^2}\right)Q^{-1}(P_d)$$

$$W_d = 2(1+2\gamma)\left(\frac{Q^{-1}(1-\delta)\sigma_w^2}{\lambda-(1+\gamma)\sigma_w^2}\right)^2 \qquad \text{(III.2.8)}$$

where $Q^{-1}(.)$ denotes the inverse Q-function. Since the sensing window must be an integer:

$$W_d = \left\lfloor 2(1+2\gamma)\left(\frac{Q^{-1}(1-\delta)\sigma_w^2}{\lambda-(1+\gamma)\sigma_w^2}\right)^2 \right\rfloor \qquad \text{(III.2.9)}$$

However, with the constraint $W_{min} \leq W_d \leq W_{max}$, we round $W_d = W_{min}$ if $W_d < W_{min}$ and $W_d = W_{max}$ if $W_d > W_{max}$.

In order to optimize for the sensing window W_{sen}, the weight β is considered to be adaptive and defined as:

$$\beta = \frac{\varsigma_1}{\varsigma_1+\varsigma_2} \qquad \text{(III.2.10)}$$

where

$$\varsigma_1 \triangleq \hat{U}_h(W_u) + P_d(W_u) \qquad \text{(III.2.11)}$$

$$\varsigma_2 \triangleq \hat{U}_h(W_d) + P_d(W_d) \qquad \text{(III.2.12)}$$

It is noted that $\hat{U}_h(.)$ and $P_d(.)$ are a function of the sensing window and are computed by using Eq. (II.2.8) and Eq. (I.2.5), respectively.

Thus far, an adaptive sensing window method for energy detection is proposed using Eq. (III.2.1) and the corresponding expressions that can optimize the sensing

performance in terms of the spectrum hole utilization as well as in terms of the probability of detection for the received SNR that fluctuates.

III.3 OPTIMIZING SENSING WINDOW WITH HEURISTIC ALGORITHM

Similar to the method presented in Section III.2, in this method, an energy-based spectrum sensing that adapts the size of the sensing window is also considered to provide reliable detection of an active PU and spectrum opportunities with optimal sensing time in dynamic scenarios. The key concept is that, here, the sensing method presented in the previous section is combined with the method presented in Chapter II such that the detector can improve the sensing performance by computing an optimal size of the sensing window. The block diagram of the proposed method is shown in Fig. 14 in which the sensing window adaptation procedure uses the channel state information at the SU as well as the decision output of the energy detector to compute and adapt the duration of the sensing procedure.

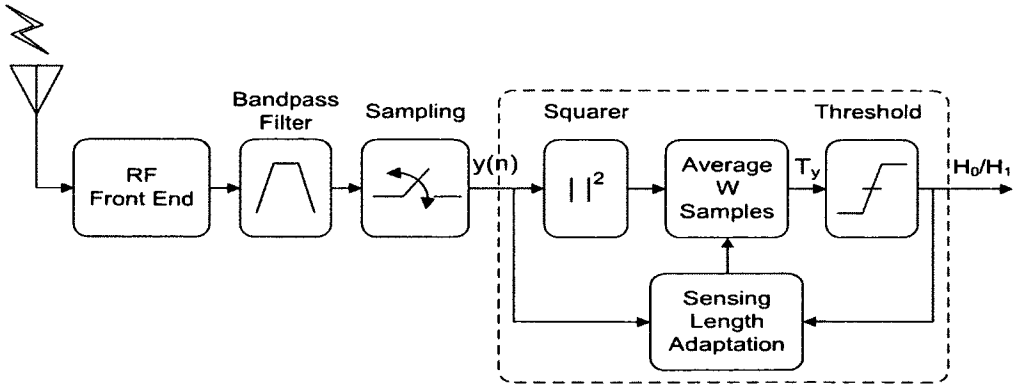

Fig. 14: Energy detector with adaptive sensing window based on heuristic adaptation.

As discussed in the previous section, the dependence of $\hat{U}_h$ and P_d on the size of the sensing window shown in Fig. 13 indicates that using an energy detector with a fixed sensing window size may limit the spectrum sensing performance of the CR system and that increasing the size of the sensing window improves the probability of detection. There is also an optimal sensing size that maximizes the spectrum hole utilization for a given SNR value. With these perspectives, the proposed spectrum sensing technique is presented by formally defining the following parameters:

- W_{sen} is the actual size of the sensing window.
- W_{min} denotes the minimum size allowed for the sensing window, and ensures that as long as $W_{sen} \geq W_{min}$, the CR has the minimum acceptable performance of PU detection.
- W_{max} denotes the maximum allowed size of the sensing window, and is used to limit the degradation of the spectrum hole utilization when the sensing window becomes too long.
- W_{lo} and W_{up} denote the lower bound and upper bound, respectively, of the sensing window, such that $W_{min} \leq W_{lo}, W_{up} \leq W_{max}$.

It is noted that all these parameters are positive integers denoting the size of the sensing window in terms of the number of samples.

In this proposed method, the sensing window W_{sen} varies between W_{lo} and W_{up} whose values depend on the received SNR and average duration of spectrum holes. The parameter W_{lo} is determined from:

$$W_{lo} = \underset{W_{min} \leq W \leq W_{max}}{\arg\max} \hat{U}_h(W) \tag{III.3.1}$$

whose solution can be found by solving for the necessary condition $\partial \hat{U}_h / \partial W = 0$. However, as derived previously, an integer W' can be found such that $\Delta(W')$ given in Eq. (III.2.6) can be close to 0 and then the condition can be approximately satisfied. Hence, W_{lo} can be obtained from:

$$W_{lo} = \underset{W_{min} \leq W \leq W_{max}}{\arg\min} \quad \Delta(W) \tag{III.3.2}$$

Furthermore, the parameter W_{up} is determined by:

$$W_{up} = \underset{W_{min} \leq W \leq W_{max}}{\arg\max} \quad P_d(W) \tag{III.3.3}$$

Similar to computing W_d in the previous section, W_{up} is computed by setting a tolerance δ in the vicinity of 1 such that P_d is set to $1 - \delta \approx 1$ in order to considerably reduce the size of the sensing window while it still maintains good PU detection with P_d very close to 1. With this perspective, W_{up} is then computed as:

$$W_{up} = \left\lfloor 2(1+2\gamma) \left[\frac{Q^{-1}(1-\delta)\sigma_w^2}{\lambda - (1+\gamma)\sigma_w^2} \right]^2 \right\rfloor \tag{III.3.4}$$

Noting also the constraint $W_{min} \leq W_{up} \leq W_{max}$, one must set $W_{up} = W_{min}$ if $W_{up} < W_{min}$, respectively $W_{up} = W_{max}$ if $W_{up} > W_{max}$.

In order to reduce the possibility of missing utilizable spectrum holes with short duration, the size of the sensing window should be adapted as follows:

- W_{sen} is initialized with W_{up} to ensure that maximum accuracy is used to detect active PU signals.
- If $W_{sen} > W_{lo}$ during an interval when a PU is active the sensing window size is decreased by W_{lo} in order to reduce possibility of missing an incoming utilizable spectrum hole with small duration. However, W_{sen} will not decrease below W_{lo}.

- During an interval when no PU is active $W_{sen} = W_{up}$ to have high performance in detecting an incoming PU signal.

By combining the concept of the method presented in Chapter II with the parameters defined, a new heuristic algorithm for spectrum sensing with adaptive sensing window is presented, which also uses variable *window_count* to keep track of the number of consecutive windows with active PU signals, and variable α as the number of consecutive windows after which the size of the sensing window is decreased by W_{lo}. The algorithm is described by using the flowchart shown in Fig. 8 and the transition diagram shown in Fig. 9 but the parameters W_{min} and W_{max} are replaced with W_{lo} which is computed from Eq. (III.3.2) and respectively W_{up} which is computed by Eq. (III.3.4). Considering the transition diagram in Fig. 9, the size of the sensing window in this proposed algorithm is maintained at its maximum value W_{up} in the case of *absence* state, while the size of the sensing window is decreased until W_{lo} is reached or maintained at this lowest acceptable value in the case of *presence* state.

III.4 SIMULATION AND NUMERICAL RESULTS

In this section numerical results obtained from simulations are presented to illustrate the performance of the two methods presented in this chapter for spectrum sensing with adaptive sensing window size and compare it with that of a conventional energy detector with fixed size of the spectrum sensing window. Similar to the simulation in Chapter II, the simulation in this study is set up as follows: the minimum and maximum size of the sensing window are set to $W_{min} = 100$ and $W_{max} = 1000$ samples, respectively. During the simulations the SNR is varied and the performance

of the proposed spectrum sensing technique with adaptive sensing window is evaluated in terms of the hole utilization measure U_h, as well as in terms of the probability of detection P_d.

Empirically, the performance measures U_h and P_d are computed by Eq. (II.2.1) and respectively Eq. (II.4.1) while analytically, the performance measures are computed by using Eq. (II.2.8) and Eq. (I.2.5), respectively, when the adaptive sensing window and a fixed sensing window size are used. In order to discuss the performance of all the methods proposed, the methods presented in Section II.3, Section III.2, and Section III.3 are referred to as *Method#1*, *Method#2*, and *Method#3*, respectively and the simulations are presented in the following subsections.

Simulation for Adaptive Sensing with Method#2

Two simulation scenarios are performed corresponding to two different dynamics of the PU activity, as follows. In the first simulation, the average durations describing the PU activity are taken as $\tau = 140$ and $\mu = 30$ symbol intervals, respectively. The results are shown in Fig. 15. From Fig. 15(a), it is noted that when energy detectors with fixed window size $W_{sen} = W_{min}$ and $W_{sen} = W_{max}$ are used, the results are the same as those plotted in Fig. 10(a) for which it is recalled that the fixed sensing window size scenario with $W_{sen} = W_{min}$ yields better spectrum hole utilization but poorer probability of detection than the fixed sensing window size scenario with $W_{sen} = W_{max}$. By comparison, using Method#2 for adaptive sensing window size improves the utilization of spectrum holes compared to the fixed sensing window size scenario with $W_{sen} = W_{max}$ while having comparable probability of detection with a fraction less than 0.05.

Moreover, the proposed adaptive sensing window is also studied with a fixed value of the weight β instead of the adaptive one computed from Eq. (III.2.10). In this scenario, β is fixed to 0.4, 0.2, and 0, respectively and it is noted that $\beta \rightarrow 0$ implies that $W_{sen} \rightarrow W_d$ which means that the sensing performance is optimized in terms of the probability of detection rather than in terms of the hole utilization. The plots show that when β decreases the probability of detection can be slightly improved at the expense of significantly degrading the spectrum hole utilization. In comparison with Method#1, Method#2 obviously has better performance in terms of spectrum hole utilization than Method#1, especially in the high SNR regime where the PU signal variance is larger than the noise variace.

In the second simulation, the PU activity is considered to be less dynamic than in the first simulation by setting $\tau = 800$ and $\mu = 240$ symbol intervals. The results are shown in Fig. 16(a) and (b) for the spectrum hole utilization and respectively the probability of detection, which look similar to Fig. 11(a) and respectively (b) in Section II.4 and the simulated results agree with the analytical results. Method#2 shows to apparently improve the spectrum utilization when compared to the fixed sensing size scenarios and also has slightly improved utilization of spectrum holes over Method#1 for the high SNR values.

From these results, it can be concluded that using Method#2 for energy-based sensing with adaptive sensing window can efficiently improve the sensing performance measures when compared to the method with fixed sensing size and that Method#2 outperforms Method#1, especially in highly dynamic scenarios.

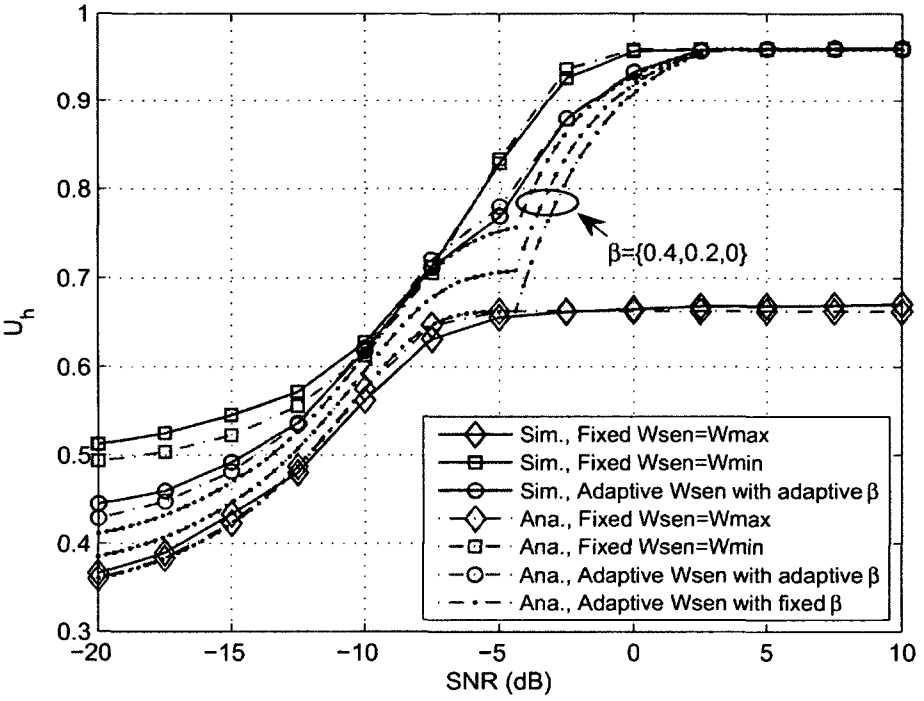

(a) Spectrum hole utilization vs. SNR.

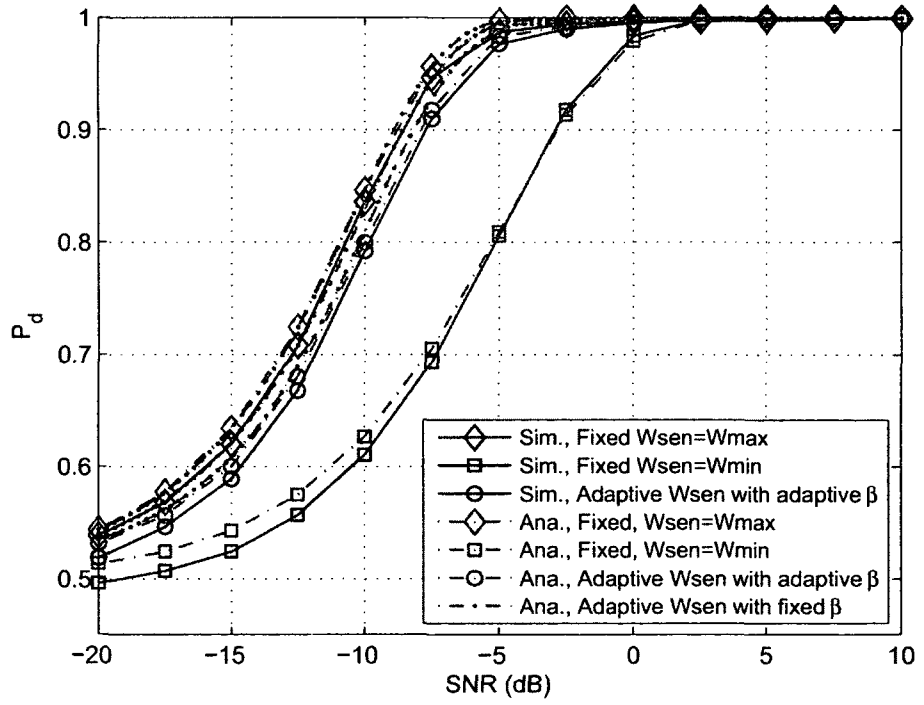

(b) Probability of detection vs. SNR.

Fig. 15: Spectrum hole utilization and probability of detection vs. SNR for performance evaluation of the proposed sensing method with weighted adaptation when $\tau = 140$ and $\mu = 30$.

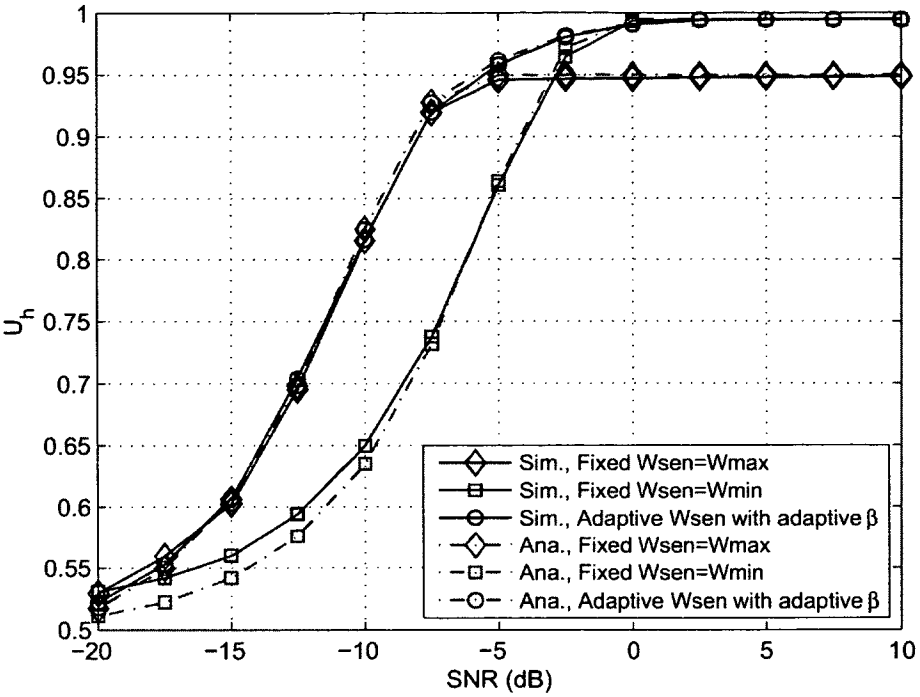

(a) Spectrum hole utilization vs. SNR.

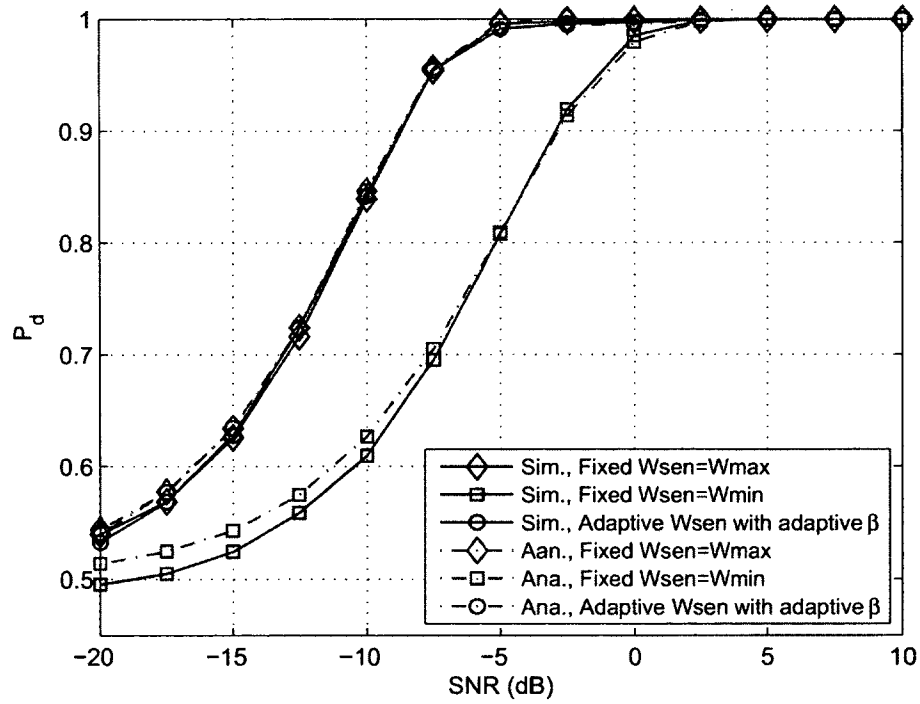

(b) Probability of detection vs. SNR.

Fig. 16: Spectrum hole utilization and probability of detection vs. SNR for performance evaluation of the proposed sensing method with weighted adaptation when $\tau = 800$ and $\mu = 240$.

Simulation for Adaptive Sensing with Method#3

Using the algoithm of Method#3, three different values are considered for the variable α = 10, 5, and 1. Similar to the previous adaptive methods proposed, two simulation scenarios are performed corresponding to the two dynamics of the PU activity as follows. In the first simulation, the average durations of the PU active periods and spectrum holes are taken as τ = 140 and μ = 30 symbol intervals, respectively, and the results for this simulation are shown in Fig. 17. Fig. 17(a) and (b) show that this proposed method for spectrum sensing with adaptive sensing window size optimally improves the spectrum hole utilization as well as the probability of detection when compared to the fixed sensing size scenario with $W_{sen} = W_{min}$ and $W_{sen} = W_{max}$ and as the value of its parameter α decreases, the spectrum hole utilization is improved while the probability of detection does not change significantly. It is also shown under this dynamic PU scenario that this method with $\alpha = 1$ also outperforms Method#1 in terms of spectrum hole utilization and have better probability of detection with the expense of slightly reduced spectrum hole utilization for low SNR values, when compared to Method#2.

In the second simulation, the PU activity is considered to be less dynamic than in the first simulation by setting the average durations of the PU active periods and spectrum holes to τ = 800 and μ = 240 symbol intervals, respectively. The results for this experiment are plotted in Fig. 18(a) and (b) which show that this method obviously has better sensing performance than the methods with fixed sensing size and also have comparable performance when compared to Method#2, under this dynamic PU scenario.

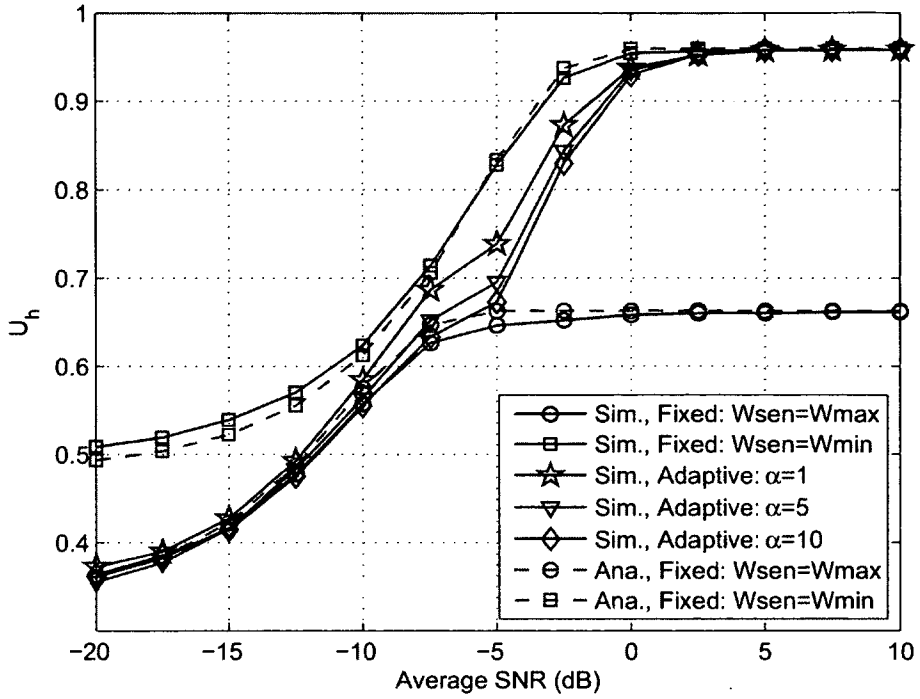

(a) Spectrum hole utilization vs. SNR.

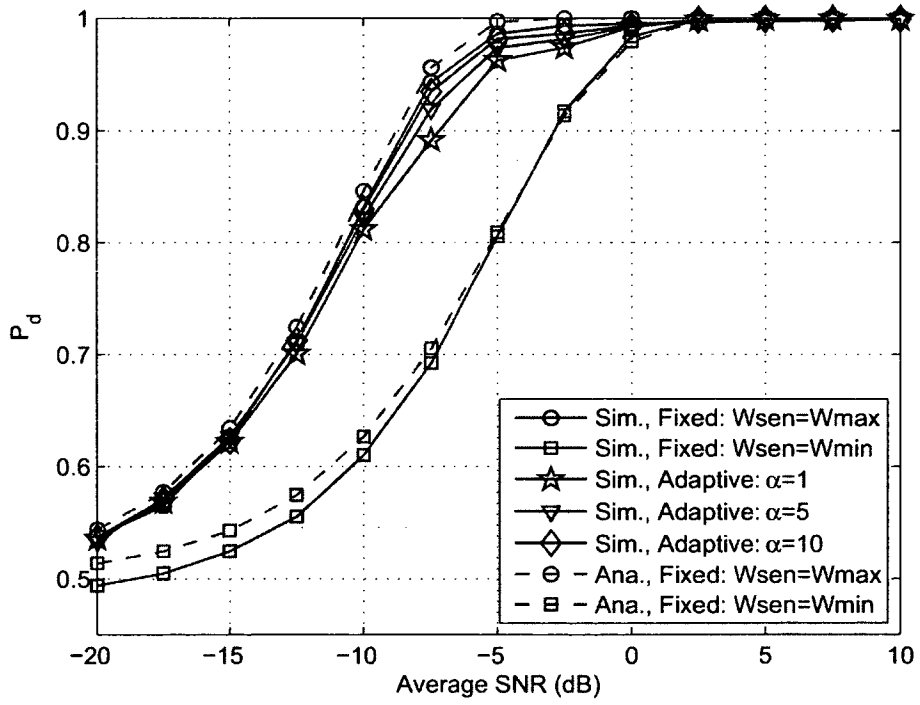

(b) Probability of detection vs. SNR.

Fig. 17: Spectrum hole utilization and probability of detection vs. SNR for performance evaluation of the proposed sensing method with heuristic adaptation when $\tau = 140$ and $\mu = 30$.

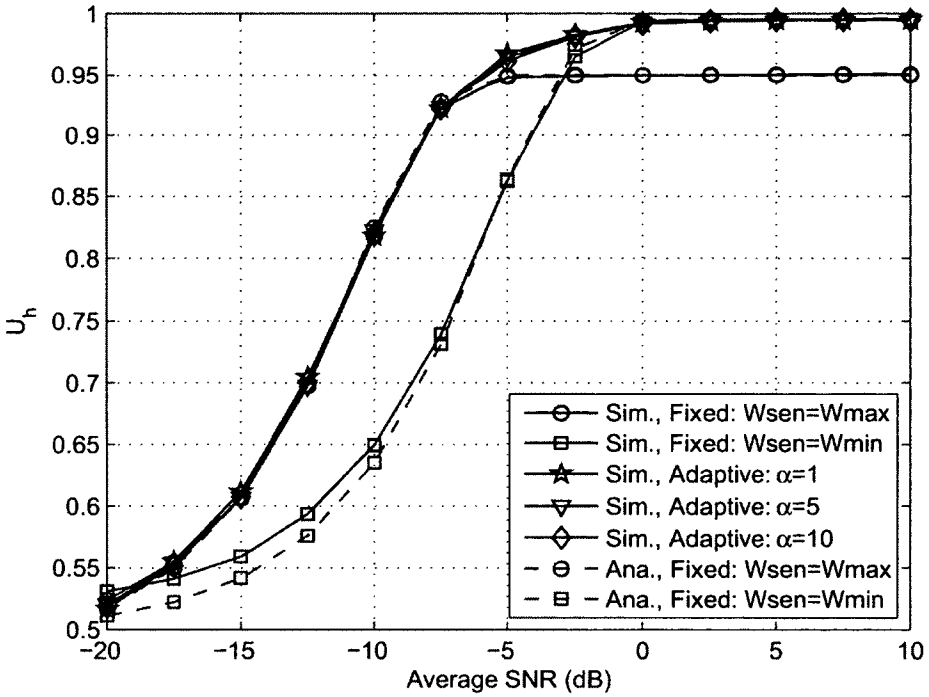

(a) Spectrum hole utilization vs. SNR.

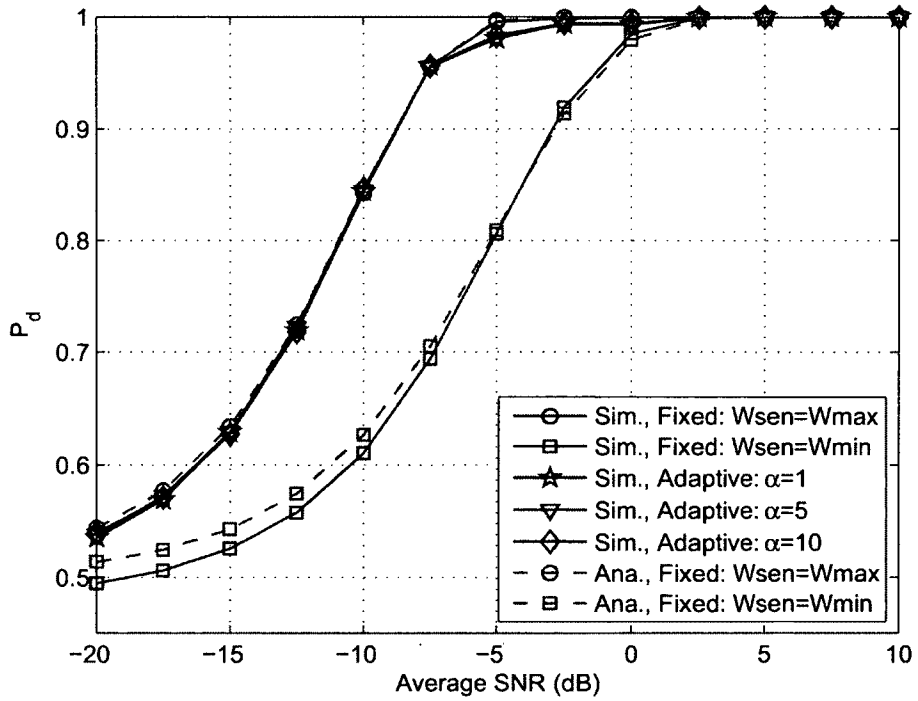

(b) Probability of detection vs. SNR.

Fig. 18: Spectrum hole utilization and probability of detection vs. SNR for performance evaluation of the proposed sensing method with heuristic adaptation when $\tau = 800$ and $\mu = 240$.

This section concludes by noting that the simulation results confirm the expected tradeoff between the size of the sensing window and the spectrum hole utilization, showing that a fixed size of the sensing window may not achieve good hole utilization and probability of detection at the same time, especially with highly dynamic spectrum opportunities and low received SNRs. The two proposed algorithms with adaptive sensing window improves both the spectrum hole utilization and the probability of detection when compared to spectrum sensing with fixed size of the sensing window.

III.5 CHAPTER SUMMARY

In this chapter, spectrum hole utilization of energy-based spectrum sensing in dynamic scenarios is studied by taking the size of the sensing window, SNR, and average duration of the spectrum opportunities into account. Specifically, this chapter proposes two new methods for spectrum sensing based on energy detection in which its sensing window is optimized corresponding to the received SNR and the spectrum opportunities. The performance of the proposed methods was illustrated with numerical results obtained from simulations which show the improvement on the probability dectection and spectrum hole utilization of the proposed methods with adaptive sensing size over the conventional energy detection with fixed sensing size and that these two methods also show to outperform the adaptive method proposed in Chapter II.

CHAPTER IV

OPTIMIZING PERFORMANCE OF COOPERATIVE SENSING FOR INCREASED SPECTRUM UTILIZATION

Cooperative spectrum sensing is a promising technique that has been proposed to enhance the performance of local spectrum sensing by employing spatial and multiuser diversities [17]. Specifically, cooperative spectrum sensing has received increased attention from researches working in the area of CR systems since it has the potential of increasing the utilization of spectrum holes in poor radio environments where the PU signal is affected by noise with high variance and/or multipath fading [17, 18].

When a network of CRs uses cooperative sensing to determine the availability of a specific frequency band, the local sensing information at individual CRs is forwarded to a CR fusion center (FC) which makes the final decision regarding the use of the sensed frequency band. Optimizing the size of the sensing window to maximize the achievable throughput for SUs is discussed in [30], while optimization of the FC voting rule, threshold, and number of cooperating SUs is presented in [22]. Furthermore, choosing the number of SUs in cooperative CR networks is investigated in [75–78]. It can be noted that, in the case of cooperative spectrum sensing, the time duration needed to detect spectrum holes consists of the actual time required for local spectrum sensing at individual CRs along with the delay associated with transmission of the local sensing information to the FC and FC processing to make the cooperative spectrum sensing decision. This latter time delay is part of the overhead associated

with cooperative spectrum sensing and affects the utilization of spectrum holes, especially in dynamic scenarios where these have finite time duration, and in this chapter, the cooperative spectrum sensing is studied by taking into account both the spectrum hole utilization and the FC transmission/processing delay.

Specifically, using the spectrum hole utilization measure introduced in Chapter I along with the probability of PU detection, a formal metric is defined for evaluating the performance of cooperative spectrum sensing that explicitly includes the time delay associated with FC processing. This metric describes the sensing performance of a network of cooperating CR systems in terms of both the capabilities of detecting active PU signal and of utilizing spectrum holes, and in this chapter, this metric is used to study the effect of the sensing window size and the FC time delay on the performance of cooperative sensing in dynamic scenarios where the activity of the PU changes in time and/or is affected by fading.

The rest of this chapter is organized as follows: the system model is introduced in Section IV.1, followed by presentation of the proposed total performance measure in Section IV.2. In Section IV.3, numerical results obtained from simulations are presented and this chapter is summarized with final remarks in Section IV.4.

IV.1 SYSTEM MODEL

The cooperative sensing network [17] considered is shown in Fig. 19 with K SUs transmitting 1-bit local sensing information H_1/H_0 corresponding to PU active/idle, to a FC that makes the final decision on the state of the PU using hard AND/OR combining. A dynamic scenario is assumed, where PU transmissions and spectrum

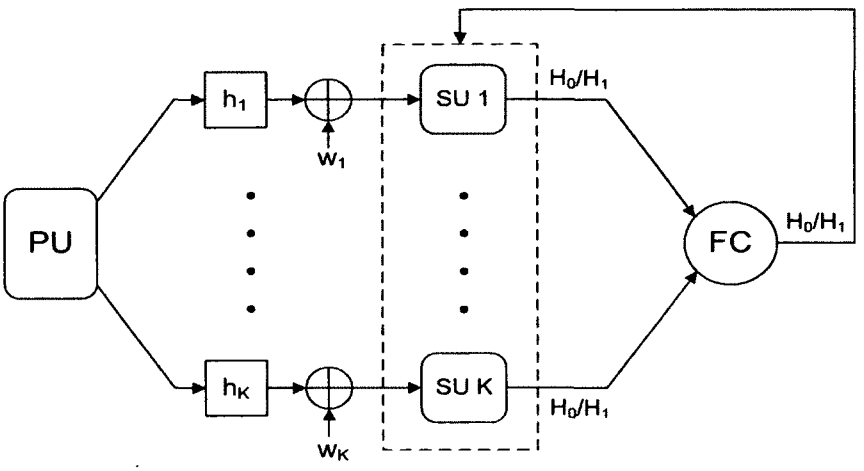

Fig. 19: Cooperative spectrum sensing with K SUs and one FC.

holes are exponentially distributed with means μ and τ, respectively, and the sampled received signal at a given SU i is given by:

$$y_i(n) = \begin{cases} w_i(n), & \text{for } H_0 \\ h_i s(n) + w_i(n), & \text{for } H_1 \end{cases} \tag{IV.1.1}$$

where $s(n)$ denotes the transmitted PU signal, h_i denotes the channel gain between the PU and SU i, $w_i(n)$ denotes the additive white Gaussian noise (AWGN) with zero mean and variance $\sigma^2_{w,i}$ at SU i, and n denotes the sample index. The sensing duration is assumed to be smaller than the coherence time of the channel such that h_i can be assumed constant during the sensing process.

The SNR at SU i is denoted by $\gamma_i = E\{[h_i s(n)]^2\}/\sigma^2_{w,i}$ and it is assumed that $\sigma^2_{w,1} = ... = \sigma^2_{w,K} = \sigma^2_w$ and the PU signal undergoes independent and identically distributed (i.i.d.) Rayleigh fading such that the received SNRs γ_i at all SUs are exponential random variables with same mean value $\bar{\gamma}$ [79], i.e.,

$$f(\gamma_i) = \frac{1}{\bar{\gamma}} \exp(-\frac{\gamma_i}{\bar{\gamma}}), \ \gamma_i \geq 0 \tag{IV.1.2}$$

Each SU uses an energy detector with the same sensing window size W and decision threshold λ such that the estimated energy $T_{y,i}$ and local decision $\mathfrak{D}_i$ for SU i are given by:

$$T_{y,i} = \frac{1}{W}\sum_{n=0}^{W-1}|y_i(n)|^2 \text{ and } \mathfrak{D}_i = \begin{cases} 0, \text{ for } T_{y,i} < \lambda \\ 1, \text{ for } T_{y,i} \geq \lambda \end{cases} \tag{IV.1.3}$$

When W is sufficiently long and the SNR is given, the estimated energy can be assumed to follow a normal distribution corresponding to the hypothesis that is true and the probabilities of detection $P_{d,i}$ and false alarm $P_{f,i}$ for SU i are [30]:

$$P_{d,i} = Q\left(\frac{\lambda - (1+\gamma_i)\,\sigma_w^2}{\sigma_w^2\sqrt{(1+2\gamma_i)\,2/W}}\right) \tag{IV.1.4}$$

$$P_{f,i} = Q\left(\frac{\lambda - \sigma_w^2}{\sigma_w^2\sqrt{2/W}}\right) \tag{IV.1.5}$$

where $Q(\cdot)$ denotes the standard Q-function. With the Rayleigh fading assumption, the probability of detection for SU i is then computed as [79]:

$$\bar{P}_{d,i} = \int_0^\infty P_{d,i}\,\frac{1}{\bar{\gamma}}\exp(-\frac{\gamma}{\bar{\gamma}})d\gamma \tag{IV.1.6}$$

In the considered dynamic scenario, the spectrum hole utilization implied by the local sensing decisions, representing the fraction of usable duration of the spectrum holes correctly detected by the SU i as introduced in Chapter II, is expressed as:

$$U_{h,i} = \exp\Big(-\frac{W}{\mu}\Big)\Big[1 - P_{f,i}\Big] \tag{IV.1.7}$$

It is assumed that the control channels between the FC and the SUs are error-free and synchronized in time-slotted fashion, where K SUs can be assumed, sense the spectrum at the same time. However, it is considered that there is delay D_c

in the control channel caused by the time-slotted medium access control and data transmissions for the FC's decision, accumulation, and dissemination processes, and W_c is denoted the cooperative spectrum sensing duration, defined as:

$$W_c = W + D_c \tag{IV.1.8}$$

Furthermore, it can be assumed that the actual PU status stays unchanged during the delay time D_c, which is usually the case in dynamic scenarios where the durations of active PU transmissions and of the spectrum holes are in general larger than the control channel delay D_c.

In order to study optimization of cooperative spectrum sensing, a metric is proposed for evaluating the total performance of cooperative sensing, that takes into account the delay D_c associated with FC processing, and the effect of D_c is studied on the spectrum hole utilization. The optimal number of SUs and sensing window size that improve the cooperative sensing performance in terms of the probability of detection as well as in terms of the hole utilization are also studied.

IV.2 THE TOTAL SENSING PERFORMANCE OF THE COOPERATIVE CR NETWORK

When the OR or AND combining scheme is used at the FC, the decision output $\mathcal{Y}$ of the FC is given by:

$$\mathcal{Y} = \begin{cases} H_0, & \text{if} \quad \sum_{i=1}^{K} \mathfrak{D}_i < k \\ H_1, & \text{otherwise} \end{cases} \tag{IV.2.1}$$

where $k = 1$ for OR combining and respectively $k = K$ for AND combining [22].

The corresponding cooperative probabilities of detection P_D and false alarm P_F are written as [30]:

$$\text{OR:} \quad \begin{cases} P_D = 1 - \prod_{i=1}^{K} (1 - \bar{P}_{d,i}), \\ P_F = 1 - \prod_{i=1}^{K} (1 - P_{f,i}) \end{cases} \tag{IV.2.2}$$

$$\text{AND:} \quad \begin{cases} P_D = \prod_{i=1}^{K} \bar{P}_{d,i}, \\ P_F = \prod_{i=1}^{K} P_{f,i} \end{cases} \tag{IV.2.3}$$

and, under the assumption that the PU state does not change during the FC processing delay D_c, the cooperative probabilities of detection and false alarm are not affected by the value of D_c. Using Eq. (IV.2.2) and Eq. (IV.2.3), the cooperative spectrum utilization U_H for the OR and AND rules is written as:

$$\text{OR:} \quad U_H = \exp\Big(-\frac{W + D_c}{\mu}\Big)\Big[\prod_{i=1}^{K} (1 - P_{f,i})\Big] \tag{IV.2.4}$$

$$\text{AND:} \quad U_H = \exp\Big(-\frac{W + D_c}{\mu}\Big)\Big[1 - \prod_{i=1}^{K} P_{f,i}\Big] \tag{IV.2.5}$$

To study the effect of the FC processing delay D_c, the sensing window size W, and the number of SUs on the cooperative sensing performance in terms of both the probability of detection and the spectrum hole utilization, the total sensing performance of the CR network is defined as:

$$T_p = \nu P_D + (1 - \nu) U_H \tag{IV.2.6}$$

where $\nu \in [0, 1]$ is a constant value that weights between P_D and U_H. It is noted that when $\nu = 1/2$ both P_D and U_H have equal weight in the total performance T_p, while when $\nu \neq 1/2$ one has more weight than the other.

Generally the FC performs spectrum sensing periodically with a constant period of time and in order to study how the sensing window size W and the delay D_c affects the total performance, W_c is set to a constant value and define the ratio:

$$\theta = \frac{W}{D_c} \tag{IV.2.7}$$

Subsequently, values for D_c and W can be computed from:

$$D_c = \left\lceil \frac{1}{\theta + 1} \cdot W_c \right\rceil, \tag{IV.2.8}$$

$$W = \left\lceil \frac{\theta}{\theta + 1} \cdot W_c \right\rceil \tag{IV.2.9}$$

where $\lceil \cdot \rceil$ denotes rounding up to the nearest integer value. It is noted that time and duration are taken in a discrete context (samples) according to the sampling process of energy detection to which the timing and delay in the control channel are related.

Thus far, the total performance has been calculated using Eq. (IV.2.6) with $\nu = 1/2$ and the corresponding expressions (IV.2.2) and (IV.2.4) for OR rule and respectively (IV.2.3) and (IV.2.5) for AND rule, to which the number of SUs K, the sensing window W and the delay D_c are accounted. The goal is to identify an optimal value for K and an optimal value for θ along with its corresponding values D_c and W that maximize the total performance T_p.

IV.3 SIMULATION AND NUMERICAL RESULTS

To study the effects of the sensing window size W and the delay D_c on the total performance T_p, the total performance of the cooperative CR network is evaluated in conjuction with the ratio θ of the local sensing window length W to the channel delay D_c and set the simulation as follows. The cooperative sensing duration is set

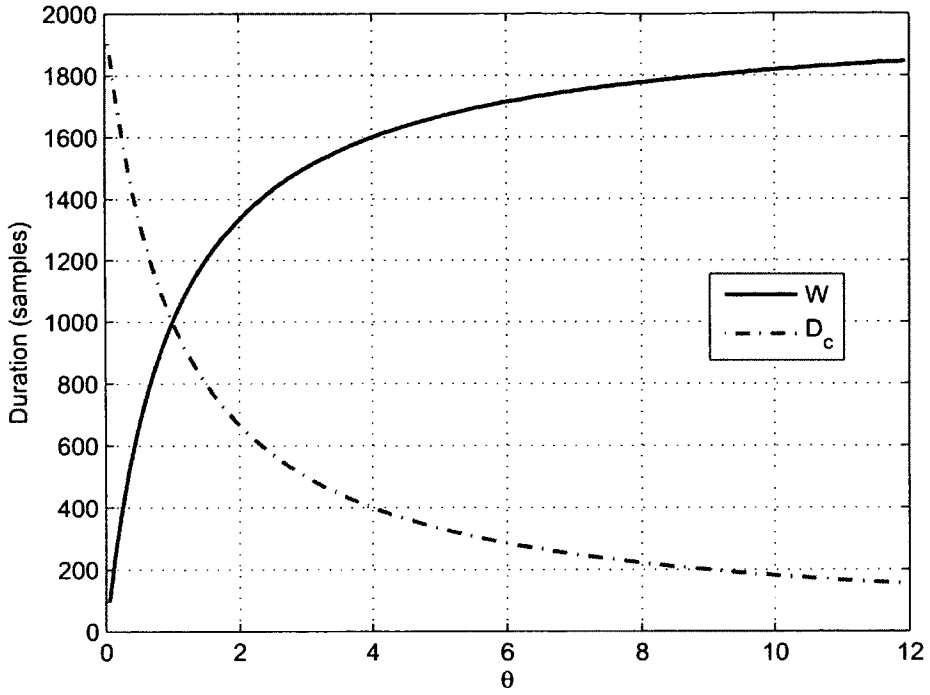

Fig. 20: Durations of the sensing window W and delay D_c in accordance with the ratio θ.

to $W_c = 2000$ samples and θ was varied from 0.05 to 12, which allows W and D_c to vary between 95 and 1,846 samples, respectively 1,905 and 154 samples, as shown in Fig. 20, which is plotted by using Eq. (IV.2.9) and Eq. (IV.2.8), such that the values for W are sufficiently long for the normal distribution assumption in the system model to be valid.

The noise variance and the average SNR $\bar{\gamma}$ corresponding to the SU Rayleigh fading channels are set to $\sigma_w^2 = 1$ and $\bar{\gamma} = -10$ dB, respectively, for all the simulations. The average duration of PU transmissions is taken $\tau = 1000$ symbol intervals, where one symbol interval has a duration of 81 samples, and different numbers of cooperating SUs K varying from 1 to 5 are considered, where $K = 1$ implies no cooperative

sensing. Two simulation scenarios are considered in this study corresponding to average spectrum hole durations $\mu = 250$ and 1000 symbol intervals, respectively. For each scenario, the sensing threshold λ is determined by setting either $P_{f,i} = 0.1$ in (IV.1.5) or $P_{d,i} = 0.99$ in (IV.1.4), assuming that $\gamma_i = \bar{\gamma}$, for all i, and the total sensing performance measure is calculated with a weighting constant $\nu = 1/2$.

Numerical results for the first scenario are shown in Fig. 21 from where it is noted that the simulated total sensing performance of the cooperating CR network closely follows the analytical curves which were plotted by assuming that the PU activity is known to the FC. From Fig. 21(a), it is also noted that when the sensing threshold λ is chosen by setting $P_{f,i}$, the OR rule outperforms the AND rule, and that in this case applying the AND rule at the FC is not meaningful as it degrades the total sensing performance below that of non-cooperative sensing. By contrast, Fig. 21(b) shows that, when the sensing threshold λ is chosen by setting $P_{d,i}$, the AND rule outperforms the OR rule and should be applied at the FC.

Numerical results for the second scenario, shown in Fig. 22, are similar to ones for the first scenario, with the notable difference being that the maximum values of the total sensing performance in this scenario are slightly higher than in the previous one. This is due to the fact that the longer average duration of spectrum holes in the second scenario results in improved spectrum utilization as the actual duration of spectrum holes is likely to be larger than the cooperative sensing length W_c leading to improved total performance as a consequence.

The total sensing performance measure can also be used to select an optimal number of cooperating SUs that implies a maximum T_p value. For the numerical

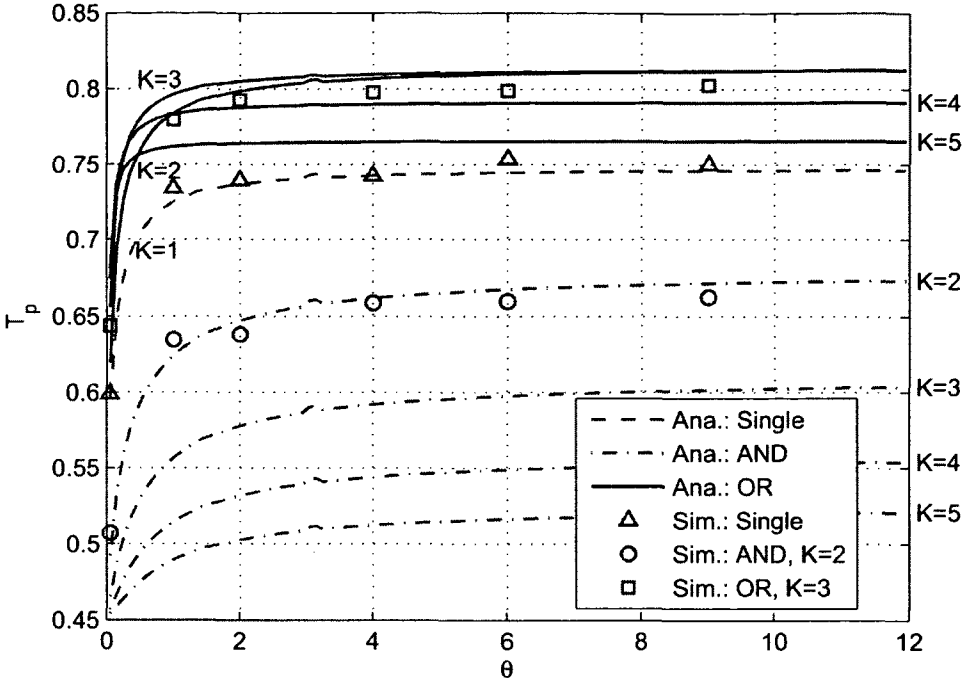

(a) The threshold λ is computed based on $P_{f,i} = 0.1$.

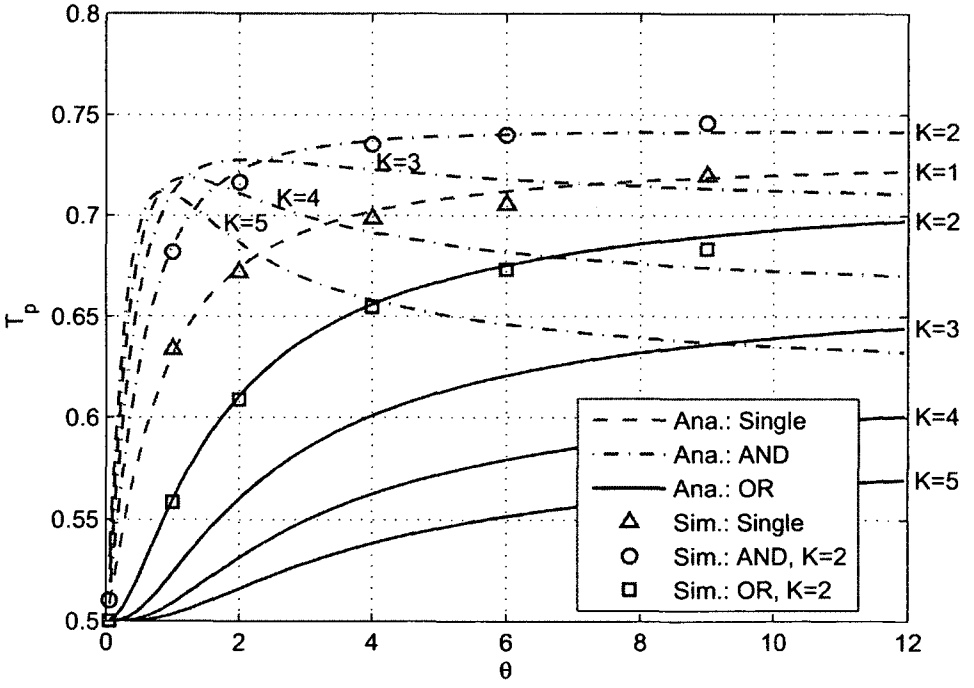

(b) The threshold λ is computed based on $P_{d,i} = 0.99$.

Fig. 21: Total sensing performance versus θ for OR and AND rules, $\tau = 1000$, $\mu = 250$, and increasing number of SUs K.

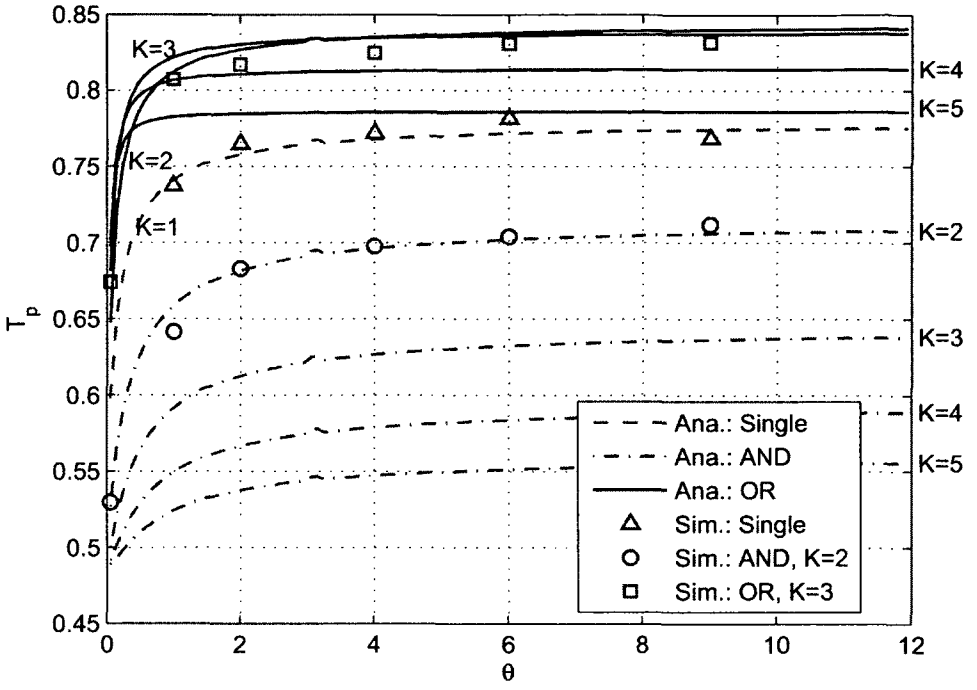

(a) The threshold λ is computed based on $P_{f,i} = 0.1$.

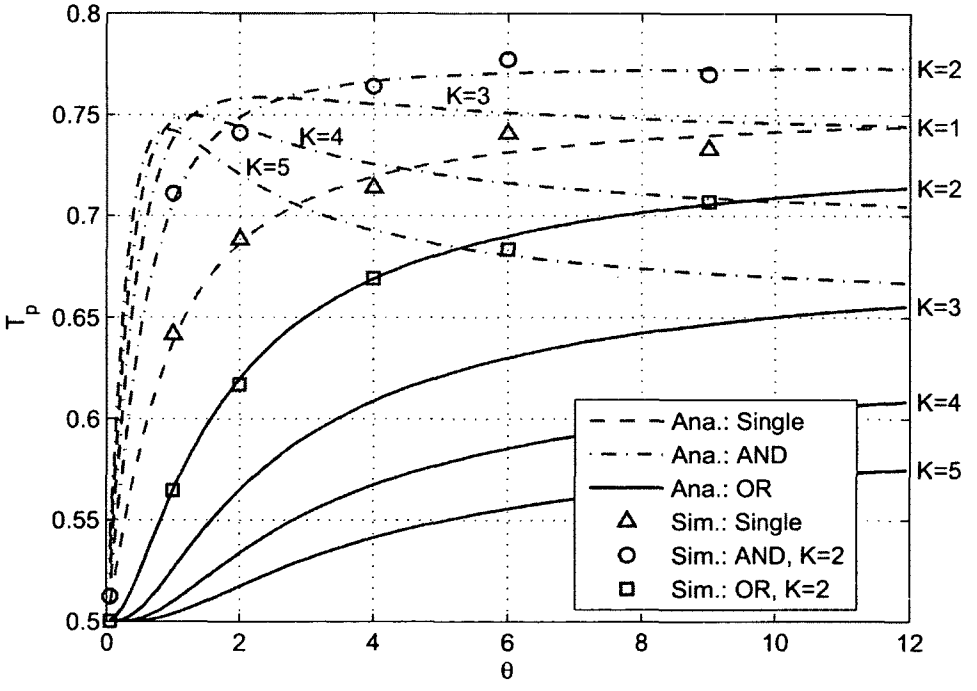

(b) The threshold λ is computed based on $P_{d,i} = 0.99$.

Fig. 22: Total sensing performance versus θ for OR and AND rules, $\tau = 1000$, $\mu = 1000$, and increasing number of SUs K.

values presented in Fig. 21 and 22, $K = 2$ and/or 3 appears to maximize T_p in all scenarios. In addition, for a given number K of SUs, an optimal value of θ that maximizes T_p can be found, which allows the selection of a sensing window size that implies maximum total sensing performance for given delay time on the control channel. For instance, for the numerical results in Fig. 21(a) a ratio $\theta \geq 2$ with $K = 2$ implies that for $D_c \leq 667$ samples, a sensing window size $W \geq 1333$ samples results in maximum $T_p \approx 0.8$, while for those in Fig. 21(b) $\theta \geq 4$ and $K = 2$ a shorter $D_c \leq 400$ samples with a longer sensing window length $W \geq 1600$ samples result in maximum $T_p \approx 0.74$.

IV.4 CHAPTER SUMMARY

This chapter studies optimization of spectrum sensing performance of cooperative spectrum sensing and introduces a new metric to evaluate the total sensing performance of a network of cooperating CR systems that includes both the cooperative probability of detection and the cooperative spectrum hole utilization. Numerical studies for specific dynamic scenarios have been performed and simulation results have shown that increasing the number of cooperating CRs and the size of local spectrum sensing does not always improve the total sensing performance, and that an optimal number of cooperating CRs and optimal durations for the local spectrum sensing and FC processing delay that result in increased spectrum utilization can be identified.

CHAPTER V

USING HMM FOR PERFORMANCE EVALUATION OF CR SPECTRUM SENSING

As introduced previously, the PU activity is unknown to SUs in practice. Hence an important functionality of CR systems is spectrum sensing which enables the detection of active PU, and allows SU to decide whether specific frequency bands are idle and available for unlicensed secondary access. In order for CR systems to maintain and/or improve their spectrum utilization efficiency as well as to sufficiently protect PUs from interference caused by their spectrum usage, CR systems need to evaluate their spectrum sensing performance which can be done through performance measures such as the probabilities of detection and false alarm.

In this chapter, performance evaluation of CR spectrum sensing is studied, which includes local spectrum sensing where CRs perform spectrum sensing individually and locally as well as cooperative spectrum sensing where multiple CRs share their local sensing information to deciding on the state of a PU. In this study, all CRs are considered to use energy detection for spectrum sensing since it does not require prior knowledge of PU signals and has low complexity, as introduced in Chapter I.

Specifically, the use of a Hidden Markov Model (HMM) is studied to describe the output of energy detectors used for local spectrum sensing as well as to describe the output of cooperative spectrum sensing and a method using HMM is presented to estimate the probabilities of detection and false alarm using past sensing decisions in local and cooperative spectrum sensings. It is noted that HMMs have been used so far

in the context of various spectrum sensing procedures [42–55], but their application to evaluating the performance of CR spectrum sensing has not been found in the literature.

The proposed HMM-based performance evaluation method can be used to enable performance awareness of local and cooperative spectrum sensing techniques in dynamic CR systems, the details of which are separately presented in Section V.1 and Section V.2, respectivley and the study in this chapter is summarized in Section V.3.

V.1 LOCAL SPECTRUM SENSING

In order to study performance evaluation for performance awareness of local CR systems, energy-based spectrum sensing is considered, which is particularly useful for CR systems since it does not require prior knowledge of PU signals [7]. It is noted that in energy detection a proper sensing threshold is determined based on the specific values set for the probabilities of detection and false alarm, P_d and P_f, respectively, and performance of energy-based spectrum sensing in CR systems depends heavily on accurate estimation of noise energy which is needed to compute a threshold value corresponding to the desired sensing performance. As a consequence, the performance can be significantly degraded if the actual noise energy differs from the estimated one, particularly in the low SNR regime when noise is stronger than the active PU signal.

In order to ensure that the values set for P_d and P_f continue to be respected, in such cases the CR system must adapt its sensing threshold to the actual noise variance which can be accomplished by various methods [80]. In order to trigger the threshold adaptation mechanism, the CR system needs to be aware that its energy

detector operates with a threshold value that is no longer suitable for the current background noise and in this section the use of HMMs is presented to enable such performance awareness.

Specifically, the energy detector's decision output is described using a HMM with two states that correspond to the presence, respectively absence, of an active PU, and the corresponding probability elements of the HMM are used to estimate the values of P_d and P_f in order to enable the CR to check for performance degradation due to deviation of the actual received SNR from the target SNR for which the sensing threshold is optimized. In addition to estimating P_d and P_f, the presented HMM allows also estimation of the noise variance which is needed for adapting the energy detector threshold.

This study is organized as follows: in Section V.1.1, the system model is introduced followed by presentation of the use of HMMs to describe the energy detector output decision in Section V.1.2. In Section V.1.3, the proposed approach is presented to enabling performance awareness for the CR system and for estimating the noise variance, which is illustrated with numerical examples obtained from simulations in Section V.1.4.

V.1.1 SYSTEM MODEL

A CR is assumed to use energy detection for local spectrum sensing, as shown in Fig. 23 and the received signal at the CR in discrete time domain is assumed under the two hypotheses: H_0 and H_1 corresponding to the absence, respectively presence, of an active PU. At the CR, the received signal $y(n)$ and the test statistic T_y for distinguishing between the two hypotheses H_0 and H_1 are given by Eq. (I.2.1) and

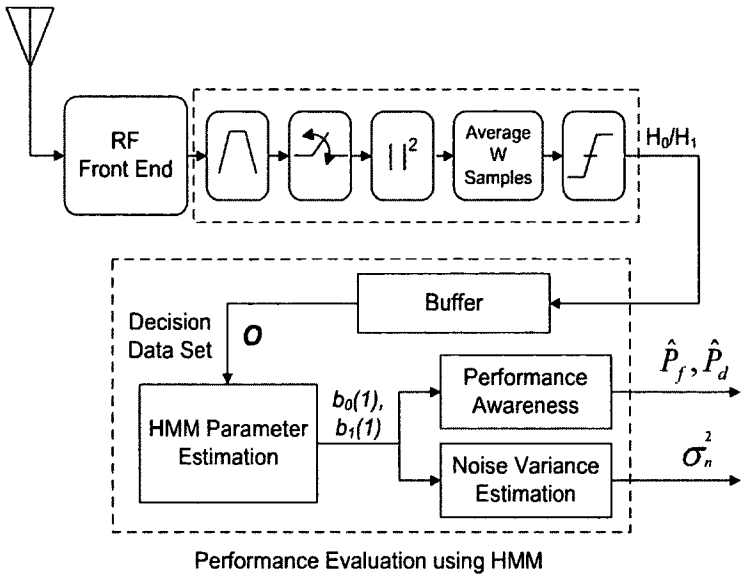

Fig. 23: Basic diagram of energy detection for spectrum sensing in CR with HMM-based performance evaluation.

respectively Eq. (I.2.2). When W is sufficiently long, the test statistic T_y is assumed to follow a normal distribution corresponding to the hypothesis that is true as given by Eq. (I.2.4) and then the probabilities of detection P_d and false alarm P_f can then be analytically computed by using Eq. (I.2.5) and Eq. (I.2.6). For convenience, the analytical P_d and P_f are expressed [30]:

$$P_d = Q\left(\frac{\lambda - (1+\gamma)\,\sigma_w^2}{\sigma_w^2\sqrt{(1+2\gamma)\,2/W}}\right) \tag{V.1.1}$$

$$P_f = Q\left(\frac{\lambda - \sigma_w^2}{\sigma_w^2\,\sqrt{2/W}}\right) \tag{V.1.2}$$

It is noted that, for a given SNR γ_t (assumed to be known at the design stage) the sensing threshold λ_t can be obtained directly from Eq. (V.1.1) or (V.1.2) when either P_d or P_f is specified. It is considered that the PU signal is transmitted with a stable variance and the received SNR is changing due to variable noise variance. If the detector is using the sensing threshold λ_t for SNR different than γ_t, then the

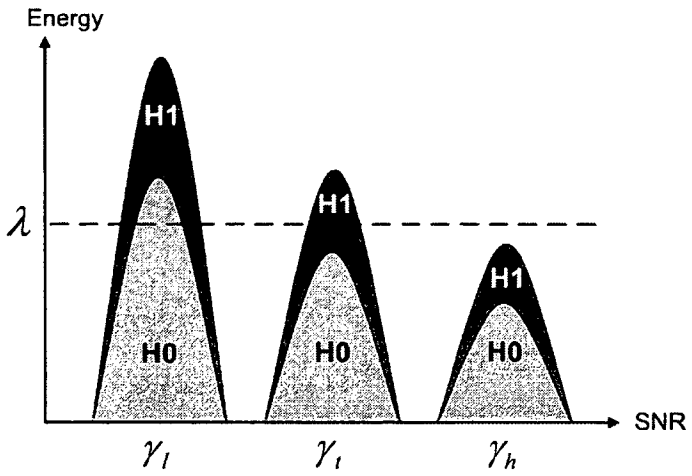

Fig. 24: Estimated energy for three different SNRs.

corresponding values for P_f and P_d will be different than the desired ones. This situation is especially true in the low SNR regime, as shown in Fig. 24, which illustrates two extreme cases of how the received SNR higher (γ_h) or lower (γ_l) than the target SNR (γ_t) affect the performance of energy detection. From the figure, it can be noted that, when the received SNR is γ_l the detector decides mostly in favor of H_1, while when the received SNR is γ_h the detector decides mostly in favor of H_0. This implies that both P_d and P_f for γ_l will be very close to 1, while for γ_h they will be close to 0. However, a good detector should have P_d close to 1 and P_f close to 0, respectively. Thus, in order to combat performance degradation, the CR should be aware of variations in the received SNR and should be able to accurately estimate noise variance in order to adapt its sensing threshold.

In this study, the use of HMMs is presented to describe the decision output of energy detection and to enable performance awareness for CR systems. As a byproduct, the proposed approach enables also estimation of the noise variance with higher accuracy than by using the sample variance method.

V.1.2 HMM FOR ENERGY DETECTOR OUTPUT

Energy detection of the CR performs spectrum sensing by deciding either H_0 or H_1, corresponding to the two possible states of the PU activity which are "idle" and respectively "active", according to Eq. (I.2.2). Over a given observation time, the detector generates a sequence of binary decisions which can be viewed as the sequence of *observed* states of the PU, since the *actual* PU states are not known to the CR. It is noted that the decision output of energy detection should change whenever the PU state changes. However, the energy detection decision may not always be accurate as the *observed* sequence of PU states may not totally agree with the *actual* sequence of PU states due to imperfections in the local sensing caused by background noise. In addition to this, it is also noted that the possibility that the PU will be active or inactive in the next time instant would be related to the previous state for which a Markov chain can be assumed.

With these perspectives on energy detection, the decision output of an energy detector is described using the 2-state HMM shown in Fig. 25, in which state 0 corresponds to PU idle, and state 1 corresponds to PU active, and where the HMM outputs represent the decisions in favor of hypothesis H_0 – PU idle, respectively hypothesis H_1 – PU active. It is noted that similar HMMs were used to model PU spectrum occupancy [45] and to describe the PU activity in spectrum sensing based on sequence detection [51].

Let $O = \{\mathcal{O}_t\}_{,1\leq t\leq T}$ be the output sequence of the energy detector with length T, where $\mathcal{O}_t \in \{H_0, H_1\}$ is the output decision corresponding to the two hypotheses at time index t. Let q_t be the state at sequence index t where $q_t \in \{0, 1\}$ corresponds to

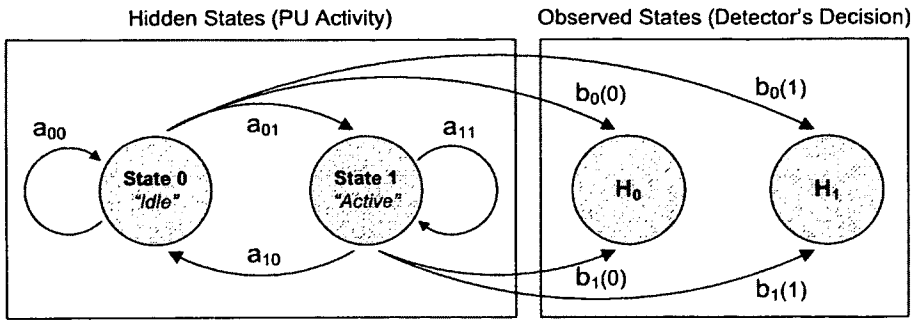

Fig. 25: Two-state HMM for describing the energy detector's decision output.

state 0 and 1 of the HMM. According to the HMM model shown in Fig. 25, it is noted that the state of the energy detector's output sequence can either stay unchanged or change to another state based on the PU activity and noise variance experienced by the detector and an output sequence is regarded as an observed sequence since the true state of the PU is unknown to the CR.

The model is described by the state transition probabilities, $\{a_{ij}\}$, where $a_{ij} = P\{q_{t+1} = j \mid q_t = i\}$ and $i, j \in \{0, 1\}$, along with the probability that the HMM generates output decision $v_k = H_k$, $k \in \{0, 1\}$ at state j and sequence index t, that is, $b_j(k) = P\{\mathcal{O}_t = v_k \mid q_t = j\}$ where $j \in \{0, 1\}$. This latter HMM parameter will be used to enable performance awareness for the energy detector and to estimate the noise variance as discussed in Section V.1.3. To complete the parameter set describing the HMM, it is denoted by $\pi_i = P\{q_1 = i\}$, $i \in \{0, 1\}$, the probability that the initial state of the HMM is state i. Hence, the complete parameter set $\varphi = (A, B, \pi)$ describing the HMM consists of:

$$A = \begin{bmatrix} a_{00} & a_{01} \\ a_{10} & a_{11} \end{bmatrix}, B = \begin{bmatrix} b_0(0) & b_0(1) \\ b_1(0) & b_1(1) \end{bmatrix}, \pi = \begin{bmatrix} \pi_0 & \pi_1 \end{bmatrix} \tag{V.1.3}$$

with the probability constraints:

$$\begin{aligned} a_{00} + a_{01} &= a_{11} + a_{10} = 1, \\ b_0(0) + b_0(1) &= b_1(0) + b_1(1) = 1, \\ \pi_0 + \pi_1 &= 1 \end{aligned} \tag{V.1.4}$$

In order to evaluate the sensing performance of the energy detector using the proposed HMM, the CR must first estimate the HMM parameters using its past decision record as shown schematically in Fig. 23. Let $\mathbf{O}$ be the training set used for estimating the HMM parameters, consisting of multiple output sequences:

$$\mathbf{O} = \{O^{(1)}, O^{(2)}, \ldots, O^{(M)}\} \tag{V.1.5}$$

$$\begin{aligned} O^{(m)} &= \{\mathcal{O}_t^{(m)}\}, 1 \leq m \leq M, 1 \leq t \leq T \\ &= \{\mathcal{E}_{\rho \cdot i}\}, 1+(m-1)T \leq i \leq T+(m-1)T \end{aligned}$$

where $\{\mathcal{E}_j\}$, $\mathcal{E}_j \in \{H_0, H_1\}$, denotes the sequence of consecutive outputs of the energy detector with the length $P = \rho TM$ and ρ is an eventual downsampling coefficient. It is noted that the observation length P should be sufficiently long to cover periods of PU being both active and idle, and that, if the number of observation samples is too large it can be reduced by downsampling with the coefficient ρ.

Using the training set $\mathbf{O}$ the set of HMM parameters φ is estimated by applying the Baum-Welch algorithm [41]. This is based on iteratively evaluating the likelihood P_φ that φ corresponds to the observations in the training set as follows:

(1) *Initialization*: The starting parameter set φ_0 is initialized as follows:

- Initial values for $\{a_{ij}\}$ and $\{b_j(k)\}$ are chosen under the constraints in (V.1.4) and

$$0 < a_{01} < a_{00} < 1,\ 0 < a_{10} < a_{11} < 1,$$

$$0 < b_0(1) < b_0(0) < 1,\ 0 < b_1(0) < b_1(1) < 1.$$

- $\pi = [1\ \ 0]$.

(2) *Estimation*: At each iteration i the parameter set φ_i and the likelihood P_{φ_i} are computed as described in [41].

(3) *Termination*: The estimation procedure (2) is repeated until $\left|P_{\varphi_i} - P_{\varphi_{i-1}}\right| < \epsilon$, where $\epsilon > 0$ denotes a given tolerance, or the number of iterations exceeds a maximum number of iterations I.

Upon termination, the algorithm yields final estimated values of the model parameters φ, and when the training data is sufficient, the procedure results in a maximum likelihood estimate of the HMM [41].

V.1.3 ESTIMATING PERFORMANCE OF ENERGY DETECTOR

This section presents the use of the HMM that describes the output decision of the energy detector to enable performance awareness for the CR system and to estimate the noise variance.

Performance Awareness

Considering now the output probabilities of the HMM $b_j(k)$, it is noted that they are computed based on the frequency of occurrence of decision H_k when the HMM is in state j, and that they do not depend on the time index t after the HMM parameters estimation. Recall that, formally, the probability of detection P_d at the CR is defined as the probability that the detector decides H_1 given that the actual PU state is

also H_1, while the probability of false alarm P_f is the probability that the detector decides H_1 given that the actual PU state is H_0. Thus, when the HMM states describe the *actual* PU state and the HMM outputs correspond to the *observed* PU state at the energy detector, the HMM output probabilities $b_j(k)$ can be used to determine estimates $\hat{P}_d$ and $\hat{P}_f$ of the probabilities of detection and false alarm, respectively. Two special cases of $b_j(k)$ are then considered as follows:

- When $j = 0$ and $k = 1$,

$$\begin{aligned} b_0(1) &= P\{\mathcal{O}_t = H_1 \mid q_t = 0\} \\ &= P\{\text{Detector decides } H_1 \mid \textit{actual} \text{ PU state is ``Idle''}\} \\ &= \hat{P}_f \end{aligned} \tag{V.1.6}$$

- When $j = 1$ and $k = 1$,

$$\begin{aligned} b_1(1) &= P\{\mathcal{O}_t = H_1 \mid q_t = 1\} \\ &= P\{\text{Detector decides } H_1 \mid \textit{actual} \text{ PU state is ``Active''}\} \\ &= \hat{P}_d \end{aligned} \tag{V.1.7}$$

For performance awareness, the energy detector uses the $\hat{P}_d$ and $\hat{P}_f$ values estimated from the HMM instead of using Eq. (V.1.1) and Eq. (V.1.2) which require knowledge (or accurate estimation) of the noise variance. Specifically, deviation of the $\hat{P}_d$ and $\hat{P}_f$ values from the prescribed/desired values for P_d and P_f indicates that the energy detector operates with a suboptimal threshold that should be adjusted for optimal performance.

Noise Variance Estimation

As a byproduct, the values $\hat{P}_f$ and $\hat{P}_d$ obtained from the HMM performance awareness estimation can be used to estimate the variance of the noise experienced by the CR. This is accomplished by using equations (V.1.2) and (V.1.1) as follows:

$$\begin{aligned} Q^{-1}\left(\hat{P}_f\right) &= \frac{\lambda - \sigma_w^2}{\sigma_w^2 \sqrt{2/W}} \\ \sigma_w^2 &= \frac{\lambda}{1 + \sqrt{\frac{2}{W}}\, Q^{-1}\left(\hat{P}_f\right)} \end{aligned} \tag{V.1.8}$$

$$Q^{-1}\left(\hat{P}_d\right) = \frac{\lambda - (1+\gamma)\,\sigma_w^2}{\sigma_w^2 \sqrt{(1+2\gamma)\,2/W}}$$

$$\sigma_w^2 = \begin{cases} \frac{-A+\sqrt{A^2+B}}{C}, & \text{for } \hat{P}_d < 0.5 \\ \frac{-A-\sqrt{A^2+B}}{C}, & \text{for } \hat{P}_d \geq 0.5 \end{cases} \tag{V.1.9}$$

where

$$\begin{aligned} A &= 2\Big[\left[2Q^{-1}\left(\hat{P}_d\right)^2/W - 1\right]\sigma_s^2 + \lambda\Big] \\ B &= 4\Big[2Q^{-1}\left(\hat{P}_d\right)^2/W - 1\Big]\left(\sigma_s^2 - \lambda\right)^2 \\ C &= 4Q^{-1}\left(\hat{P}_d\right)^2/W - 2 \end{aligned}$$

Since $Q(-\infty) = 1$ and $Q(\infty) = 0$, it is noted that Eq. (V.1.8) and Eq. (V.1.9) are applicable when the values of $\hat{P}_f$ and $\hat{P}_d$ are in the range $[\delta, 1-\delta]$, where $\delta \in \mathbb{R}^+$ is a small value close to 0.

V.1.4 SIMULATION AND NUMERICAL RESULTS

This section illustrates application of the proposed HMM for a CR system using energy detector with sensing window of length $W = 450$, a desired probability of false

alarm $P_f = 0.1$ and an operating target SNR $\gamma_t = -4$ dB. In order to evaluate the performance awareness using the proposed method in conjunction with varying noise, it is assumed that the PU signal variance σ_s^2 is not changing over the sensing period of time. Without loss of generality, it is also assumed that $\sigma_s^2 = 1$. Hence $\sigma_w^2 = 1/\gamma$ is obtained. The sensing threshold λ corresponding to the desired P_f and target SNR is obtained from Eq. (V.1.2) as:

$$\lambda = \frac{1}{\gamma}\left(\sqrt{2/W} \cdot Q^{-1}(P_f) + 1\right) \tag{V.1.10}$$

The probability of detection (P_d) can then be computed using Eq. (V.1.1) and result in $P_d = 0.9998$. For the HMM describing the energy detector output its parameters are initialized as:

$$A = \begin{bmatrix} 2/3 & 1/3 \\ 1/3 & 2/3 \end{bmatrix}, B = \begin{bmatrix} 2/3 & 1/3 \\ 1/3 & 2/3 \end{bmatrix}, \pi = \begin{bmatrix} 1 & 0 \end{bmatrix} \tag{V.1.11}$$

The other numerical values needed to estimate the HMM parameters are summarized in Table 2 and the parameter δ for estimating noise variance is set to 10^{-4}.

Table 2: Parameters settings for the HMM.

ρ	T	M	$P = \rho TM$	I	ϵ
1	200	30	6000	100	10^{-5}

Simulations were performed in which the received SNR was varied around the target SNR $\gamma_t = -4$ dB and the probabilities of detection and false alarm were evaluated using the proposed HMM-based method in comparison with those using the analytical and simulated approaches. It is noted that the HMM-based estimates $\hat{P}_d$ and $\hat{P}_f$

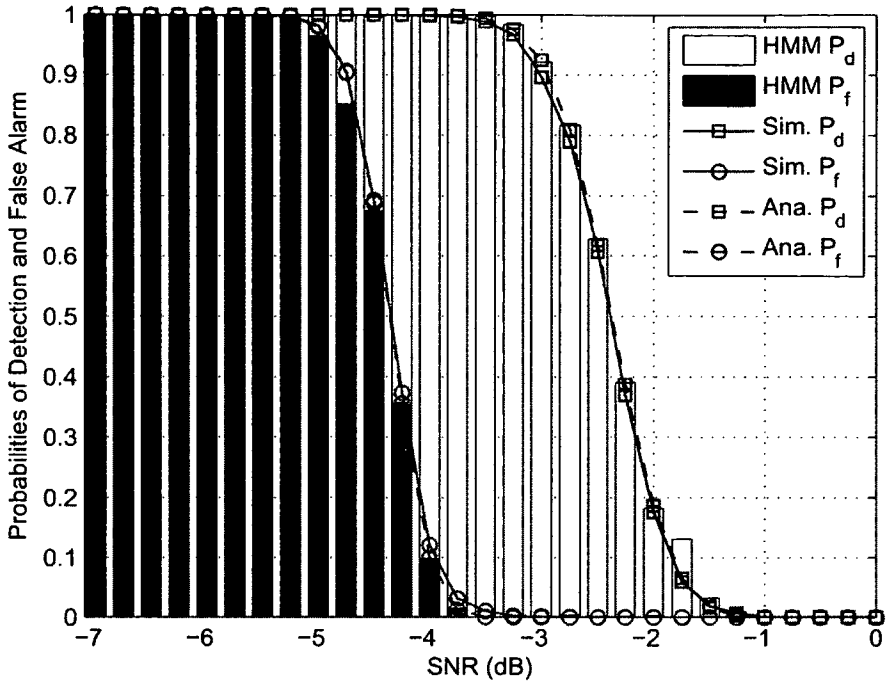

Fig. 26: HMM-based P_d and P_f in comparison with analytical and simulated results for the considered simulation scenario.

are computed from Eq. (V.1.7) and respectively Eq. (V.1.6) with no knowledge of the actual noise variance, while the analytical P_d and P_f are computed from Eq. (V.1.1) and Eq. (V.1.2) respectively, using knowledge of the noise variance. The simulated values of P_d and P_f are computed with knowledge of the actual PU activity, which implies that the detector is able to know when its detection decision is correct or incorrect. It is noted that the simulated values cannot be determined in practical scenarios as the PU activity is assumed to be unknown to the CR in real systems, and that the simulated results are presented as reference results for comparison with the proposed method.

The results are plotted in Fig. 26 from which it is noted that the values of $\hat{P}_d$ and $\hat{P}_f$ agree with those of the analytical P_d and P_f, respectively, as well as with

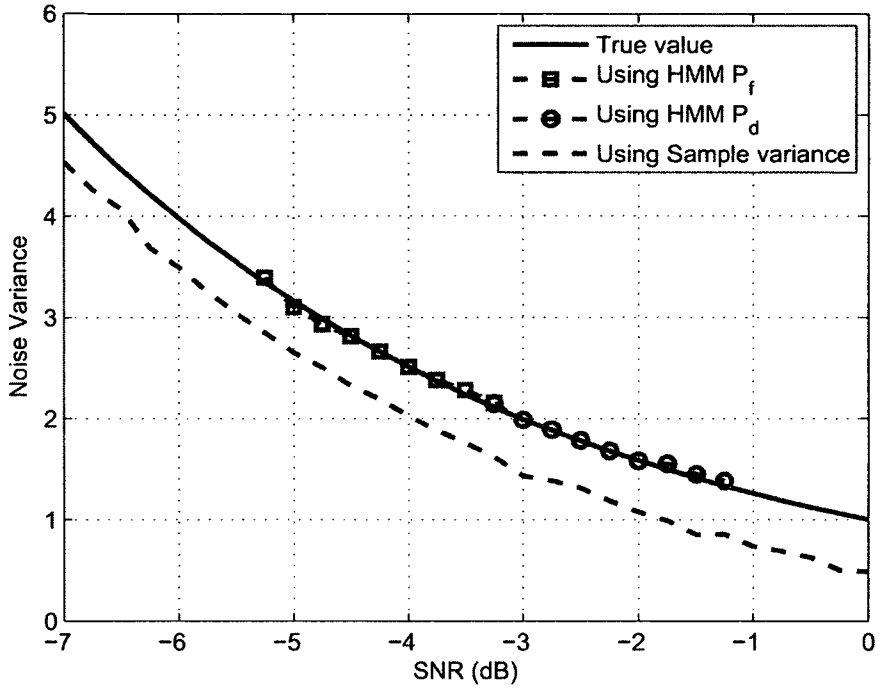

Fig. 27: Noise variance estimates for the considered simulation scenario.

those of the simulated P_d and P_f values. This implies that the proposed HMM is suitable to describe the output of energy detector and that the values of $\hat{P}_d$ and $\hat{P}_f$ can accurately indicate the performance degradation of the energy detector when either P_d or P_f is not close to their desired values which are 0.9998 and 0.1, respectively, for this example. It is also noted that, instead of estimating the actual SNR during the sensing operation and then evaluating the current sensing performance through the analytical values of P_d and P_f, the proposed approach enables the CR to evaluate the accuracy of its sensing performance by employing only a past record of its decisions.

Fig. 27 shows the results of estimating noise variance using Eq. (V.1.8) and Eq. (V.1.9) and the values $\hat{P}_f$ and $\hat{P}_d$ obtained from the HMM, along with the true

noise variance and the noise variance estimated by using the conventional sample variance method. These results show that estimation of the noise variance by using the proposed approach is very accurate resulting in estimated values that are very close to the true noise variance, and it outperforms the sample variance method using the same length of sample data as the proposed HMM method. It is noted that the SNR range over which the proposed method is applicable is not as large as that over which the sample variance is applicable due to limitations in the numerical computation of the inverse Q-function. Nevertheless, the range is adequate for the purpose of threshold adaptation corresponding to the true received SNR which gradually deviates from the target SNR.

V.2 COOPERATIVE SPECTRUM SENSING

As introduced in Chapter I, cooperative spectrum sensing can enhance the performance of local sensing in practical scenarios with noise and/or multipath fading, by combining the local sensing information of multiple SUs at a FC which makes the final decision regarding the use of the sensed frequency band [17]. The performance of cooperative sensing in terms of the cooperative probabilities of detection and false alarm can be analytically determined at the FC when all the local sensing information at all cooperating SUs is known to the FC [22, 23]. However, in order to avoid high complexity and bandwidth requirements on the control channel between SUs and the FC, in practice the FC receives only the local sensing information that is sufficient for making a cooperative decision at the FC, but that may not be enough for the FC to analytically compute the cooperative probabilities of detection and false alarm.

This section presents the use of a HMM to describe the sensing decisions of the FC and also propose a method for estimating the cooperative probabilities of detection and false alarm by using estimates of the probabilities in the corresponding HMM that are determined based on the history of the FC decisions, similar to Section V.1. The study in this section is organized as follows: the system model is introduced in Section V.2.1, followed by presentation of the HMM proposed for describing the FC in Section V.2.2. The proposed method for HMM-based performance evaluation of cooperative spectrum sensing is presented in Section V.2.3 and is illustrated with numerical results obtained from simulations in Section V.2.4.

V.2.1 SYSTEM MODEL

A cooperative approach to spectrum sensing is considered, as shown in Fig. 28 where K SUs transmit local sensing information to a FC which combines the data using a hard or soft combining scheme and makes the final binary decision on the state of the PU (0 for hypothesis H_0 when the PU is idle, respectively 1 for hypothesis H_1 when the PU is active). Similar to Chapter IV, let the sampled received signal at SU i, corresponding to the two hypotheses, be:

$$y_i(n) = \begin{cases} w_i(n), & \text{for } H_0 \\ h_i s(n) + w_i(n), & \text{for } H_1 \end{cases} \tag{V.2.1}$$

where $s(n)$ denotes the transmitted PU signal, h_i denotes the channel gain between the PU and SU i, $w_i(n)$ is a sample of an additive white Gaussian noise (AWGN) process with zero mean and variance σ_w^2, and n denotes the sample index. It is assumed the sensing duration is smaller than the coherence time of the channel such

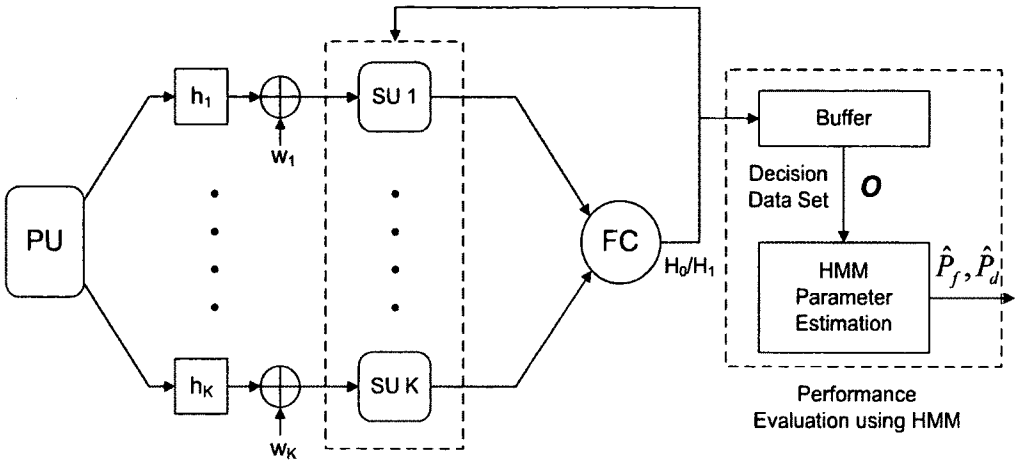

Fig. 28: Block diagram of the considered cooperative sensing network with HMM-based performance evaluation.

that h_i can be assumed constant during the sensing process, and $\gamma_i = E\{[h_i s(n)]^2\}/\sigma_w^2$ denotes the SNR at SU i.

To make local spectrum sensing decisions, all SUs employ energy detectors with the same sensing window size W and decision threshold λ, such that the test statistic $T_{y,i}$ and local decision $\mathfrak{D}_i$ for SU i are given by:

$$T_{y,i} = \frac{1}{W}\sum_{n=0}^{W-1}|y_i(n)|^2 \quad \text{and} \quad \mathfrak{D}_i = \begin{cases} 0, \text{ for } T_{y,i} < \lambda \\ 1, \text{ for } T_{y,i} \geq \lambda \end{cases} \tag{V.2.2}$$

When hard combining is used, the FC makes the cooperative sensing decision based on the local decisions as:

$$Y_h = \sum_{i=1}^{K}\mathfrak{D}_i \underset{H_0}{\overset{H_1}{\gtrless}} k \tag{V.2.3}$$

where $k = K$ for AND combining, respectively $k = 1$ for OR combining [22].

When soft combining is used, the FC makes its decision as:

$$Y_s = \sum_{i=1}^{K} g_i T_{y,i} \underset{H_0}{\overset{H_1}{\gtrless}} \lambda_f \tag{V.2.4}$$

where g_i denotes the weight for SU i test statistic and λ_f denotes the decision threshold at the FC [23]. Weight computations based on *Equal Gain Combining* (EGC) and *Maximal Ratio Combining* (MRC) in [23] are considered, which are given by $g_i = 1/\sqrt{K}$ and $g_i = \gamma_i / \sqrt{\sum_{j=1}^{K} \gamma_j^2}$, respectively.

The goal in this framework is to study the use of HMMs to describe the output decisions of the FC and to evaluate the cooperative spectrum sensing performance in terms of the cooperative probabilities of detection P_D and false alarm P_F.

V.2.2 HMM FOR THE FC DECISION

Similar to the decision output of energy detection used for local spectrum sensing, the sensing decision of the FC at any time instant is either H_0 or H_1, corresponding to the two possible states of the PU which are "idle", respectively "active". Thus, over a given observation time, the FC generates a sequence of binary decisions which can be viewed as the sequence of *observed* states of the PU, since the *actual* PU states are not known to the SUs. It is noted that the FC decision should change whenever the PU state changes, however, the FC decision may not always be accurate as the *observed* sequence of PU states may not totally agree with the *actual* sequence of PU states due to imperfections in the local sensing caused by background noise and/or fading.

Therefore the FC output can also be described using the HMM shown in Fig. 25, in which state 0 corresponds to PU idle and state 1 corresponds to PU active. It

is denoted by $O = \{\mathcal{O}_t\}_{,1\leq t\leq T}$ the sequence of FC decisions, where $\mathcal{O}_t \in \{H_0, H_1\}$, consisting of T observations, and then the complete parameter set $\varphi = (A, B, \pi)$ describing the HMM is given by (V.1.3) with the probability constraints in (V.1.4).

Similar to the case of local spectrum sensing, the HMM states represent the *actual* PU states which are unknown to the FC, and that the HMM outputs depend on the actual PU activity and on the sensing performance of the FC. Thus, the cooperative sensing performance at the FC can be estimated from the output probabilities $b_j(k)$ when the HMM parameter set is optimized as discussed in the following section.

V.2.3 ESTIMATING COOPERATIVE SENSING PERFORMANCE

Similar to Section V.1, in order to evaluate the cooperative sensing performance using the proposed HMM, the FC must first estimate the HMM parameters using its past decision record as shown schematically in Fig. 28. Let $\mathbf{O'}$ be the training set used for estimating the HMM parameters for cooperative spectrum sensing, consisting of multiple output sequences:

$$\mathbf{O'} = \{O^{(1)}, O^{(2)}, \ldots, O^{(M)}\} \tag{V.2.5}$$

$$O^{(m)} = \{\mathcal{E}_{\rho \cdot i}\}_{,1+(m-1)T\leq i\leq T+(m-1)T}$$

where $\{\mathcal{E}_j\}$, $\mathcal{E}_j \in \{H_0, H_1\}$, denotes the sequence of consecutive outputs of the FC with the length $P = \rho TM$. The observation length P should be sufficiently long to cover periods of PU being both active and idle, and the observation samples can be downsampled with the coefficient ρ if the number of observation samples is too large. Using the training set $\mathbf{O'}$, the set of HMM parameters φ is estimated by applying the Baum-Welch algorithm [41], as described in Section V.1.2, and it is

noted that when the training data set is sufficient, the procedure results in a maximum likelihood estimate of the HMM and then the HMM can yield accurate estimates on the cooperative sensing performance.

Using the same concept as local spectrum sensing using energy detection, the HMM states represent the *actual* PU state and the HMM outputs correspond to the *observed* PU state at the FC. Two of the HMM probabilities $b_j(k)$ are then considered to determine estimates $\hat{P}_D$ and $\hat{P}_F$ of the cooperative probabilities of detection and false alarm, respectively, as follows:

$$\begin{aligned} b_0(1) &= P\{\text{FC decides } H_1 \mid \textit{actual} \text{ PU state is "Idle"}\} \\ &= \hat{P}_F \end{aligned} \tag{V.2.6}$$

$$\begin{aligned} b_1(1) &= P\{\text{FC decides } H_1 \mid \textit{actual} \text{ PU state is "Active"}\} \\ &= \hat{P}_D \end{aligned} \tag{V.2.7}$$

V.2.4 SIMULATION AND NUMERICAL RESULTS

In order to illustrate the accuracy of the proposed method for evaluating the performance of cooperative spectrum sensing, extensive simulations were performed with the following setup: a dynamic scenario was considered where the PU activity consists of active transmissions and idle periods that have random durations with exponential distribution and means $\tau = 1000$ and $\mu = 500$ symbol intervals, respectively [72]. However, it is noted that the proposed method is general and other types of random variables may also be assumed for the PU activity. The sensing window size is $W = 400$ samples for all SUs and, without loss of generality, the noise variance is set at $\sigma_w^2 = 1$.

The local sensing threshold λ at individual SUs is determined by constraining the local probability of false alarm [30]:

$$P_{f,i} = Q\left(\frac{\lambda - \sigma_w^2}{\sigma_w^2\sqrt{2/W}}\right) \tag{V.2.8}$$

to have a prescribed value. The initial values for the HMM parameters and the parameter values for the Baum-Welch algorithm are set as in Eq. (V.1.11) and Table 2. Application of the proposed method is illustrated in both AWGN and Rayleigh fading environments, and its effectiveness is demonstrated by comparing its results with analytical and simulated results obtained by assuming that the FC has perfect local sensing information and knowledge of PU activity, respectively.

For the AWGN case, the low SNR regime is considered, where the PU signal variance is lower than the AWGN variance and the same SNR value is assumed at all SUs. The receiver operating characteristic (ROC) curves obtained by simulating the proposed method for AWGN with hard and soft combining schemes at different SNRs are plotted in Fig. 29 and 30. It is noted that all ROC curves in Fig. 29 and 30 are close to each other which confirms the accuracy of our proposed HMM-based method for estimating cooperative sensing performance. In addition to the results, it is also noted that the soft combining schemes EGC and MRC outperform the hard combining schemes AND and OR and that OR combining scheme outperforms AND combining scheme while EGC and MRC combining schemes are equivalent since MRC scheme has equal weights like EGC combining scheme in this simulation scenario.

For the Rayleigh fading case, it is assumed that the PU signal undergoes independent and identically distributed (i.i.d.) Rayleigh fading such that the received SNRs γ_i at all SUs are exponential random variables with same mean value $\bar{\gamma}$ [79]. ROC

curves obtained by simulating the proposed method for Rayleigh fading with $K = 5$ and 8 SUs are shown in Fig. 31 along with corresponding analytical and simulated ROC curves. These plots confirm that the proposed HMM-based method for estimating cooperative sensing performance is effective also when the PU signal is affected by Rayleigh fading. The results in this simulation scenario also show that MRC combining scheme outperform all the other combining schemes and with the exception of the AND combining scheme, the cooperative sensing performance improves when the number of cooperating SUs increases from 5 to 8.

In order to see how the cooperative sensing performance changes when the number of cooperating SUs increases, the cooperative probabilities of detection P_D and false alarm P_F for increasing K in separate plots are shown in Fig. 32. It is noted that in this case the FC threshold λ_f for EGC and MRC soft combining schemes are pre-computed based on minimizing the probability of error $P_e = 1 - P_D + P_F$ in order to observe optimal performance. This is different than in Fig. 30 and 31 where λ_f for EGC and MRC were pre-computed based on fixing $P_F = P_{f,i}$ in order to determine the ROC curves. The plots in Fig. 32 confirm again that the proposed HMM-based method yields accurate estimates for P_D and P_F in all cases. In addition to the plots, it is noted that there is a tradeoff between P_D and P_F when using AND and OR combining schemes with the increasing number of cooperative SUs while using MRC and EGC combining schemes can improve both P_D and P_F when the number of cooperating SUs increases.

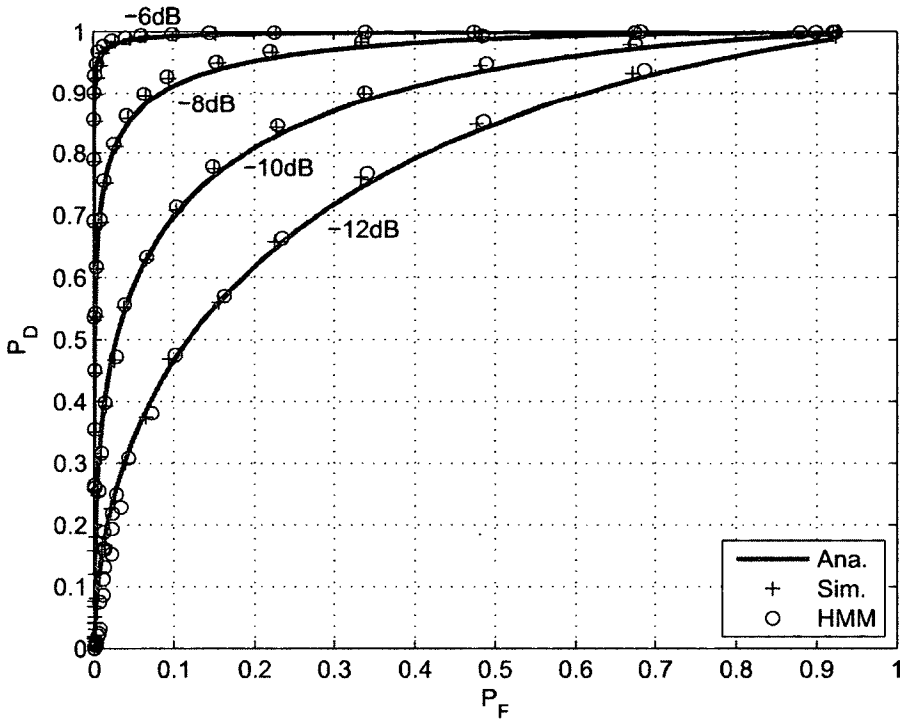

(a) AND.

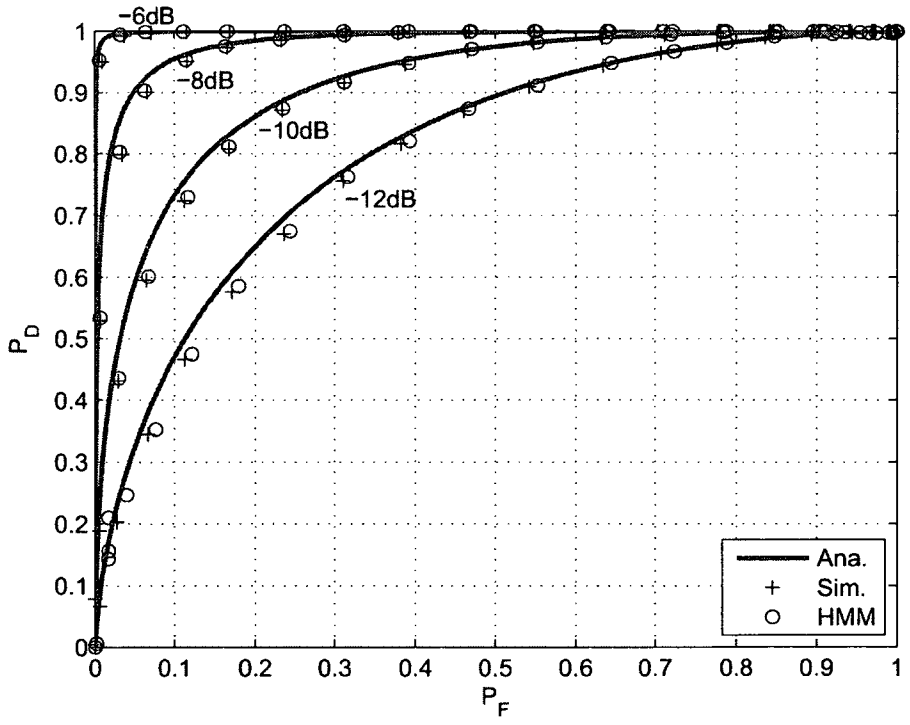

(b) OR.

Fig. 29: ROC curves for hard combining schemes with $K = 3$ in AWGN at different SNRs.

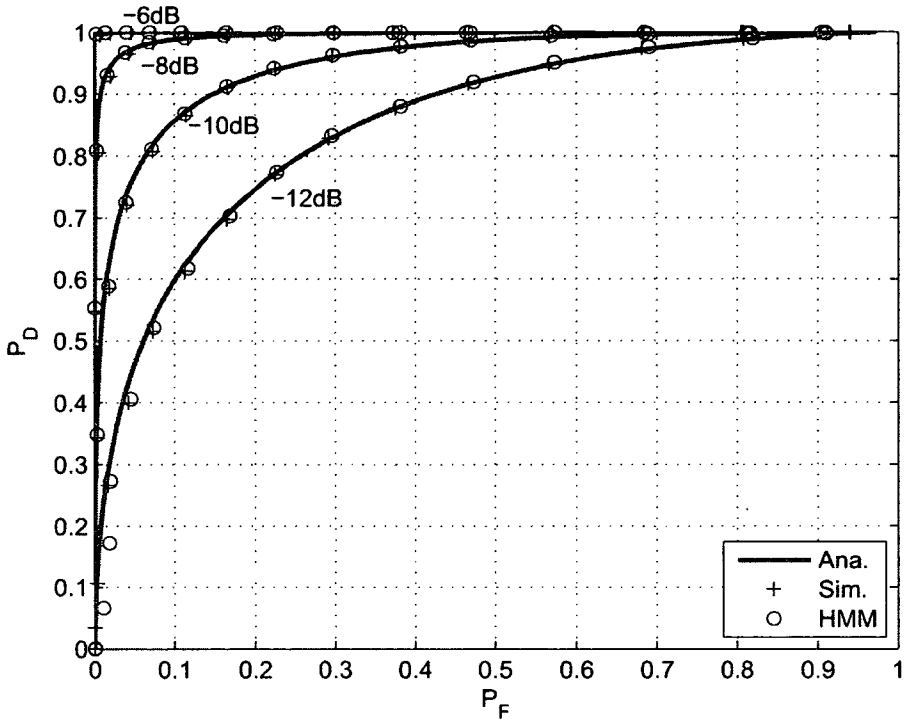

(a) EGC.

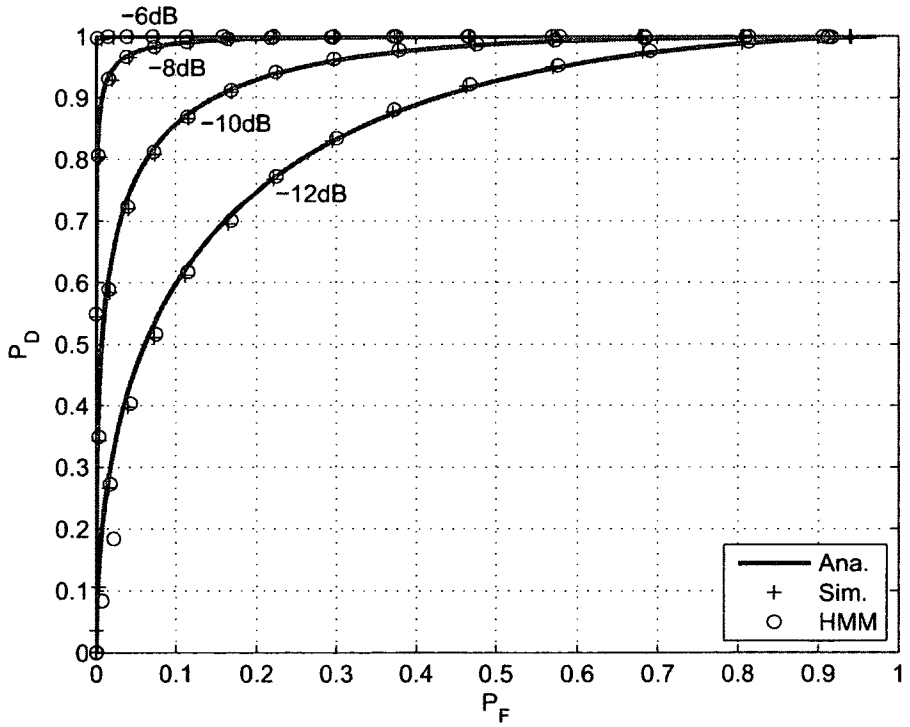

(b) MRC.

Fig. 30: ROC curves for soft combining schemes with $K = 3$ in AWGN at different SNRs.

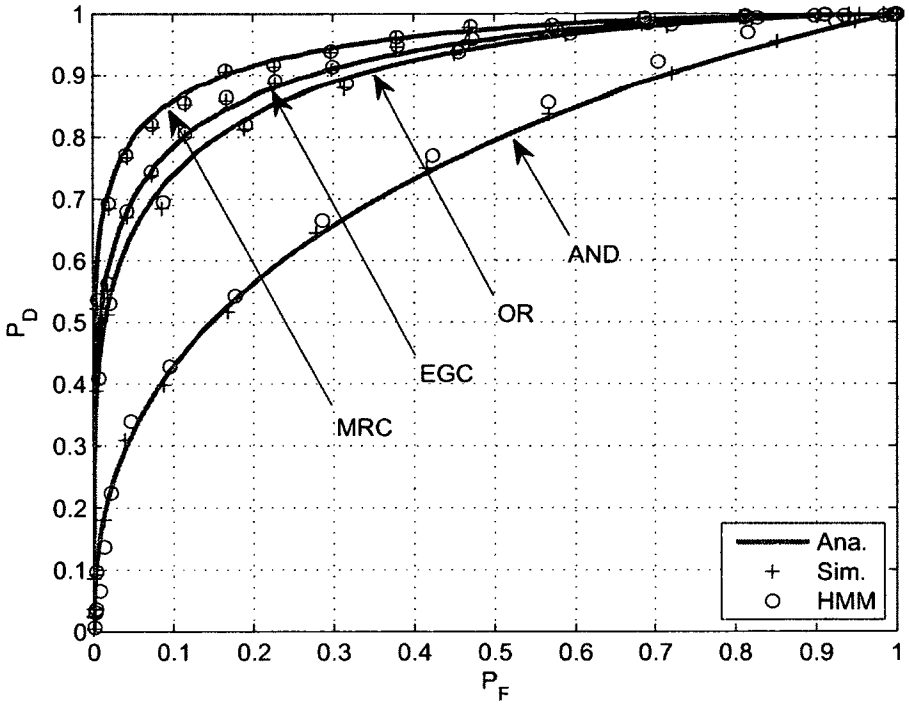

(a) K=5.

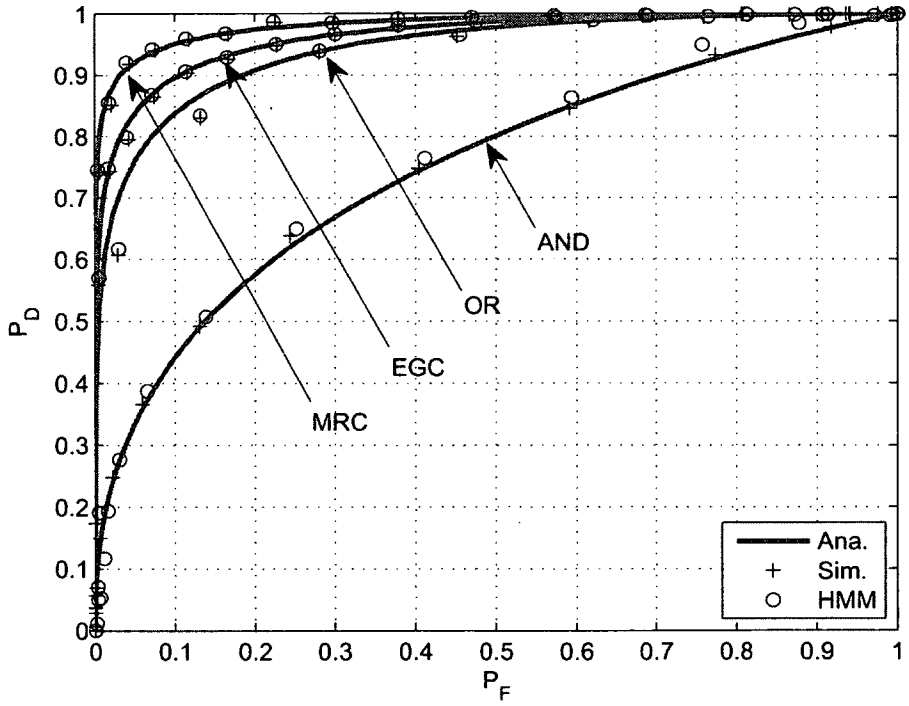

(b) K=8.

Fig. 31: ROC curves for hard and soft combining in Rayleigh fading with $\bar{\gamma} = -11$ dB and different K.

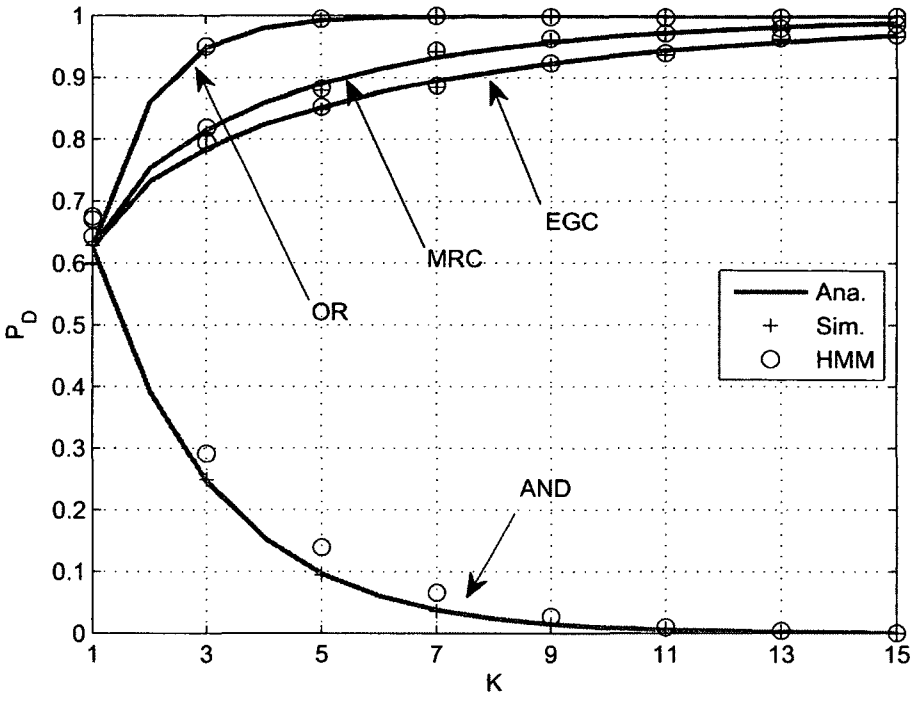

(a) K=5.

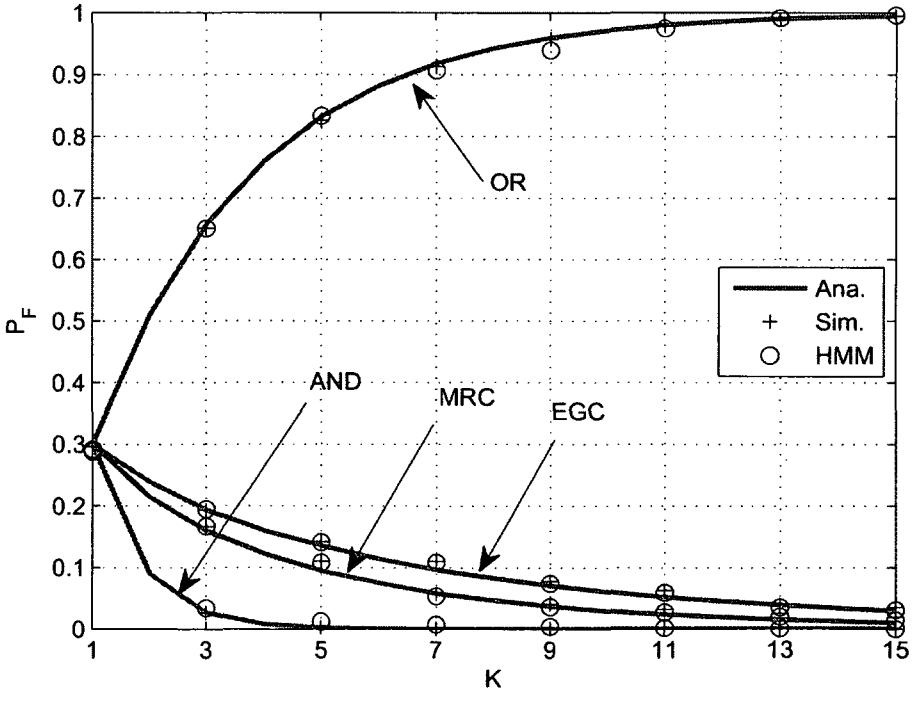

(b) K=8.

Fig. 32: Cooperative probabilities of detection and false alarm vs. K for hard and soft combining schemes in Rayleigh fading with $\bar{\gamma} = -11$ dB.

V.3 CHAPTER SUMMARY

This chapter presents the use of HMM to describe the output of energy detectors used for local spectrum sensing in CR systems and proposes a HMM-based method that can be used to determine when detector performance degrades due to changes in the noise variance. The proposed method uses the probability elements in the HMM which are estimated based on the past decisions of the energy detector. Numerical results show that the proposed HMM method can accurately estimate the performance of the energy detector in terms of the probabilities of detection and false alarm. This also indicates that the proposed HMM is suitable to model the energy detection output.

The presented HMM is also applied to describe the FC decision in cooperative spectrum sensing and to estimate the cooperative probabilities of detection and false alarm using only a record of past decisions of the FC, without knowledge of the actual PU state and of the local sensing information. The proposed method is illustrated with numerical results obtained from simulations which confirm its effectiveness and show that it can accurately estimate the cooperative sensing performance for hard and soft combining schemes in practical scenarios where the cooperating SUs experience AWGN and/or Rayleigh fading.

The proposed approach can be used as an alternative to dynamic estimation of the noise variance leading to enabling the threshold adaptation mechanism of energy-based spectrum sensing and is applicable to performance awareness of CR systems when they become aware that their performance no longer meets the desired values for the probabilities of detection and false alarm.

CHAPTER VI

CONCLUSIONS AND FUTURE RESEARCH

In this chapter, the contributions of this dissertation are concluded and some useful directions for future research are discussed.

VI.1 CONCLUSIONS

CR is a recently introduced concept in wireless communications, that aims at reusing the licensed radio frequencies in order to alleviate spectrum congestion in future generations of wireless technologies. The physical layer of CR serves as the foundation of the whole system, in which sensing, adaptation, and awareness of spectrum opportunities are essential functionalities. This dissertation has presented a number of contributions applicable to implementation of the CR physical layer, which are summarized as follows:

First, the utilization of spectrum holes by energy-based spectrum sensing in dynamic CR systems has been investigated and a performance measure for spectrum hole utilization was formally defined. The dependence of this measure on the duration of the sensing procedure, SNR value, and average duration of spectrum holes was analyzed, and the proposed measure was applied to enhancing the spectrum hole utilization in CR systems.

Next, the parameters that influence the spectrum hole utilization to spectrum sensing design were taken and three new methods that adapt the size of the sensing window for improving the spectrum hole utilization as well as the probability of

detecting an active PU were proposed. Numerical studies of the proposed methods were performed showing that they outperform spectrum sensing with fixed size of the sensing window.

The performance of centralized cooperative spectrum sensing was also evaluated, which is affected by both the sensing window size of local spectrum sensing and the time delay introduced by the FC for processing of the local sensing information. A new metric for evaluating the performance of cooperative sensing was introduced, that includes the cooperative probability of detection and spectrum hole utilization. Using the metric, an optimal number of cooperative SUs and optimal durations for the local spectrum sensing and the FC processing delay can be identified, in dynamic scenarios where the activity of the PU changes in time and/or is affected by fading, such that the cooperative sensing performance can be optimized.

Finally, HMM was applied to describe the spectrum sensing decision in local and cooperative scenarios. Specifically, a HMM-based method was proposed to estimate the sensing performance in terms of the probabilities of detection and false alarm for both local and cooperative spectrum sensing, such that performance awareness can be enabled for both local and cooperative sensing schemes and that the noise variance can also be estimated for enabling threshold adaptation of energy-based sensing. The proposed method is illustrated with numerical results which confirm its effectiveness for all the considered spectrum sensing schemes in practical scenarios with noise and/or multipath fading.

VI.2 FUTURE RESEARCH

The contributions of this dissertation may be extended in future research in the following directions:

The key concepts of the adaptive sensing methods presented in Chapter II and III, can be studied in conjunction with other spectrum sensing methods introduced in Chapter I, such as waveform-based detection, cyclostationary detection, and cooperative spectrum sensing, for which adapting the sensing window may lead to similar improvements in the spectrum hole utilization and probability of detection. Furthermore, other types of degraded radio environments can also be studied with the presented methods, such as Rayleigh and Nakagami multipath fadings.

For the study on optimization of the cooperative sensing performance presented in Chapter IV, the presented method for the optimization assumes that the PU status stays unchanged during the delay time for the FC processing. Hence, one interesting direction in this context is to study optimizing the sensing performance of the cooperative sensing network when it is assumed that the PU may change its state during the FC processing duration.

For the use of the presented HMM for performance evaluation of CR systems proposed in Chapter V, a challenge is to apply the presented HMM-based method to enabling threshold adaptation of energy-based spectrum sensing as mentioned in the chapter. Moreover, the proposed method may be studied in other types of degraded radio environments beyond AWGN and Rayleigh fading.

BIBLIOGRAPHY

[1] S. Haykin, "Cognitive Radio: Brain-Empowered Wireless Communications," *IEEE Journal on Selected Areas in Communications*, vol. 23, no. 2, pp. 201–220, Feb. 2005.

[2] W. Krenik, A. M. Wyglinsky, and L. Doyle, "Cognitive Radios for Dynamic Spectrum Access," *IEEE Communications Magazine*, vol. 45, no. 5, pp. 64–65, May 2007.

[3] R. Tandra, A. Sahai, and M. Mishra, "What is a Spectrum Hole and What Does It Take to Recognize One?" *Proceedings of the IEEE*, vol. 97, no. 5, pp. 824–848, May 2009.

[4] J. Mitola, "Cognitive Radio: An Integrated Agent Architecture for Software Defined Radio," Ph.D. dissertation, Royal Institute of Technology, 2000.

[5] J. Mitola, "The Software Radio Architecture," *IEEE Communications Magazine*, vol. 33, no. 5, pp. 26–38, May 1995.

[6] J. Mitola and G. Q. Maguire, "Cognitive Radio: Making Software Radios More Personal," *IEEE Personal Communications Magazine*, vol. 6, no. 6, pp. 13–18, Aug. 1999.

[7] T. Yucek and H. Arslan, "A Survey of Spectrum Sensing Algorithms for Cognitive Radio Applications," *IEEE Communications Surveys and Tutorials*, vol. 11, no. 1, pp. 116–130, Mar. 2009.

[8] Federal Communications Commission, "Notice of Proposed Rule Making and Order: Facilitating Opportunities for Flexible, Efficient, and Reliable Spectrum Use Employing Cognitive Radio Technologies," *ET Docket*, no. 03-108, Feb. 2005.

[9] B. Wang and K. J. R. Liu, "Advances in Cognitive Radio Networks: A Survey," *IEEE Journal of Selected Topics in Signal Processing*, vol. 5, no. 1, pp. 5–23, Feb. 2011.

[10] H. Urkowitz, "Energy Detection of Unknown Deterministic Signals," *Proceedings of the IEEE*, vol. 55, no. 4, Apr. 1967.

[11] H. Tang, "Some Physical Layer Issues of Wide-band Cognitive Radio Systems," in *Proceedings of IEEE International Symposium on New Frontiers in Dynamic Spectrum Access Networks*, Baltimore, MD, Nov. 2005, pp. 151–159.

[12] W. A. Gardner, "Signal Interception: A Unifying Theoretical Framework for Feature Detection," *IEEE Transactions on Communications*, vol. 36, no. 8, pp. 897–906, Aug. 1988.

[13] W. A. Gardner, A. Napolitano, and L. Paura, "Cyclostationarity: Half a Century of Research," *Elsevier Signal Processing*, vol. 86, no. 4, pp. 639–697, Apr. 2006.

[14] P. D. Sutton, K. E. Nolan, and L. E. Doyle, "Cyclostationary Signatures in Practical Cognitive Radio Applications," *IEEE Journal on Selected Areas in Communications*, vol. 26, no. 1, pp. 13–24, Jan. 2008.

[15] M. Ghozzi, F. Marx, M. Dohler, and J. Palicot, "Cyclostationarity-based Test for Detection of Vacant Frequency Bands," in *Proceedings of IEEE International*

Conference on Cognitive Radio Oriented Wireless Networks and Communications, Jun. 2006, pp. 1–5.

[16] K. Kim, I. A. Akbar, K. K. Bae, J. Um, C. M. Spooner, and J. H. Reed, "Cyclostationary Approaches to Signal Detection and Classification in Cognitive Radio," in *Proceedings of IEEE International Symposium on New Frontiers in Dynamic Spectrum Access Networks*, Apr. 2007, pp. 212–215.

[17] I. F. Akyildiz, B. F. Lo, and R. Balakrishnan, "Cooperative Spectrum Sensing in Cognitive Radio Networks: A Survey," *Elsevier Physical Communications*, vol. 4, no. 1, pp. 40–62, Mar. 2011.

[18] K. B. Letaief and W. Zhang, "Cooperative Communications for Cognitive Radio Networks," *Proceedings of the IEEE*, vol. 97, no. 5, pp. 878–893, May 2009.

[19] S. Zarrin and T. J. Lim, "Cooperative Spectrum Sensing in Cognitive Radios with Incomplete Likelihood Functions," *IEEE Transactions on Signal Processing*, vol. 58, no. 6, pp. 3272–3281, Jun. 2010.

[20] Z. Quan, S. Cui, and A. H. Sayed, "Optimal Linear Cooperation for Spectrum Sensing in Cognitive Radio Networks," *IEEE Journal of Selected Topics in Signal Processing*, vol. 2, no. 1, pp. 28–40, Feb. 2008.

[21] T. C. Aysal, S. Kandeepan, and R. Piesiewicz, "Cooperative Spectrum Sensing with Noisy Hard Decision Transmissions," in *Proceedings of IEEE International Conference on Communications*, Jun. 2009, pp. 1–5.

[22] W. Zhang, R. K. Mallik, and K. B. Letaief, "Optimization of Cooperative Spectrum Sensing with Energy Detection in Cognitive Radio Networks," *IEEE Transactions on Wireless Communications*, vol. 8, no. 12, pp. 5761–5766, Dec. 2009.

[23] J. Ma and Y. Li, "Soft Combination and Detection for Cooperative Spectrum Sensing in Cognitive Radio Networks," in *Proceedings of IEEE Globecom*, Nov. 2007, pp. 3139–3143.

[24] M. Gandetto and C. Regazzoni, "Spectrum Sensing: A Distributed Approach for Cognitive Terminals," *IEEE Journal on Selected Areas in Communications*, vol. 25, no. 3, pp. 546–557, Apr. 2007.

[25] W. Ejaz, N. U. Hasan, H. S. Kim, and M. A. Azam, "Fully Distributed Cooperative Spectrum Sensing for Cognitive Radio Ad Hoc Networks," in *Proceedings of the 2011 Frontiers of Information Technology*, Dec. 2011, pp. 9–13.

[26] R. Chen, J. Park, and K. Bian, "Robust Distributed Spectrum Sensing in Cognitive Radio Networks," in *Proceedings of the 2008 IEEE Conference on Computer Communications*, Apr. 2008, pp. 1876–1884.

[27] W. Zhang and K. B. Letaief, "Cooperative Spectrum Sensing with Transmit and Relay Diversity in Cognitive Radio Networks," *IEEE Transactions on Wireless Communications*, vol. 7, no. 12, pp. 4761–4766, Dec. 2008.

[28] G. Ganesan and Y. Li, "Cooperative Spectrum Sensing in Cognitive Radio, Part I: Two User Networks," *IEEE Transactions on Wireless Communications*, vol. 6, no. 6, pp. 2204–2213, Jun. 2007.

[29] G. Ganesan and Y. Li, "Cooperative Spectrum Sensing in Cognitive Radio, Part II: Multiuser Networks," *IEEE Transactions on Wireless Communications*, vol. 6, no. 6, pp. 2214–2222, Jun. 2007.

[30] Y. C. Liang, Y. Zeng, E. C. Peh, and A. T. Hoang, "Sensing-Throughput Tradeoff for Cognitive Radio Networks," *IEEE Transactions on Wireless Communications*, vol. 7, no. 4, pp. 1326–1337, Apr. 2008.

[31] A. Mariani, A. Giorgetti, and M. Chiani, "Energy Detector Design for Cognitive Radio Applications," in *Proceedings of International Waveform Diversity and Design Conference (WDD)*, Aug. 2010, pp. 53–57.

[32] F. F. Digham, M. S. Alouini, and M. K. Simon, "On the Energy Detection of Unknown Signals Over Fading Channels," *IEEE Transactions on Communications*, vol. 55, no. 1, pp. 21–24, Jan. 2007.

[33] S. Ciftci and M. Torlak, "A Comparison of Energy Detectability Models for Spectrum Sensing," in *Proceedings of IEEE Global Telecommunications Conference*, New Orleans, LO, Dec. 2008, pp. 1–5.

[34] J. G. Proakis and D. G. Manolakis, *Digital Signal Processing: Principles, Algorithms, and Applications.* Pearson Prentice Hall, 2007.

[35] D. Cabric, A. Tkachenko, and R. W. Brodersen, "Experimental Study of Spectrum Sensing based on Energy Detection and Network Cooperation," in *Proceedings of International Workshop on Technology and Policy for Accessing Spectrum (TAPAS)*, Aug. 2006.

[36] S. M. Kay, *Fundamentals of Statistical Signal Processing: Detection Theory.* Prentice Hall, 1998.

[37] L. E. Baum and T. Petrie, "Statistical Inference for Probabilistic Functions of Finite State Markov Chains," *The Annals Mathematical Statistics*, vol. 37, no. 6, pp. 1554–1563, Dec. 1966.

[38] L. E. Baum and J. A. Eagon, "An Inequality with Applications to Statistical Estimation for Probabilistic Functions of a Markov Process and to a Model for Ecology," *Bulletin of The American Mathematical Society*, vol. 73, no. 3, pp. 360–363, 1967.

[39] L. E. Baum, T. Petrie, G. Soules, and N. Weiss, "A Maximization Technique Occurring in the Statistical Analysis of Probabilistic Functions of Markov Chains," *The Annals Mathematical Statistics*, vol. 41, no. 1, pp. 164–171, 1970.

[40] L. E. Baum, "An Inequality and Associated Maximization Technique in Statistical Estimation for Probabilistic Functions of Markov Processes," *Inequalities*, vol. 3, no. 1, pp. 1–8, 1972.

[41] L. R. Rabiner, "A Tutorial on Hidden Markov Models and Selected Applications in Speech Recognition," *Proceedings of the IEEE*, vol. 7, no. 22, pp. 257–286, Feb. 1989.

[42] A. J. Coulson, "Spectrum Sensing using Hidden Markov Modeling," in *Proceedings of IEEE International Conference on Communications (ICC'09)*, Jun. 2009, pp. 1–6.

[43] A. B. Reid and A. J. Coulson, "Blind Wideband Spectrum Sensing using Cluster Analysis," in *Proceedings of Australian Communications Theory Workshop (AusCTW)*, Feb. 2010, pp. 133–138.

[44] A. J. Coulson, "Blind Spectrum Sensing using Bayesian Sequential Testing with Dynamic Update," in *Proceedings of IEEE International Conference on Communications (ICC'11)*, New Zealand, Jun. 2011, pp. 1–6.

[45] C. Ghosh, C. Cordeiro, D. P. Agrawal, and M. B. Rao, "Markov Chain Existence and Hidden Markov Models in Spectrum Sensing," in *Proceedings of IEEE International Conference on Pervasive Computing and Communications (PerCom)*, Mar. 2009, pp. 1–6.

[46] Z. Chen, N. Guo, Z. Hu, and R. C. Qiu, "Experimental Validation of Channel State Prediction Considering Delays in Practical Cognitive Radio," *IEEE Transactions on Vehicular Technology*, vol. 60, no. 4, pp. 1314–1325, May 2011.

[47] Z. Chen, N. Guo, Z. Hu, and R. C. Qiu, "Channel State Prediction in Cognitive Radio, Part II: Single-User Prediction," in *Proceedings of IEEE Southeastcon*, Mar. 2011, pp. 50–54.

[48] Z. Chen and R. C. Qiu, "Prediction of Channel State for Cognitive Radio Using Higher-Order Hidden Markov Model," in *Proceedings of IEEE Southeastcon*, Mar. 2010, pp. 276 – 282.

[49] C. H. Park, S. W. Kim, S. M. Lim, and M. S. Song, "HMM Based Channel Status Predictor for Cognitive Radio," in *Proceedings of Asia-Pacific Microwave Conference (APMC)*, Dec. 2007, pp. 1–4.

[50] C. Devanarayana and A. S. Alfa, "Predictive Channel Access in Cognitive Radio Networks Based on Variable Order Markov Models," in *Proceedings of IEEE Global Telecommunications Conference*, Dec. 2011, pp. 1–6.

[51] Z. Sun, G. J. Bradford, and J. N. Laneman, "Sequence Detection Algorithms for PHY-Layer Sensing in Dynamic Spectrum Access Networks," *IEEE Journal of Selected Topics in Signal Processing*, vol. 5, no. 1, pp. 97–109, Feb. 2011.

[52] Z. Sun, J. N. Laneman, and G. J. Bradford, "Sequence Detection Algorithms for Dynamic Spectrum Access Networks," in *Proceedings of IEEE Symposium on New Frontiers in Dynamic Spectrum*, Singapore, Apr. 2010, pp. 1–9.

[53] K. W. Choi and E. Hossain, "Opportunistic Access to Spectrum Holes Between Packet Bursts: A Learning-Based Approach," *IEEE Transactions on Wireless Communications*, vol. 10, no. 8, pp. 2497–2509, Aug. 2011.

[54] T. Nguyeny, B. L. Mark, and Y. Ephraim, "Hidden Markov Process Based Dynamic Spectrum Access for Cognitive Radio," in *Proceedings of 45th Annual Conference on Information Sciences and Systems (CISS)*, Mar. 2011, pp. 1–6.

[55] Y. Li, S. K. Jayaweera, M. Bkassiny, and K. A. Avery, "Optimal Myopic Sensing and Dynamic Spectrum Access in Cognitive Radio Networks with Low-Complexity Implementations," *IEEE Transactions on Wireless Communications*, vol. 11, no. 7, pp. 2412–2423, Jul. 2012.

[56] R. Durbin, S. R. Eddy, A. Krogh, and G. Mitchison, *Biological Sequence Analysis.* Cambridge, UK: Cambridge University Press, 1998.

[57] Y. Xin, H. Zhang, and S. Rangarajan, "SSCT: A Simple Sequential Spectrum Sensing Scheme for Cognitive Radio," in *Proceedings of IEEE Globecom*, Dec. 2009, pp. 1–6.

[58] T. S. Shehata and M. El-Tanany, "A Novel Adaptive Structure of The Energy Detector Applied to Cognitive Radio Networks," in *Proceedings of 11th Canadian Workshop on Information Technology*, May 2009, pp. 95–98.

[59] J. Y. Xu and F. Alam, "Adaptive Energy Detection for Cognitive Radio: An Experimental Study," in *Proceedings of 12th International Conference on Computer and Information Technology*, Dec. 2009, pp. 547–551.

[60] Y. Zou, Y. D. Yao, and B. Zheng, "Spectrum Sensing and Data Transmission Tradeoff in Cognitive Radio Networks," in *Proceedings of 19th Annual Wireless and Optical Communications Conference*, May 2010, pp. 1–5.

[61] D. Treeumnuk and D. C. Popescu, "Adaptive Sensing for Increased Spectrum Utilization in Dynamic Cognitive Radio Systems," in *Proceedings of 2012 IEEE Radio and Wireless Symposium (RWS 2012)*, Jan. 2012, pp. 319–322.

[62] D. Treeumnuk and D. C. Popescu, "Energy Detector with Adaptive Sensing Window for Improved Spectrum Utilization in Dynamic Cognitive Radio Systems," in *Proceedings of IEEE International Conference on Communications (ICC 2012)*, Ottawa, Canada, Jun. 2012.

[63] D. Treeumnuk and D. C. Popescu, "Enhancing Spectrum Hole Utilization Through Adaptive Sensing in Cognitive Radio Systems," in *Proceedings of IEEE*

Global Telecommunications Conference (GLOBECOM 2012), CA, USA, Dec. 2012.

[64] D. Treeumnuk and D. C. Popescu, "Enhanced Spectrum Utilization in Dynamic Cognitive Radios with Adaptive Sensing," *Submitted to IEEE Transactions on Wireless Communications*, Aug. 2012.

[65] D. Treeumnuk, S. L. Macdonald, and D. C. Popescu, "Optimizing Performance of Cooperative Sensing for Increased Spectrum Utilization in Dynamic Cognitive Radio Systems," *Submitted to the 2013 IEEE International Conference on Communications (ICC 2013)*, Sep. 2012.

[66] D. Treeumnuk and D. C. Popescu, "Using Hidden Markov Models to Enable Performance Awareness and Noise Variance Estimation for Energy Detection in Cognitive Radio," in *Proceedings of the 46th Annual Conference on Information Sciences and Systems (CISS)*, NJ, USA, March 2012.

[67] D. Treeumnuk and D. C. Popescu, "Using Hidden Markov Models to Evaluate Performance of Cooperative Spectrum Sensing," *Submitted to IEEE Communications Letters*, Aug. 2012.

[68] Y. Zou, Y. D. Yao, and B. Zheng, "Cognitive Transmissions with Multiple Relays in Cognitive Radio Networks," *IEEE Transactions on Wireless Communications*, vol. 10, no. 2, pp. 648–659, Feb. 2011.

[69] L. H. Jiang and Z. Qi, "Tradeoff between Utilization and Collision in Cognitive Radio," in *Proceedings of International Conference on Wireless Communications and Signal Processing*, Nov. 2009, pp. 1–5.

[70] J. E. Salt and H. H. Nguyen, "Performance Prediction for Energy Detection of Unknown Signals," *IEEE Transactions on Vehicular Technology*, vol. 57, no. 6, pp. 3900–3904, Nov. 2008.

[71] R. Fantacci and A. Tani, "Performance Evaluation of a Spectrum-Sensing Technique for Cognitive Radio Applications in B-VHF Communication Systems," *IEEE Transactions on Vehicular Technology*, vol. 58, no. 4, pp. 1722–1730, May 2009.

[72] S. Geirhofer, L. Tong, and B. M. Sadler, "Cognitive Medium Access: Constraining Interference Based on Experimental Models," *IEEE Journal on Selected Areas in Communications*, vol. 26, no. 1, pp. 95–105, Jan. 2008.

[73] R. Tandra and A. Sahai, "SNR Walls for Signal Detection," *IEEE Journal of Selected Topics in Signal Processing*, vol. 2, no. 1, pp. 4–17, Feb. 2008.

[74] M. Abramowitz and I. A. Stegun, *Handbook of Mathematical Functions with Formulas, Graphs, and Mathematical Tables.* Dover Publications, 1972.

[75] Y. Chen, "Optimum Number of Secondary Users in Collaborative Spectrum Sensing Considering Resources Usage Efficiency," *IEEE Communications Letters*, vol. 12, no. 12, pp. 877–889, Dec. 2008.

[76] S. Wu, M. Zhao, and J. Zhu, "Optimal Number of Secondary Users through Maximizing Utility in Cooperative Spectrum Sensing," in *Proceedings of IEEE 70th Vehicular Technology Conference Fall*, Sep. 2009, pp. 1–5.

[77] L. Zhang, D. Zhang, and G. Huang, "Optimal Number of Secondary users for Cooperative Sensing in Cognitive Radio Networks," in *Proceedings of IEEE Youth Conference on Information, Computing and Telecommunication*, Sep. 2009, pp. 347–350.

[78] E. Peh and Y. C. Liang, "Optimization for Cooperative Sensing in Cognitive Radio Networks," in *Proceedings of IEEE Wireless Communications and Networking Conference*, Mar. 2007, pp. 27–32.

[79] F. F. Digham, M. S. Alouini, and M. K. Simon, "On The Energy Detection of Unknown Signals Over Fading Channels," in *Proceedings of IEEE ICC*, Anchorage, AK, May 2003, pp. 3575–3579.

[80] D. R. Joshi, D. C. Popescu, and O. A. Dobre, "Gradient-Based Threshold Adaptation for Energy Detector in Cognitive Radio Systems," *IEEE Communication Letters*, vol. 15, no. 1, pp. 19–21, Jan. 2011.

VITA

Dusadee Treeumnuk
Department of Electrical and Computer Engineering
Old Dominion University
Norfolk, VA 23529

EDUCATION

- M.S. Electrical Engineering, 2009, Old Dominion University, USA
- M.E. Microelectronics, 2001, Asian Institute of Technology, Thailand
- B.E. Electrical Engineering, 1995, Kasetsart University, Thailand

PUBLICATIONS

- Dusadee Treeumnuk and Dimitrie C. Popescu, "Enhancing Spectrum Hole Utilization Through Adaptive Sensing in Cognitive Radio Systems," in *Proc. IEEE GLOBECOM 2012*, Dec. 2012, CA, USA.
- Dusadee Treeumnuk and Dimitrie C. Popescu, "Energy Detector with Adaptive Sensing Window for Improved Spectrum Utilization in Dynamic Cognitive Radio Systems," in *Proc. IEEE ICC 2012*, Jun. 2012, Ottawa, Canada.
- Dusadee Treeumnuk and Dimitrie C. Popescu, "Using Hidden Markov Models to Enable Performance Awareness and Noise Variance Estimation for Energy Detection in Cognitive Radio," in *Proc. IEEE CISS 2012*, Mar. 2012, NJ, USA.
- Dusadee Treeumnuk and Dimitrie C. Popescu, "Adaptive Sensing for Increased Spectrum Utilization in Dynamic Cognitive Radio Systems," in *Proc. IEEE RWS 2012*, pp. 319-322, Jan. 2012, CA, USA.